Electronic Supplementary Material (ESI) for Dalton Transactions
This journal is © The Royal Society of Chemistry 2015

Electronic Supplementary Information

Phase development during high-energy ball-milling of zinc oxide and iron – the impact of grain size on the source and the degree of contamination

Goran Štefanić,* Stjepko Krehula and Ivka Štefanić

Ruđer Bošković Institute, Bijenička 54, HR-10000 Zagreb, Croatia

Table of Contents

Section 1 *Colors of the Products*

Fig. 1 Colors of the starting zincite (S1-0) and the products obtained after ball-milling of zincite for 1 h, 2 h, 5 h, 9 h, 14 h, 20 h and 25 h.

Fig 2 Colors of the powder mixtures of zincite and iron with weight ratio 3:1 (S2-0) and the corresponding products obtained after ball-milling for 1 h, 2 h, 5 h, 9 h, 14 h, 20 h and 25 h.

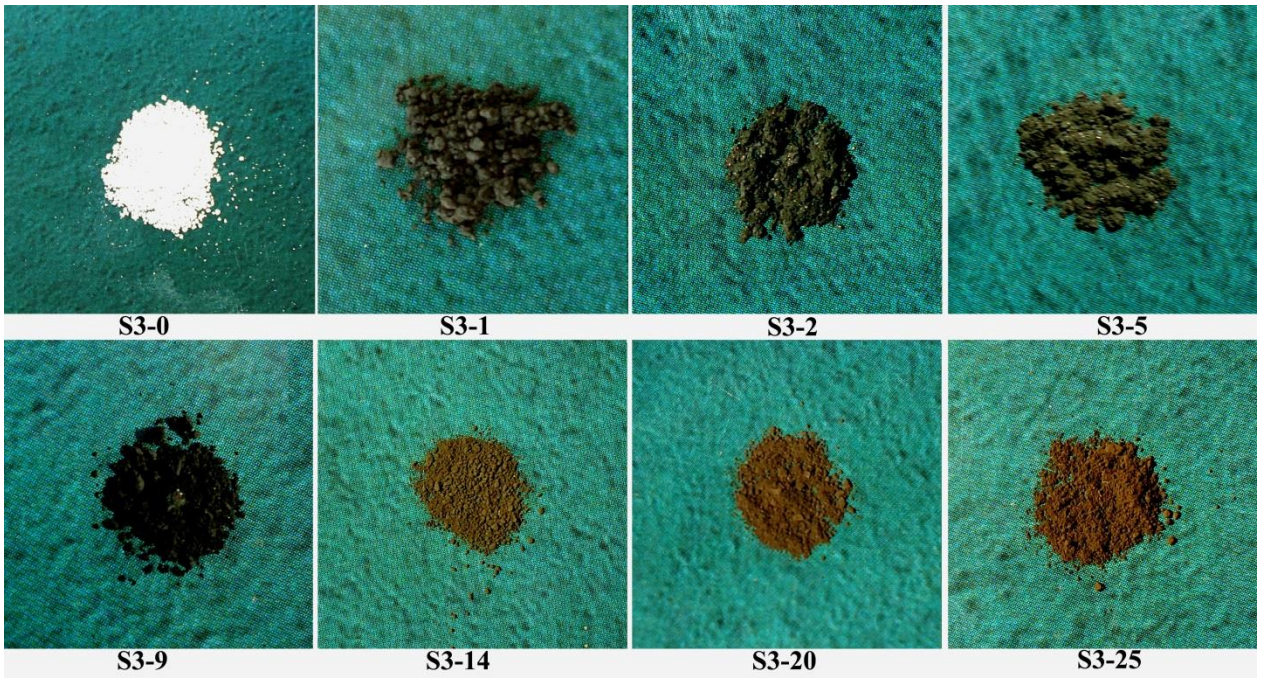

Fig 3 Colors of the powder mixtures of zincite and iron with weight ratio 1:1 (S3-0) and the corresponding products obtained after ball-milling for 1 h, 2 h, 5 h, 9 h, 14 h, 20 h and 25 h.

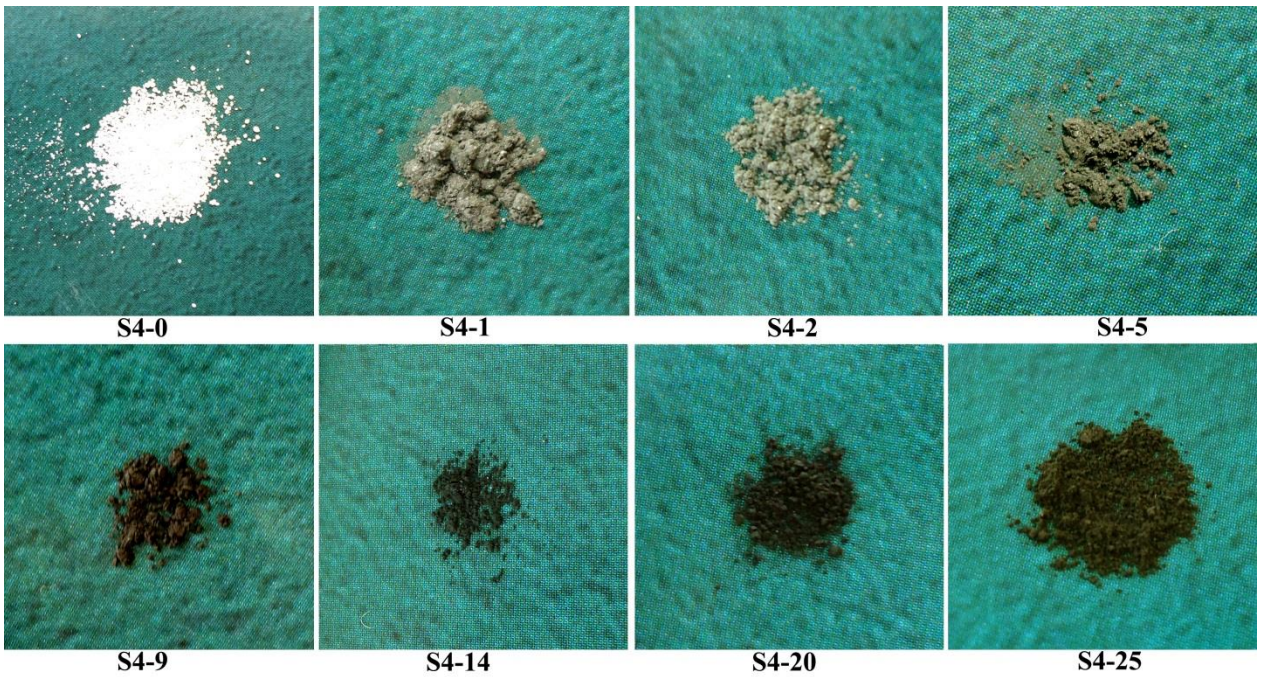

Fig 4 Colors of the powder mixtures of zincite and iron with weight ratio 1:3 (S4-0) and the corresponding products obtained after ball-milling for 1 h, 2 h, 5 h, 9 h, 14 h, 20 h and 25 h.

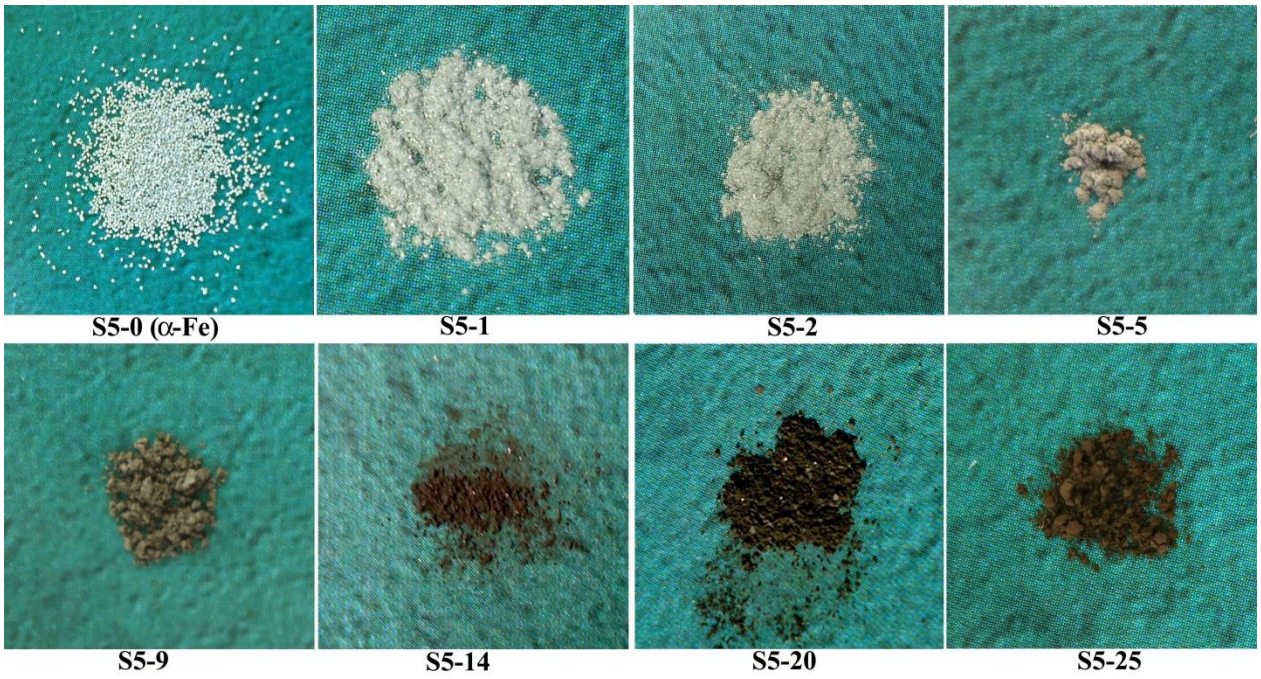

Fig. 5 Colors of the starting α-iron (S5-0) and the corresponding products obtained after ball-milling for 1 h, 2 h, 5 h, 9 h, 14 h, 20 h and 25 h.

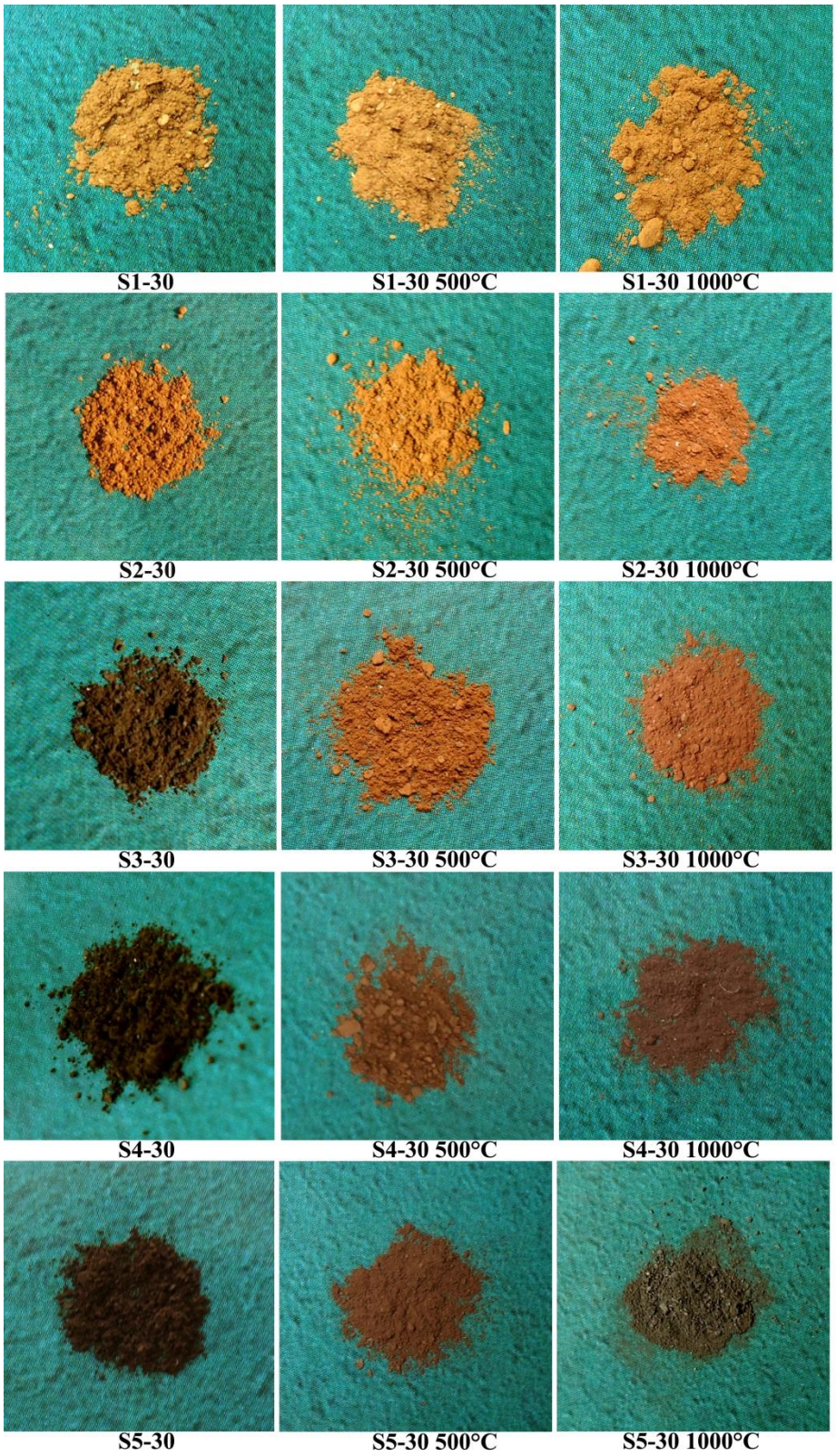

Fig. 6 Colors of the final milling products (30 h) of samples S1, S2, S3, S4 and S5 and the corresponding products obtained after their annealing at 500 °C and 1000 °C.

Section 2 *Quantitative Crystal Phase Analysis*

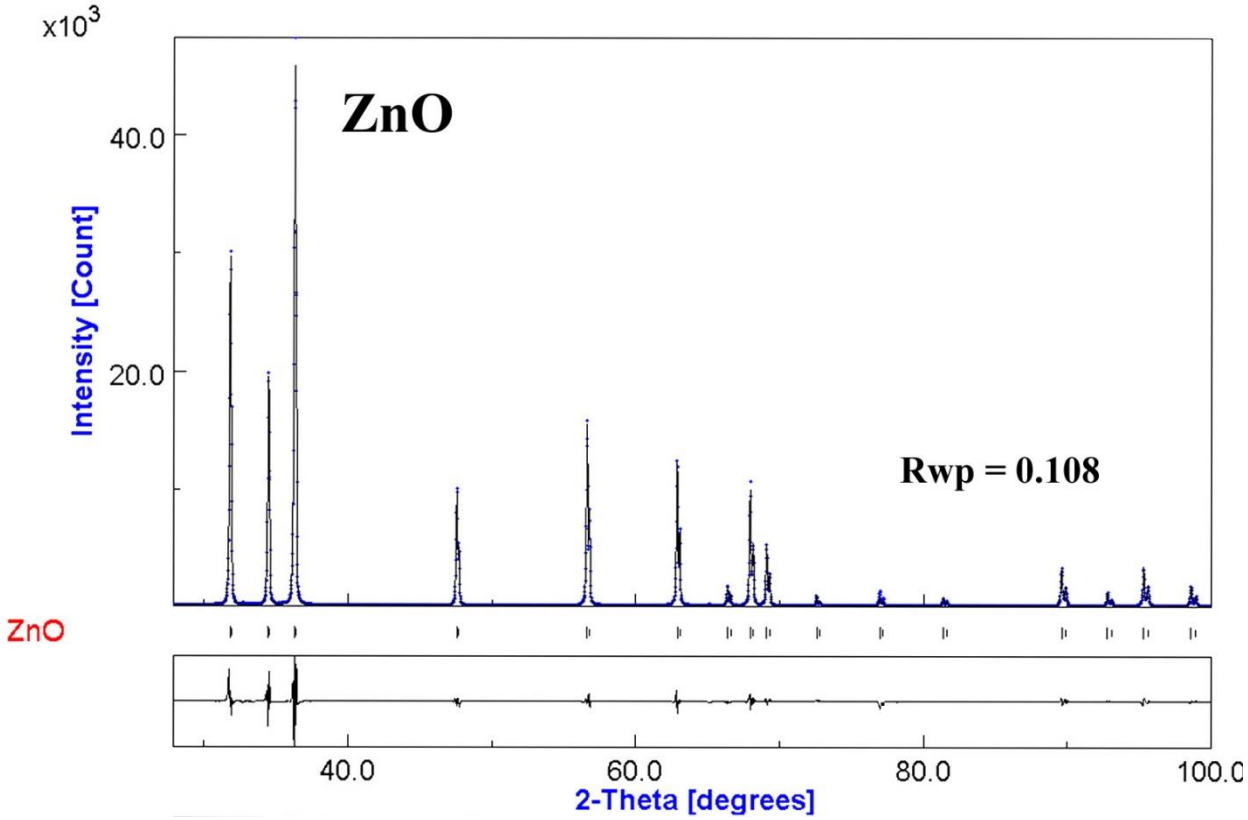

Fig. 7 Rietveld refinements on powder diffraction patterns of the starting zincite (ZnO). The difference between the observed and calculated patterns is shown in the box below.

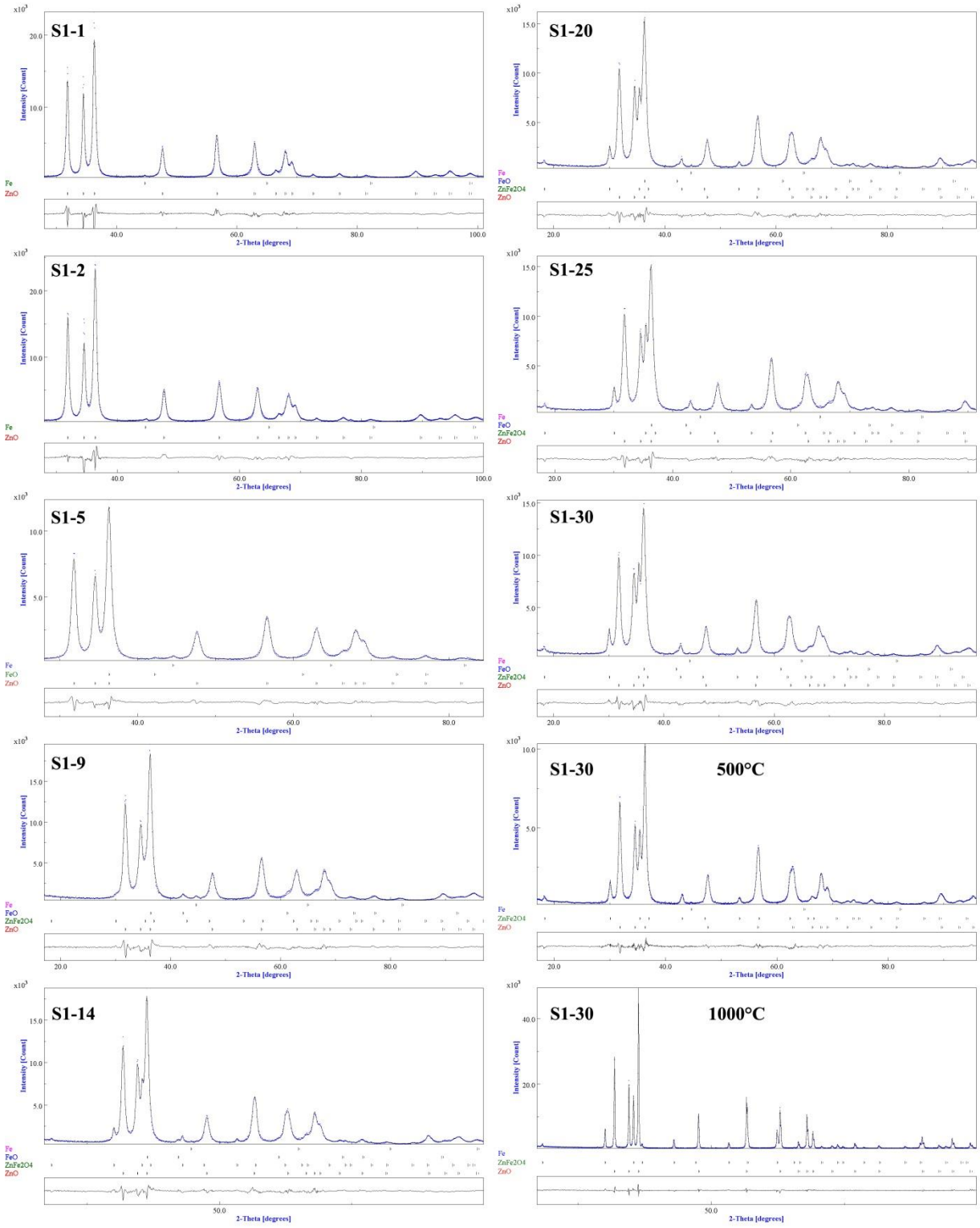

Fig. 8 Rietveld refinements on powder diffraction patterns of the products obtained after high-energy ball-milling of pure zincite (sample S1-0) and annealing of the final milling product (30 h) at 500 and 1000 °C. The difference between the observed and calculated patterns is shown in the box below.

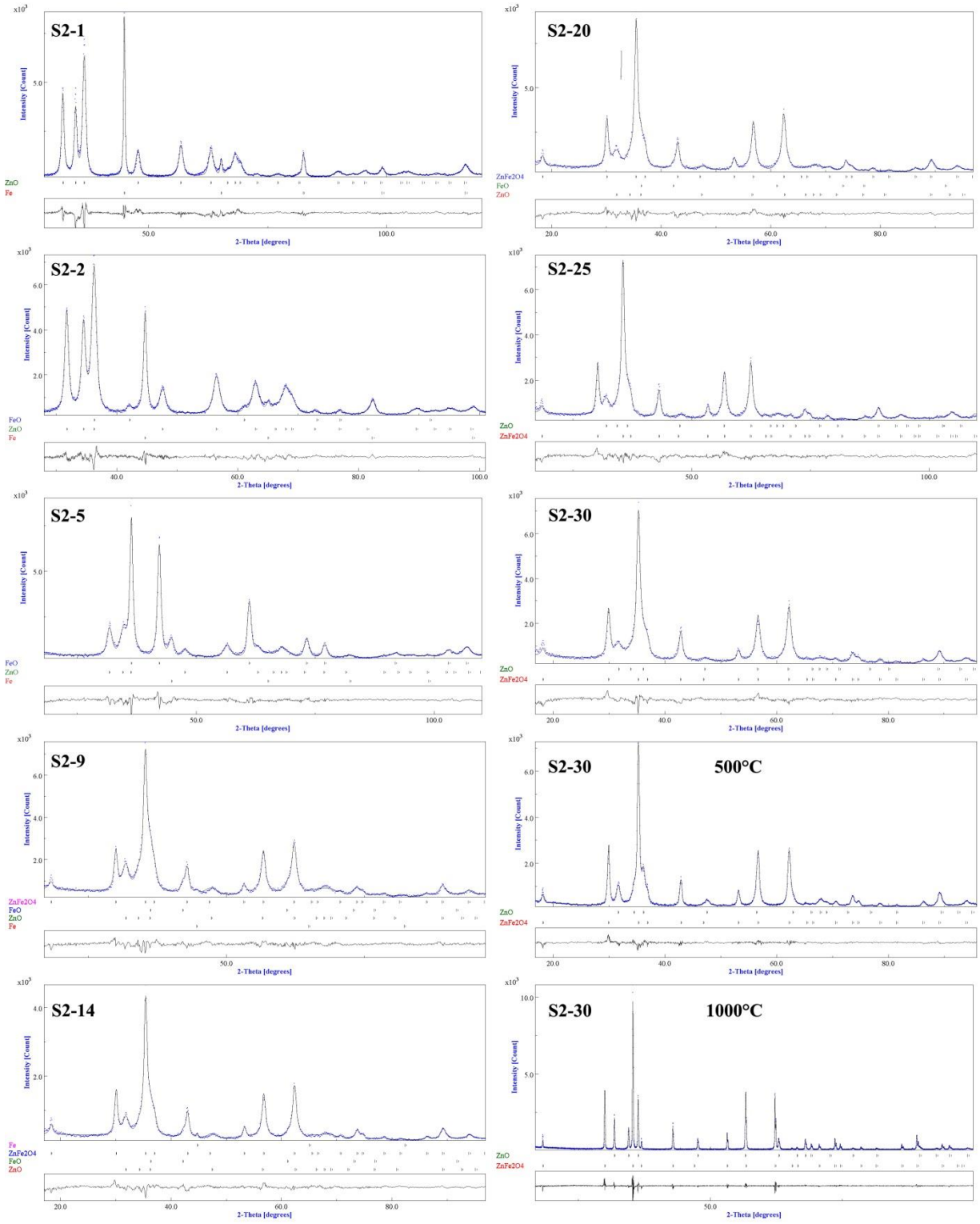

Fig. 9 Rietveld refinements on powder diffraction patterns of the products obtained after high-energy ball-milling of the powder mixtures of zincite and iron with weight ratio 3:1 (sample S2-0) and annealing of the final milling product (30 h) at 500 and 1000 °C. The difference between the observed and calculated patterns is shown in the box below.

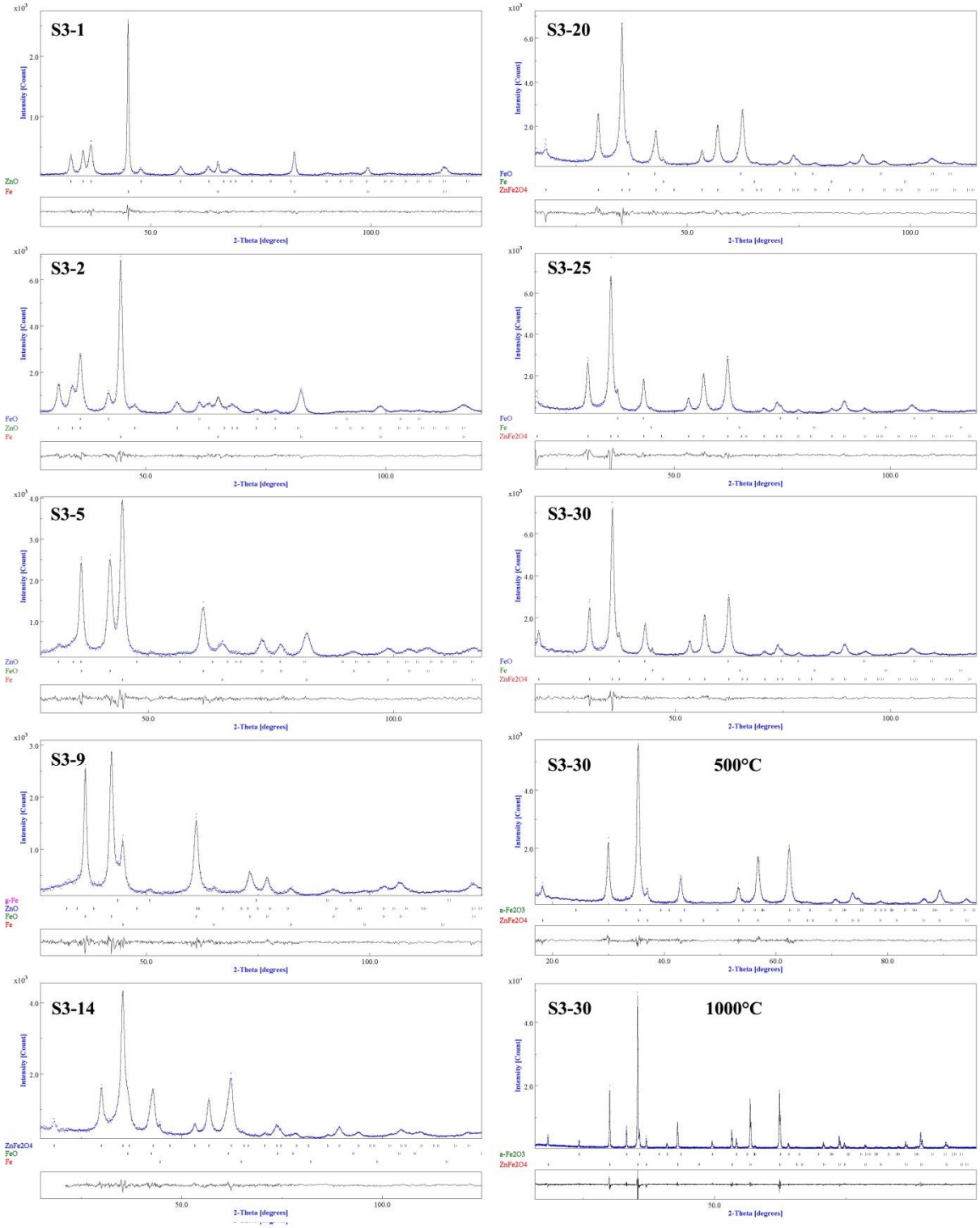

Fig. 10 Rietveld refinements on powder diffraction patterns of the products obtained after high-energy ball-milling of the powder mixtures of zincite and iron with weight ratio 1:1 (sample S3-0) and annealing of the final milling product (30 h) at 500 and 1000 °C. The difference between the observed and calculated patterns is shown in the box below.

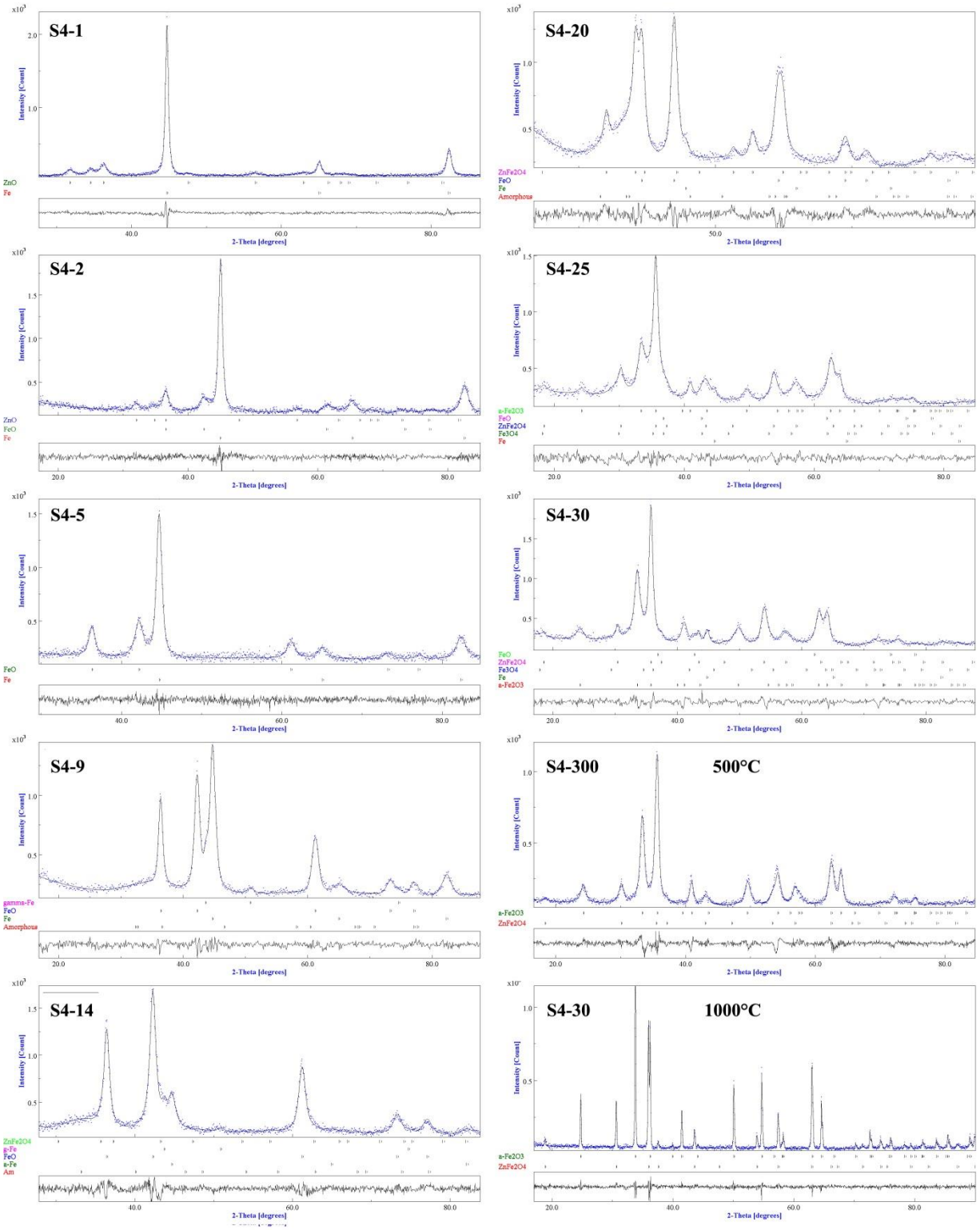

Fig. 11 Rietveld refinements on powder diffraction patterns of the products obtained after high-energy ball-milling of the powder mixtures of zincite and iron with weight ratio 1:3 (sample S4-0) and annealing of the final milling product (30 h) at 500 and 1000 °C. The difference between the observed and calculated patterns is shown in the box below.

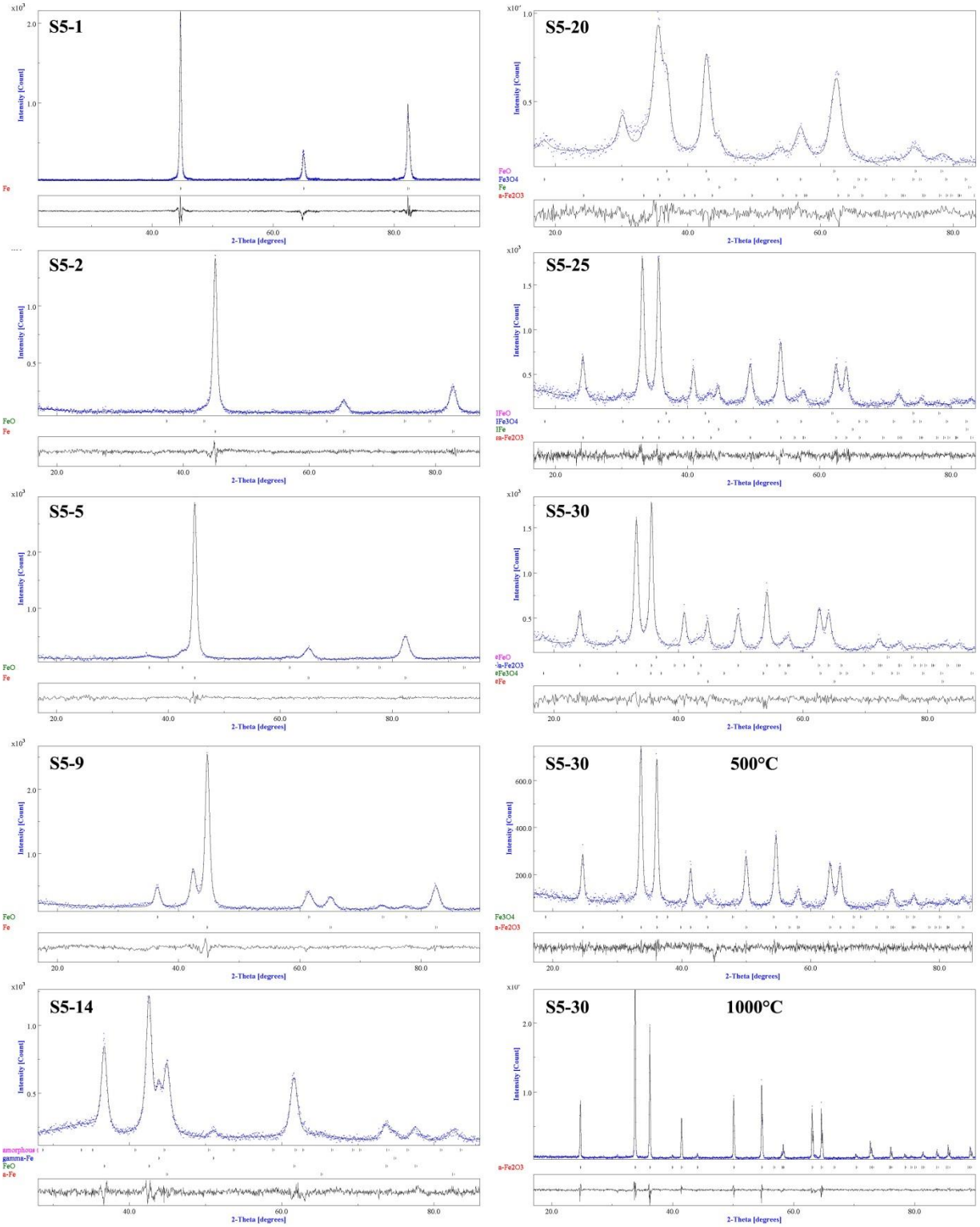

Fig. 12 Rietveld refinements on powder diffraction patterns of the products obtained after high-energy ball-milling of pure α-iron (sample S5-0) and annealing of the final milling product (30 h) at 500 and 1000 °C. The difference between the observed and calculated patterns is shown in the box below.

Table 1

The results of quantitative phase analysis of the products obtained upon ball-milling of the samples S1, S2, S3, S4 and S5 and calcination of the final milling products (30 h) at 500 and 1000 °C. The volume fraction of the obtained crystalline phases was determined from the results of Rietveld refinements with the weighted residual error indexes (R_{wp}) given in the last column.

Sample	Time	Temperature	Phase composition (volume fraction)	R_{wp}
S1	-	RT	ZnO	0.10
S1-1	1 h	RT	*Z* + *αFe* (traces)	0.09
S1-2	2 h	RT	*Z* (0.99) + *αFe* (0.01)	0.08
S1-5	5 h	RT	*Z* (0.98) + *αFe* (0.01) + *W* (0.01)	0.05
S1-9	9 h	RT	*Z* (0.94) + *W* (0.03) + *S* (0.03)	0.06
S1-14	14 h	RT	*Z* (0.85) + *S* (0.13) + *W* (0.02)	0.05
S1-20	20 h	RT	*Z* (0.80) + *S* (0.19) + *W* (0.01)	0.06
S1-25	25 h	RT	*Z* (0.77) + *S* (0.22) + *W* (0.01)	0.05
S1-30	30 h	RT	*Z* (0.76) + *S* (0.23) + *W* (0.01)	0.05
S1-30-500	30 h	500 °C	*Z* (0.72) + *S* (0.28)	0.06
S1-30-1000	30 h	1000°C	*Z* (0.71) + *S* (0.29)	0.09
S2	-	RT	ZnO (0.81) + *α*-Fe (0.19)*	-
S2-1	1 h	RT	*Z* (0.81) + *αFe* (0.19)	0.09
S2-2	2 h	RT	*Z* (0.80) + *αFe* (0.15) + *W* (0.05)	0.06
S2-5	5 h	RT	W (0.62) + *Z* (0.34) + *αFe* (0.04)	0.07
S2-9	9 h	RT	*S* (0.62) + *Z* (0.32) + *W* (0.05) + *αFe* (0.01)	0.06
S2-14	14 h	RT	*S* (0.71) + *Z* (0.25) + *W* (0.04)	0.06
S2-20	20 h	RT	*S* (0.76) + *Z* (0.22) + *W* (0.02)	0.06
S2-25	25 h	RT	*S* (0.79) + *Z* (0.21)	0.07
S2-30	30 h	RT	*S* (0.79) + *Z* (0.21)	0.07
S2-30-500	30 h	500 °C	*S* (0.75) + *Z* (0.25)	0.08
S2-30-1000	30 h	1000°C	*S* (0.74) + *Z* (0.26)	0.12
S3	-	RT	ZnO (0.58) + *α*Fe (0.42)*	-
S3-1	1 h	RT	*Z* (0.55) + *Fe* (0.45)	0.10
S3-2	2 h	RT	*Z* (0.44) + *αFe* (0.38) + *W* (0.18)	0.05
S3-5	5 h	RT	*W* (0.58) + *αFe* (0.30) + *Z* (0.12)	0.06
S3-9	9 h	RT	*W* (0.80) + *αFe* (0.11) + *Z* (0.09)	0.09
S3-14	14 h	RT	*S* (0.87) + *W* (0.12) + *αFe* (0.01)	0.05
S3-20	20 h	RT	*S* (0.93) + *W* (0.06) + *αFe* (0.01)	0.06
S3-25	25 h	RT	*S* (0.97) + *W* (0.02) + *αFe* (0.01)	0.09
S3-30	30 h	RT	*S* (0.99) + *W* (0.01)	0.08
S3-30-500	30 h	500 °C	*S* (0.99) + *H* (0.01)	0.06
S3-30-1000	30 h	1000°C	*S* (0.81) + *H* (0.19)	0.13

Table 1 (cont.)

Sample	Time	Temperature	Phase composition (volume fraction)	R_{wp}
S4	-	RT	*α*Fe (0.68) + *Z* (0.32)*	
S4-1	1 h	RT	*α*Fe (0.65) + *Z* (0.35)	0.09
S4-2	2 h	RT	*α*Fe (0.56) + *Z* (0.23) + *W* (0.21)	0.07
S4-5	5 h	RT	*W* (0.54) + *αFe* (0.46)	0.08
S4-9	9 h	RT	*W* (0.59) + *αFe* (0.31) + Am (0.07) + *γFe* (0.03)	0.05
S4-14	14 h	RT	*W* (0.80) + Am (0.09) + *αFe* (0.07) + *γFe* (0.02)	0.08
S4-20	20 h	RT	*W* (0.46) + *S* (0.32) + *Am* (0.21) + *αFe* (0.01)	0.06
S4-25	25 h	RT	*S* (0.63) + *H* (0.35) + *W* (0.01) + *αFe* (0.01)	0.06
S4-30	30 h	RT	*H* (0.58) + *S* (0.38) + *αFe* (0.02) + *W* (0.02)	0.08
S4-30-500	30 h	500 °C	*H* (0.70) + *S* (0.30)	0.10
S4-30-1000	30 h	1000°C	*H* (0.69) + *S* (0.31)	0.10
S5	-	RT	*αFe**	
S5-1	1 h	RT	*αFe*	0.12
S5-2	2 h	RT	*αFe* (0.93) + *W* (0.07)	0.08
S5-5	5 h	RT	*αFe* (0.80) + *W* (0.20)	0.09
S5-9	9 h	RT	*αFe* (0.54) + *W* (0.46)	0.06
S5-14	14 h	RT	*W* (0.79) + *γFe* (0.16) + *γFe* (0.05)	0.06
S5-20	20 h	RT	*S* (0.75) + *W* (0.20) + *H* (0.04) + *αFe* (0.01)	0.07
S5-25	25 h	RT	*H* (0.81) + *S* (0.15) + *αFe* (0.02) + *W* (0.02)	0.08
S5-30	30 h	RT	*H* (0.79) + *S* (0.16) + *αFe* (0.03) + *W* (0.02)	0.06
S5-30-500	30 h	500 °C	*H* (0.92) + *S* (0.08)	0.07
S5-30-1000	30 h	1000°C	*H*	0.14

*Volume fractions determined from the mass ratio of starting zincite and iron powders.

Description: *Z* = phase structurally similar to zincite (ZnO), *W* = phase structurally similar to wüstite (FeO), *αFe* = phase structurally similar to alpha iron, *γFe* = phase structurally similar to gamma iron, *S* = phase structurally similar to *franklinite (*$ZnFe_2O_4$) or magnetite (Fe_3O_4), *H* = phase structurally similar to hematite (*α*-Fe_2O_3)

Section 3 *Unit-cell parameter of spinel* ferrite *lattice*

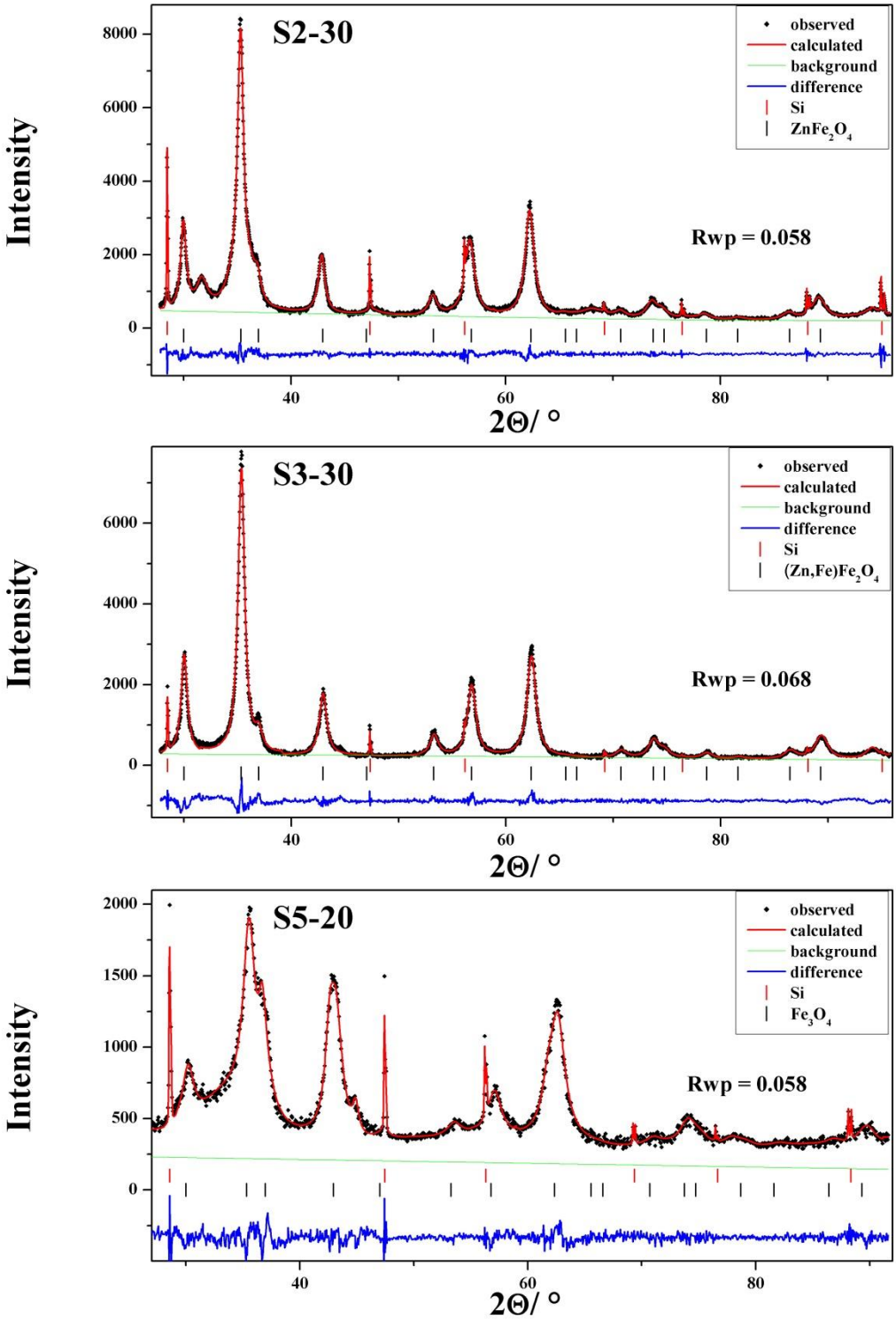

Fig 13 Le Bail refinements on powder diffraction patterns of the samples S2-30, S3-30 and S5-20 with added silicon as an internal standard. The difference between the observed and calculated patterns is shown as a line in the lower field.

Table 2

Refined values of unit-cell parameters of the *phase S (*spinel ferrite) in the milling products with different iron content as determined from the results of Le Bail refinements on powder diffraction patterns with added silicon as an internal standard.

Sample	Lattice parameter *a*/ nm	R_{wp}
S2-30	0.84368(2)	0.058
S3-30	0.84221(2)	0.068
S5-20	0.83978(8)	0.058

Section 4 *Mössbauer spectroscopy*

Table 3

^{57}Fe Mössbauer parameters (20 °C) of the products obtained from the sample S2 and corresponding iron oxidation state identification.

Sample	Spectral line	δ (mm s^{-1})	Δ or 2ε (mm s^{-1})	B_{hf} or $\langle B_{hf} \rangle$ (T)	Γ (mm s^{-1})	Area (%)	Iron oxidation state
S2-0	M	0.00	-	33.0	0.27	100	Fe^0 in α-Fe
S2-5	M	0.00	-	32.7	0.79	18.7	Fe^0 in α-Fe
	Q	1.01	1.05	-	0.72	63.5	Fe^{2+} in *W*
	Q	0.36	0.86	-	0.38	17.8	Fe^{3+} in *W* or *S*
S2-9	Q	1.01*	1.05*	-	0.80	4.8	Fe^{2+} in *W*
	Q	0.35	0.67	-	0.57	60.8	Fe^{3+} in *S*
	Q	0.27	-	22.8	0.40	34.4	Fe^{3+} in *S*
S2-14	Q	1.01*	1.05*	-	0.90	2.7	Fe^{2+} in *W*
	Q	0.34	0.63	-	0.54	53.7	Fe^{3+} in *S*
	Q	0.28	-	19.8	0.40	43.6	Fe^{3+} in *S*
S2-20	Q	1.01*	1.05*	-	0.90	2.2	Fe^{2+} in *W*
	Q	0.34	0.62	-	0.58	50.9	Fe^{3+} in *S*
	Q	0.33	-	17.7	0.40	46.9	Fe^{3+} in *S*
S2-30	Q	0.34	0.63	-	0.56	51.6	Fe^{3+} in *S*
	M	0.30	-	18.1	0.40	48.4	Fe^{3+} in *S*
S2-30-500	Q	0.34	0.48	-	0.42	100.0	Fe^{3+} in *S*
S2-30-1000	Q	0.35	0.44	-	0.32	100.0	Fe^{3+} in *S*

Description: *W* = phase structurally similar to wüstite (FeO), *S* = phase structurally similar to *franklinite* ($ZnFe_2O_4$), *H* = phase structurally similar to hematite (α-Fe_2O_3)

Errors: $\delta = \pm 0.01$ mm s^{-1}, $2\varepsilon = \pm 0.01$ mm s^{-1}, $B_{hf} = \pm 0.2$ T. Isomer shift is given relative to α-Fe.

*Imposed

Table 4

^{57}Fe Mössbauer parameters (20 °C) of the products obtained from the sample S3 and corresponding iron oxidation state identification.

Sample	Spectral line	δ (mm s^{-1})	Δ or 2ε (mm s^{-1})	B_{hf} or $\langle B_{hf} \rangle$ (T)	Γ (mm s^{-1})	Area (%)	Iron oxidation state
S3-0	M	0.00	-	33.0	0.27	100.0	Fe^0 in α-Fe
S3-5	M	0.01	-	32.7	0.31	63.3	Fe^0 in α-Fe
	Q	1.02	1.22	-	0.69	28.3	Fe^{2+} in *W*
	Q	0.37	0.88	-	0.41	8.4	Fe^{3+} in *W*
S3-9	M	0.03	-	31.3	0.32	21.2	Fe^0 in α-Fe
	Q	1.02	1.22	-	0.67	60.8	Fe^{2+} in *W*
	Q	0.35	0.72	-	0.43	18.0	Fe^{3+} in *W*
S3-14	Q	1.02*	1.22*	-	0.70*	11.7	Fe^{2+} in *W*
	Q	0.38	0.75	-	0.70	42.7	Fe^{3+} in *S* or
	M	0.65*	-	22.9	0.40*	33.0	$Fe^{2.5+}$ in *S*
	M	0.27*	-	28.8	0.40*	12.6	Fe^{3+} in *S*
S3-20	M	0.65*	-	24.0	0.40*	25.8	$Fe^{2.5+}$ in *S*
	M	0.27*	-	26.1	0.40*	41.7	Fe^{3+} in *S*
	Q	1.02*	1.22*	-	0.70*	4.1	Fe^{2+} in *W*
	Q	0.35	0.80	-	0.69	28.4	Fe^{3+} in *S* or
S3-30	M	0.38	0.01	21.1	0.41	100.0	Fe^{3+} in *S*
S4-30-500	M	0.32*	-	12.1	0.40*	34.6	Fe^{3+} in *S*
	Q	0.36	0.42	-	0.35	65.4	Fe^{3+} in *S*
S4-30-1000	M	0.37	- 0.22	51.7	0.25	29.4	Fe^{3+} in *H*
	Q	0.36	0.38	-	0.32	70.6	Fe^{3+} in *S*

Description: *W* = phase structurally similar to wüstite (FeO), *S* = phase structurally similar to *franklinite (*$ZnFe_2O_4$) or magnetite (Fe_3O_4), *H* = phase structurally similar to hematite (α-Fe_2O_3)
Errors: $\delta = \pm 0.01$ mm s^{-1}, $2\varepsilon = \pm 0.01$ mm s^{-1}, $B_{hf} = \pm 0.2$ T. Isomer shift is given relative to α-Fe.
* Imposed

Table 5

^{57}Fe Mössbauer parameters (20 °C) of the products obtained from the sample S4 and corresponding iron oxidation state identification.

Sample	Spectral line	δ (mm s^{-1})	Δ or 2ε (mm s^{-1})	B_{hf} or $\langle B_{hf} \rangle$ (T)	Γ (mm s^{-1})	Area (%)	Iron oxidation state
S4-0	M	0.00	-	33.0	0.27	100.0	Fe^0 in α-Fe
S4-5	M	0.01	-	32.8	0.25	70.1	Fe^0 in α-Fe
	Q	0.98	1.28	-	0.75	25.6	Fe^{2+} in *W*
	Q	0.28	0.67	-	0.40	4.3	Fe^{3+} in *W*
S4-9	M	0.01	-	32.9	0.30	40.9	Fe^0 in α-Fe
	Q	0.96	1.27	-	0.74	47.2	Fe^{2+} in *W*
	Q	0.28	0.67	-	0.29	11.9	Fe^{3+} in *W*
S4-14	M	0.04	-	32.1	0.33	13.0	Fe^0 in α-Fe
	Q	0.98	1.20	-	0.73	68.8	Fe^{2+} in *W*
	Q	0.32	0.66	-	0.50	18.2	Fe^{3+} in *W*
S4-20	M	0.65*	-	16.9	0.55	32.7	$Fe^{2.5+}$ in *S*
	M	0.28*	-	42.4	0.52	10.4	Fe^{3+} in *S*
	Q	0.98	1.11	-	0.94	36.6	Fe^{2+} in *W*
	Q	0.36	0.54	-	0.55	20.3	Fe^{3+} in *W* or *S*
S4-30	M	0.37	- 0.20	38.9	0.40	67.2	Fe^{3+} in *H*
	M	0.32*	-	26.0	0.40*	32.8	Fe^{3+} in *S*
S4-30-500	M	0.37	- 0.20	49.5	0.31	68.2	Fe^{3+} in *H*
	M	0.32*	-	24.7	0.40*	16.0	Fe^{3+} in *S*
	D	0.36	0.46	-	0.44	15.8	Fe^{3+} in *S*
S4-30-1000	M	0.37	- 0.22	51.6	0.28	77.1	Fe^{3+} in *H*
	D	0.35	0.40	-	0.32	22.9	Fe^{3+} in *S*

Description: *W* = phase structurally similar to wüstite (FeO), *S* = phase structurally similar to franklinite ($ZnFe_2O_4$) or magnetite (Fe_3O_4), *H* = phase structurally similar to hematite (α-Fe_2O_3)
Errors: δ = ± 0.01 mm s^{-1}, 2ε = ± 0.01 mm s^{-1}, B_{hf} = ± 0.2 T. Isomer shift is given relative to α-Fe.
*Imposed

Table 6

^{57}Fe Mössbauer parameters (20 °C) of the products obtained from the sample S5 and corresponding iron oxidation state identification.

Sample	Spectral line	δ (mm s^{-1})	Δ *or* 2ε (mm s^{-1})	B_{hf} or <B_{hf}> (T)	Γ (mm s^{-1})	Area (%)	Iron oxidation state
S5-0	M	0.00	-	33.0	0.27	100.0	Fe^{0} in α-Fe
S5-5	M	0.00	-	33.3	0.25	85.6	Fe^{0} in α-Fe
	Q	0.95	1.35	-	0.84	11.2	Fe^{2+} in *W*
	Q	0.27	0.75	-	0.43	3.2	Fe^{3+} in *W*
S5-9	M	0.00	-	33.1	0.28	57.1	Fe^{0} in α-Fe
	Q	0.95	1.22	-	0.77	35.6	Fe^{2+} in *W*
	Q	0.26	0.58	-	0.41	7.3	Fe^{3+} in *W*
S5-14	M	0.00	-	32.4	0.33	20.4	Fe^{0} in α-Fe
	S	- 0.06*	-	-	0.40*	2.7	Fe^{0} in γ-Fe
	Q	0.95	1.19	-	0.73	63.1	Fe^{2+} in *W*
	Q	0.25	0.60	-	0.51	13.8	Fe^{3+} in *W*
S5-20	M	0.65*	-	31.2	0.48	41.9	$Fe^{2.5+}$ in *S*
	M	0.27*	-	24.5	0.40	23.2	Fe^{3+} in *S*
	Q	0.98	1.11	-	0.94	27.7	Fe^{2+} in *W*
	Q	0.26	0.40	-	0.50	7.2	Fe^{3+} in *W*
S5-30	M	0.37	- 0.20	43.8	0.25	78.0	Fe^{3+} in *H*
	M	0.65*	-	40.0	1.00*	9.3	$Fe^{2.5+}$ in *S*
	M	0.27*	-	46.0	1.00*	7.7	Fe^{3+} in *S*
	Q	0.33	0.60	-	0.92	5.0	Fe^{3+} S
S5-30-500	M	0.37	- 0.21	50.0	0.28	90.7	Fe^{3+} in *H*
		0.32*	-	23.5	0.40*	9.3	Fe^{3+} in *S*
S5-30-1000	M	0.37	- 0.22	51.1	0.24	100	Fe^{3+} in *H*

Description: *W* = phase structurally similar to wüstite (FeO), *S* = phase structurally similar to magnetite (Fe_3O_4), *H* = phase structurally similar to hematite (α-Fe_2O_3)
Errors: $\delta = \pm 0.01$ mm s^{-1}, $2\varepsilon = \pm 0.01$ mm s^{-1}, $B_{hf} = \pm 0.2$ T. Isomer shift is given relative to α-Fe.
*Imposed

Section 5 *FE-SEM analysis*

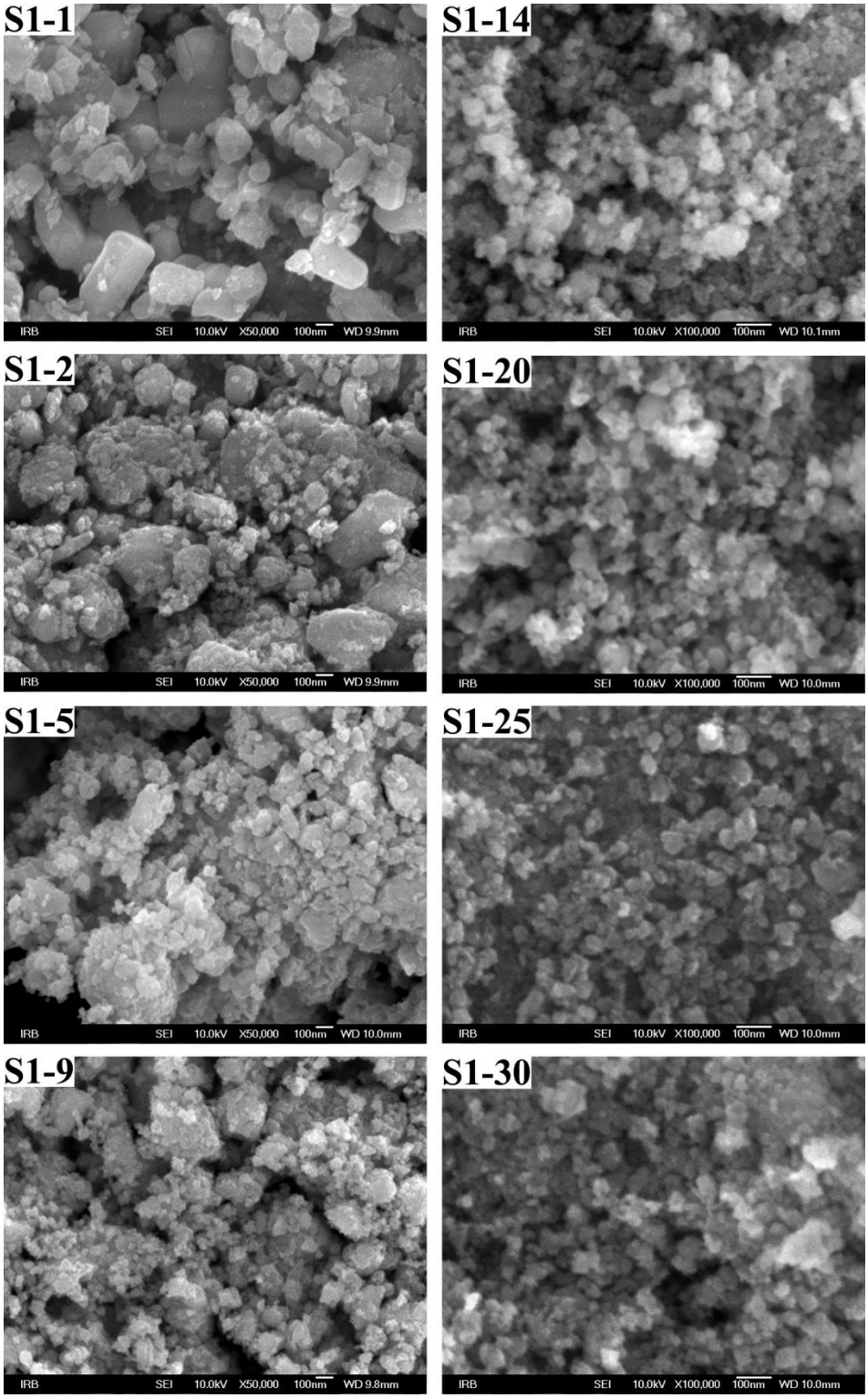

Fig 14 FE-SEM micrographs of the products obtained after 1 h, 2 h, 5 h, 9 h, 14 h, 20 h, 25 h and 30 h of high-energy ball-milling of pure zincite (sample S1-0).

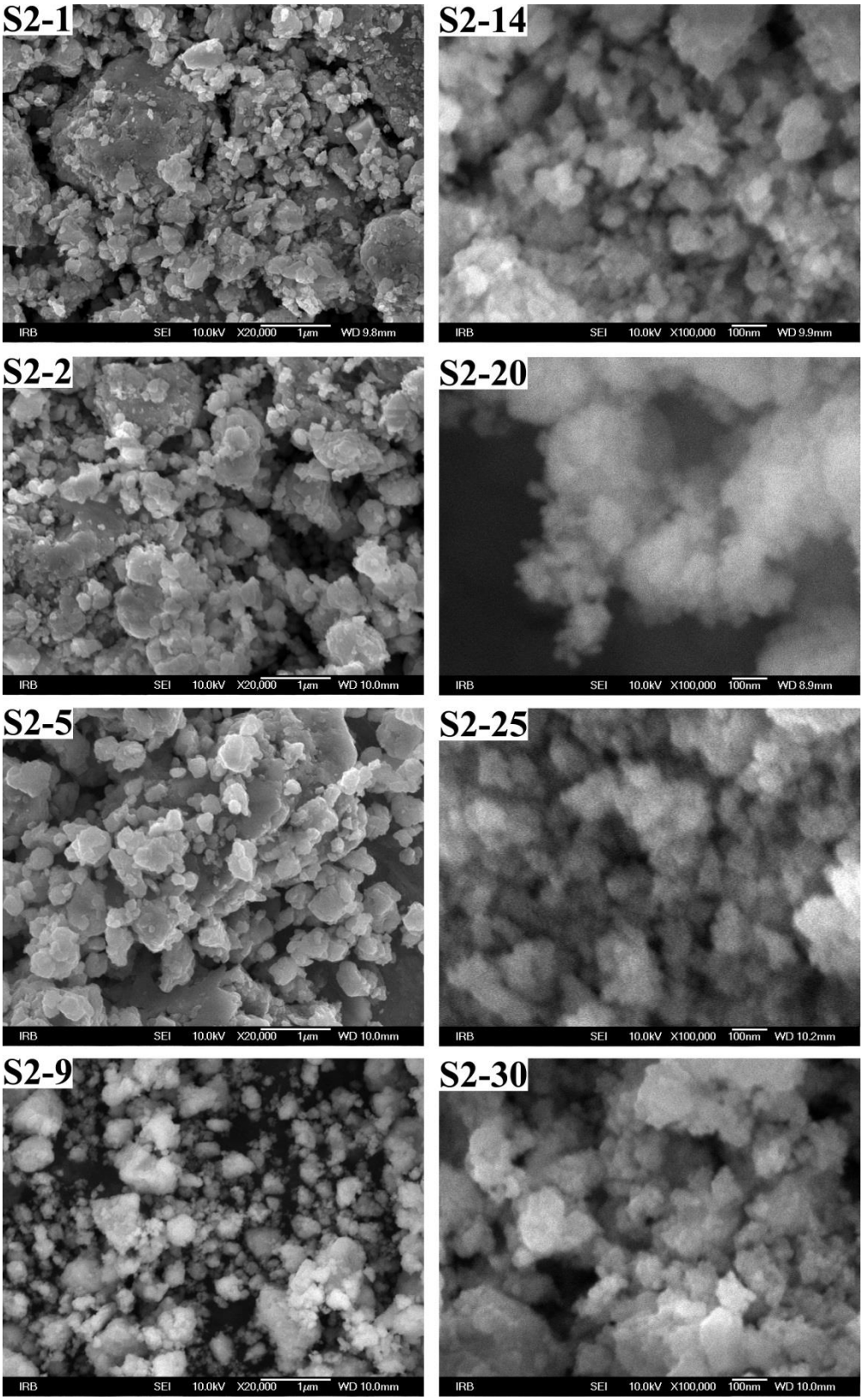

Fig 15 FE-SEM micrographs of the products obtained after 1 h, 2 h, 5 h, 9 h, 14 h, 20 h, 25 h and 30 h of high-energy ball-milling of the powder mixtures of zincite and iron with weight ratio 3:1 (sample S2-0)

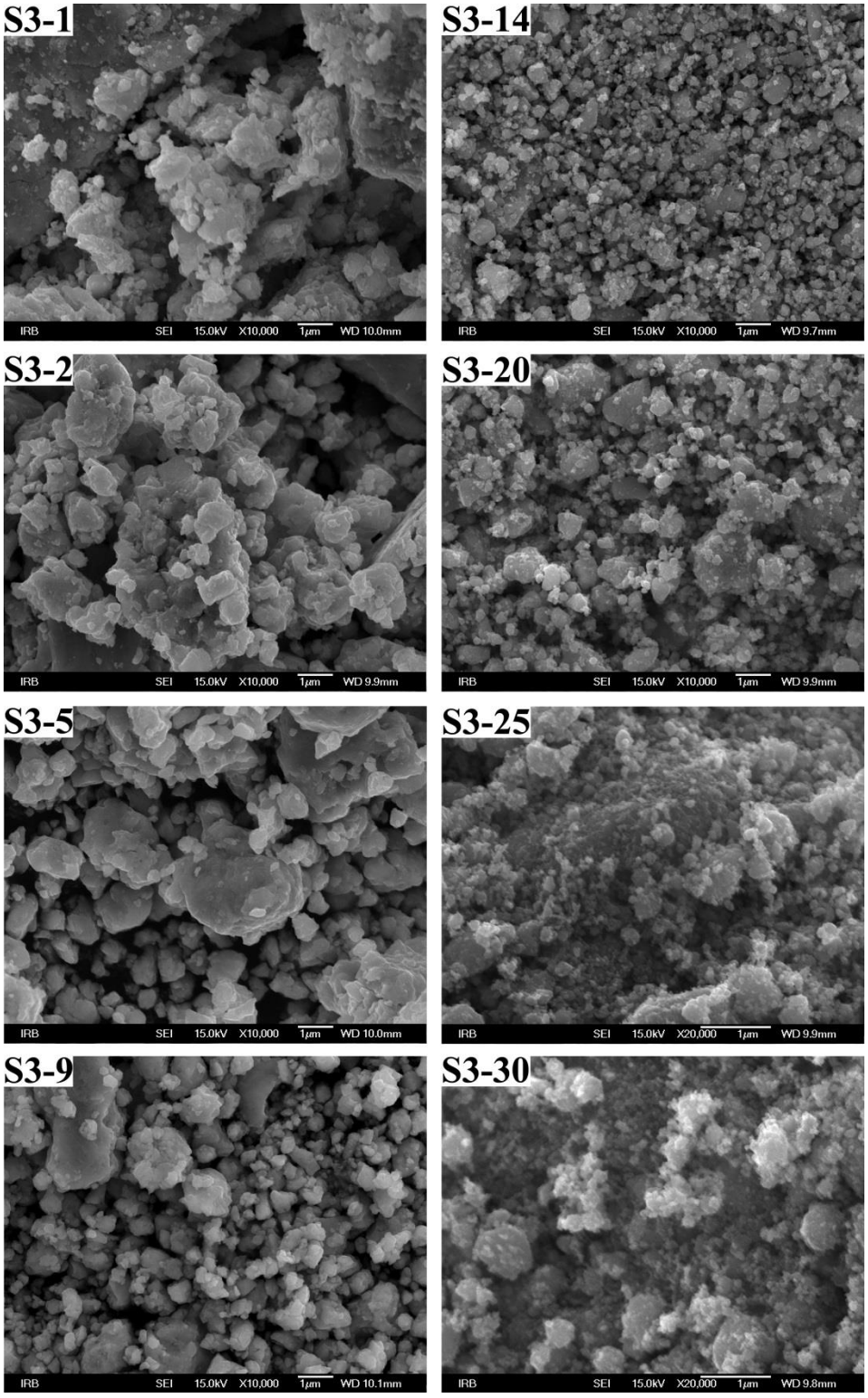

Fig 16 FE-SEM micrographs of the products obtained after 1 h, 2 h, 5 h, 9 h, 14 h, 20 h, 25 h and 30 h of high-energy ball-milling of the powder mixtures of zincite and iron with weight ratio 1:1 (sample S3-0).

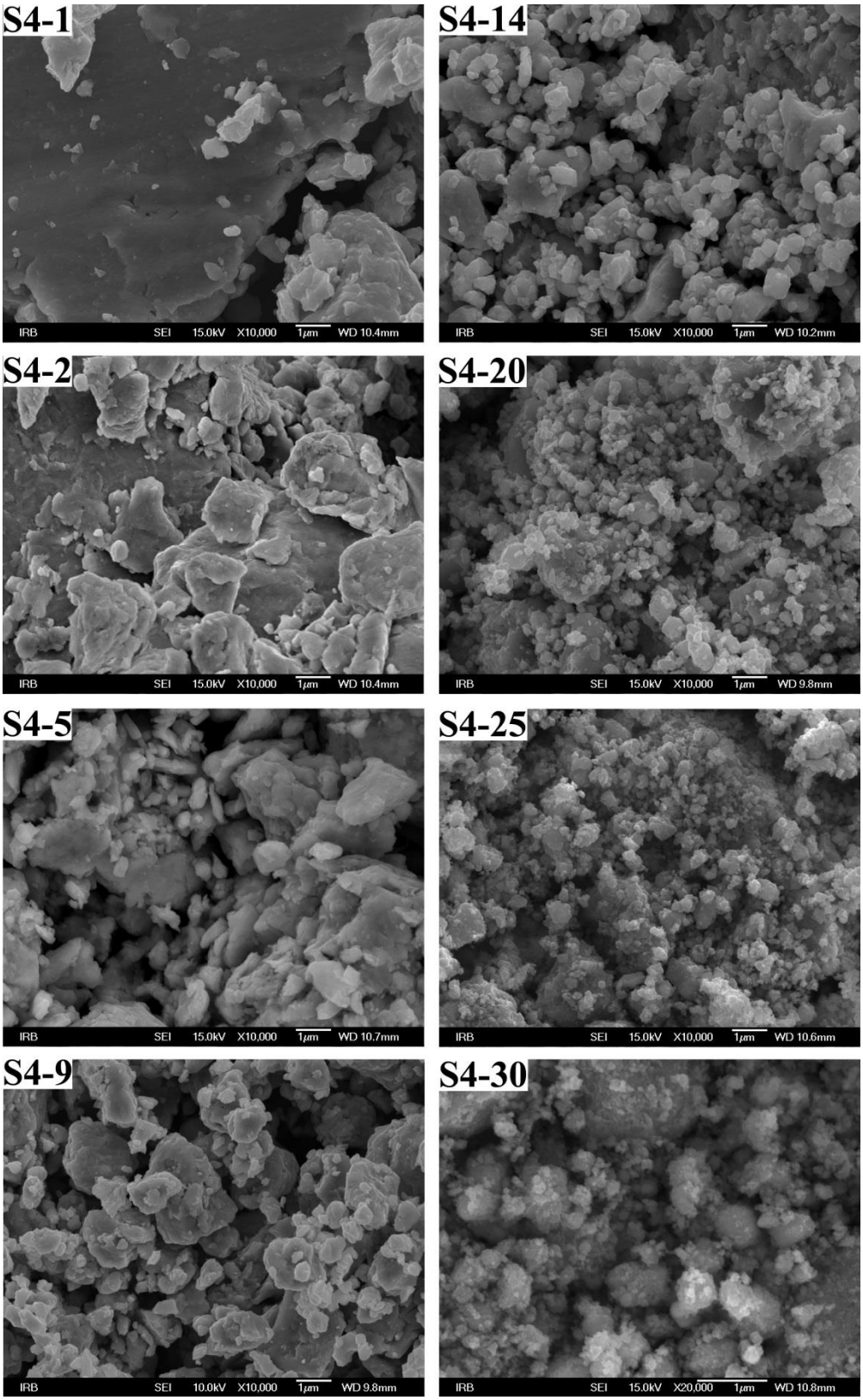

Fig 17 FE-SEM micrographs of the products obtained after 1 h, 2 h, 5 h, 9 h, 14 h, 20 h, 25 h and 30 h of high-energy ball-milling of the powder mixtures of zincite and iron with weight ratio 1:3 (sample S4-0).

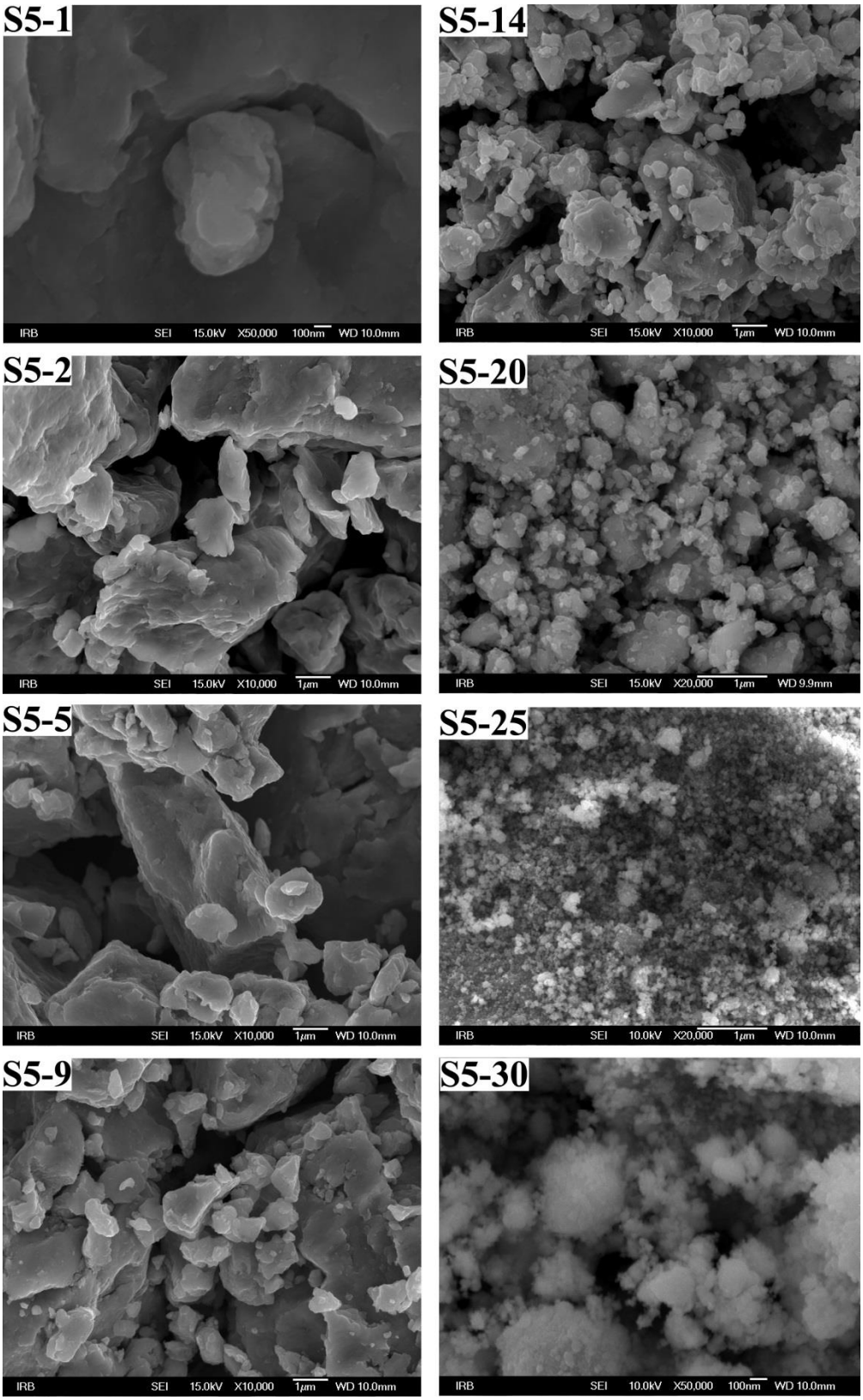

Fig 18 FE-SEM micrographs of the products obtained after 1 h, 2 h, 5 h, 9 h, 14 h, 20 h, 25 h and 30 h of high-energy ball-milling of pure iron (sample S5-0).

Section 6 *EDS analysis*

The results of elemental analysis of the milled samples were based on several (at least three) independent EDS measurements performed at low magnification.

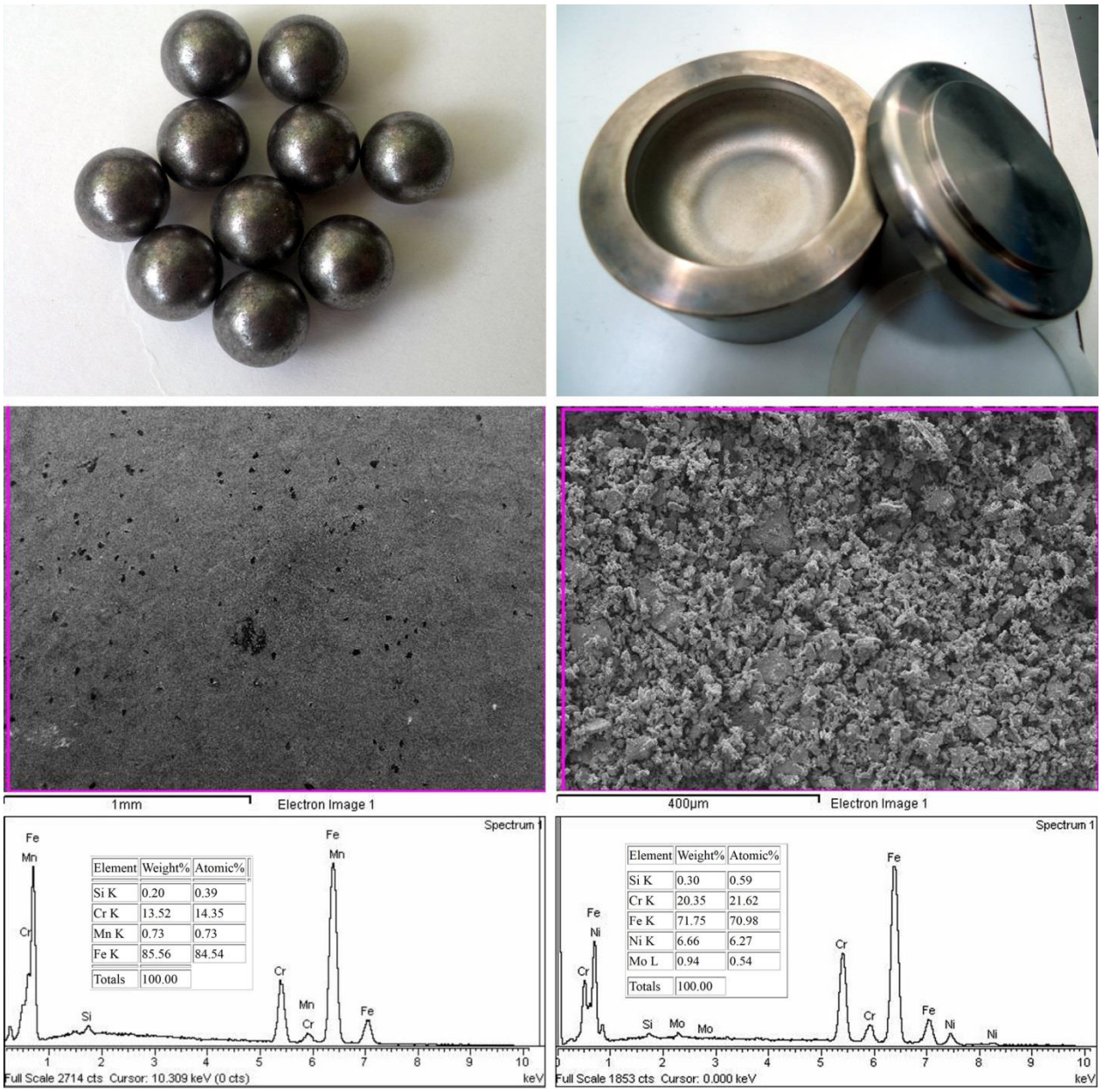

Fig. 19 FE-SEM micrographs and the corresponding EDS spectra of milling balls (left) and steel chips coming from milling vial (right). Inset tables show the results of elemental analysis.

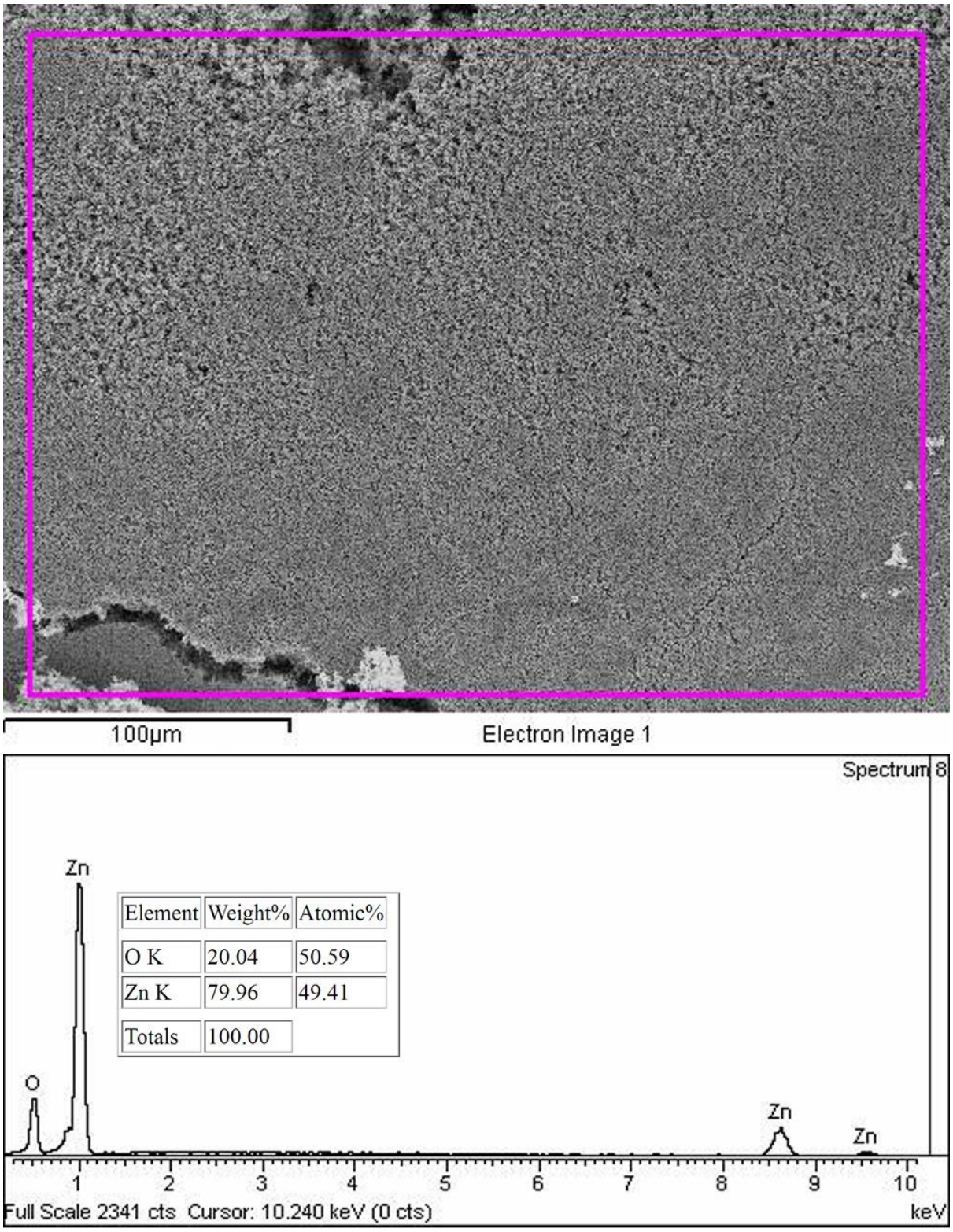

Fig. 20 FE-SEM micrograph of starting zincite powder (sample S1-0) obtained at 300 × magnification (top) and the corresponding EDS spectrum (bottom). Inset table shows the results of elemental analysis.

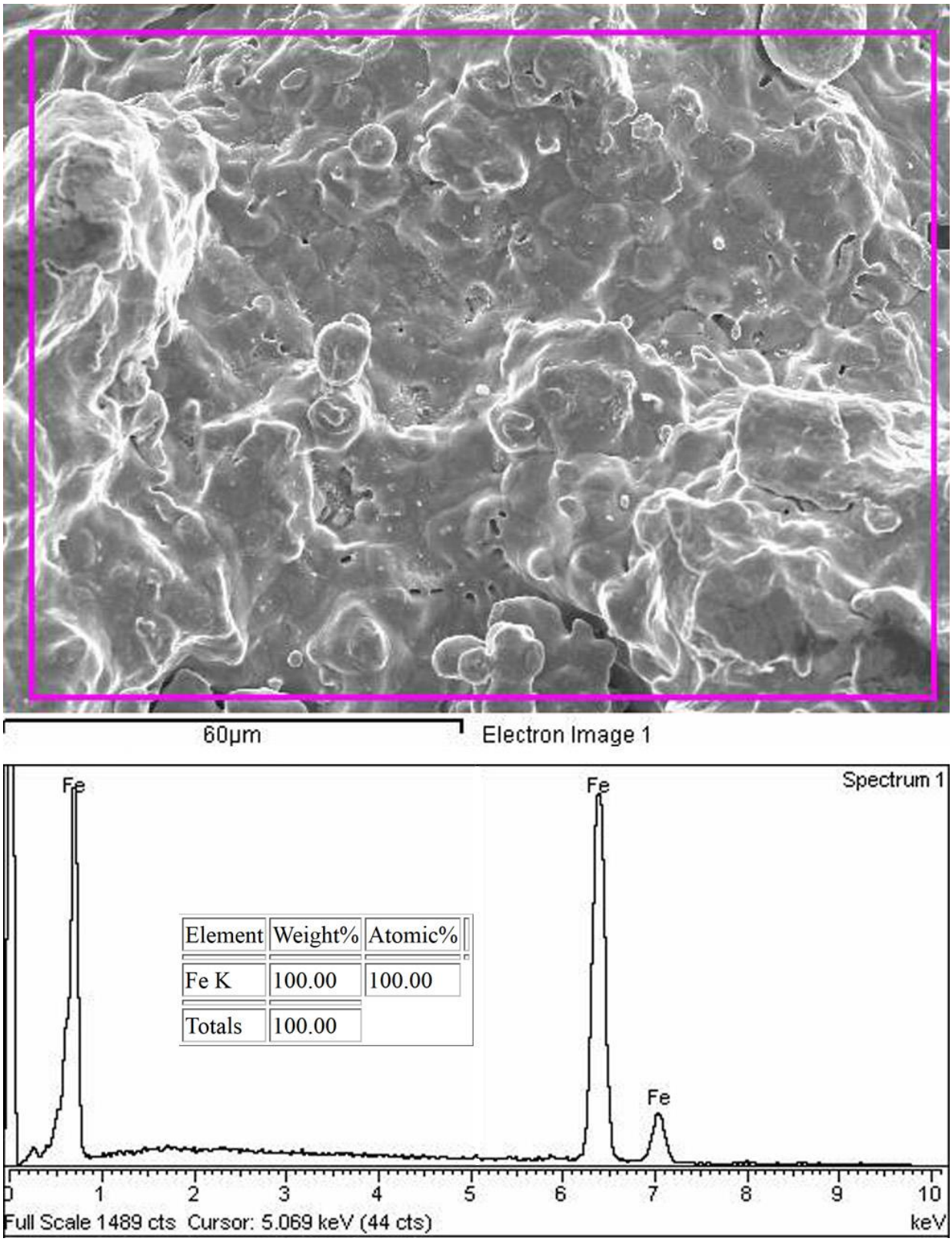

Fig. 21 FE-SEM micrograph of starting iron powder (sample S5-0) obtained at 800 × magnification (top) and the corresponding EDS spectrum (bottom). Inset table shows the results of elemental analysis.

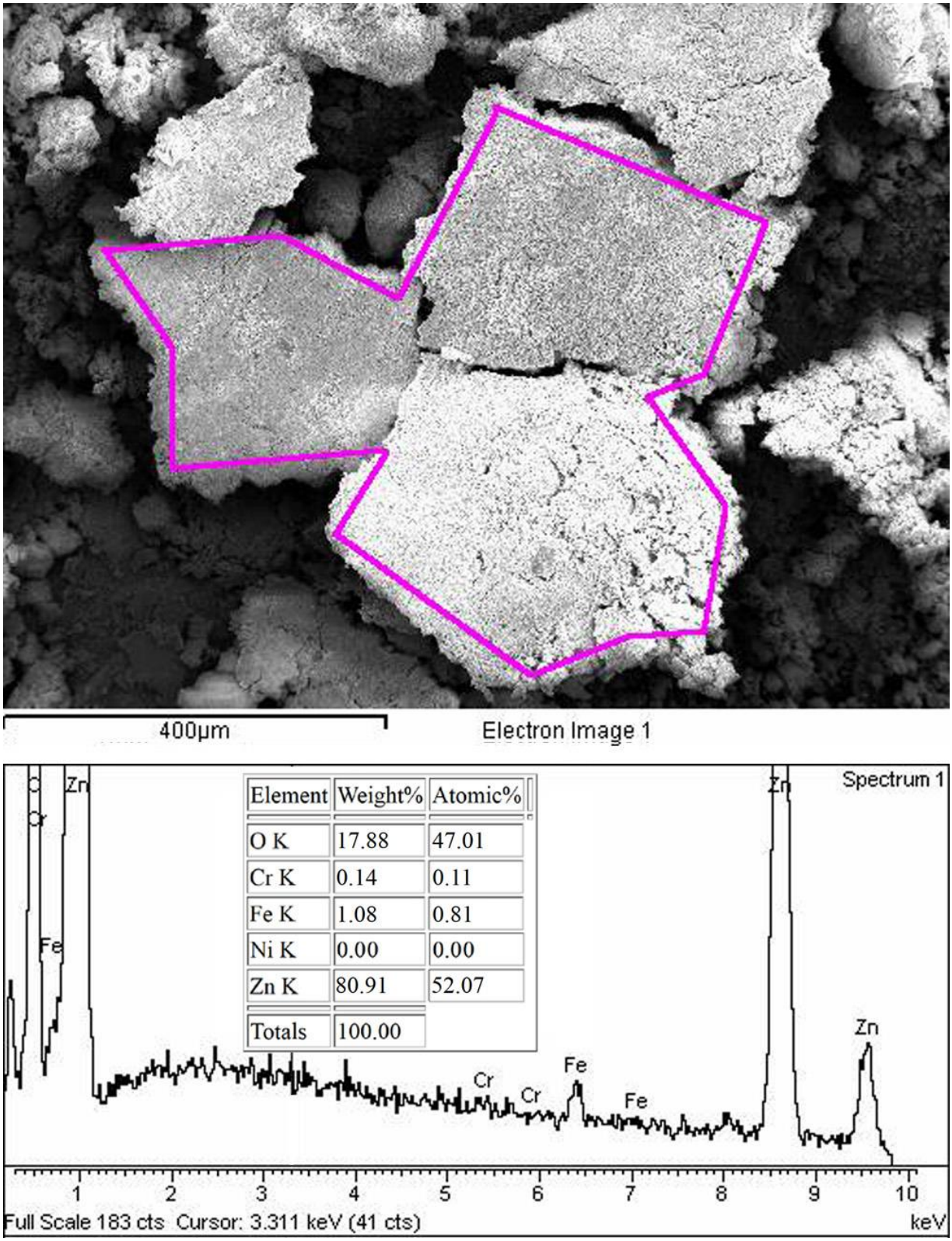

Fig. 22 FE-SEM micrograph of sample S1-1 obtained at 100 × magnification (top) and the corresponding EDS spectrum (bottom). Inset table shows the results of elemental analysis.

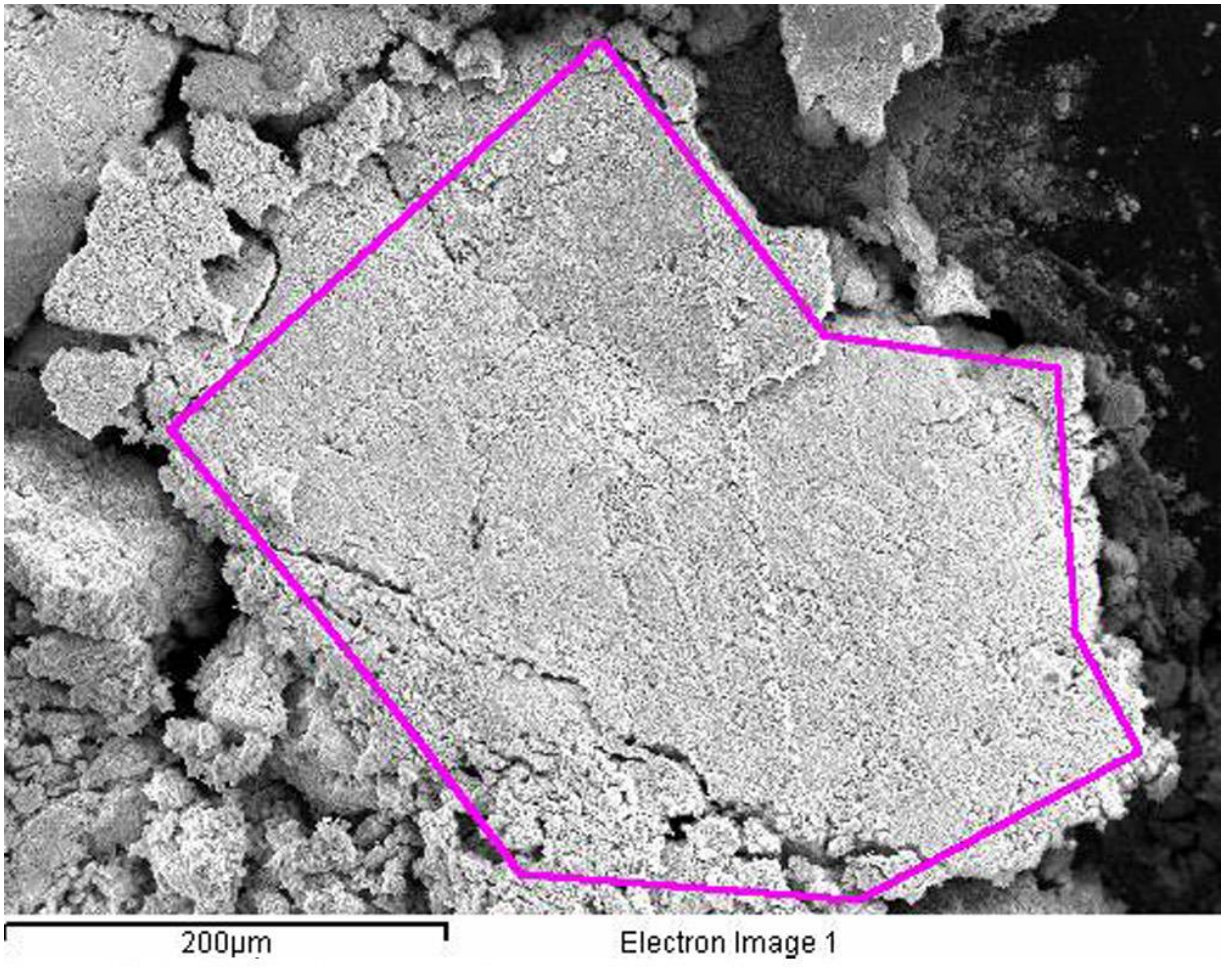

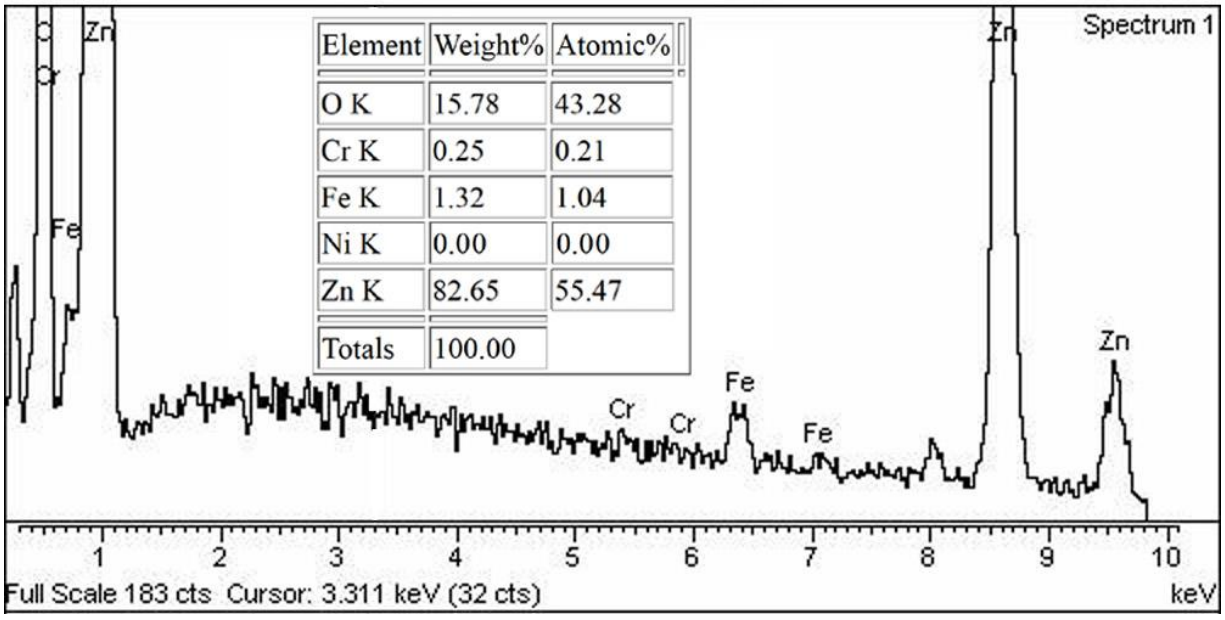

Element	Weight%	Atomic%
O K	15.78	43.28
Cr K	0.25	0.21
Fe K	1.32	1.04
Ni K	0.00	0.00
Zn K	82.65	55.47
Totals	100.00	

Fig. 23 FE-SEM micrograph of sample S1-2 obtained at 180 × magnification (top) and the corresponding EDS spectrum (bottom). Inset table shows the results of elemental analysis.

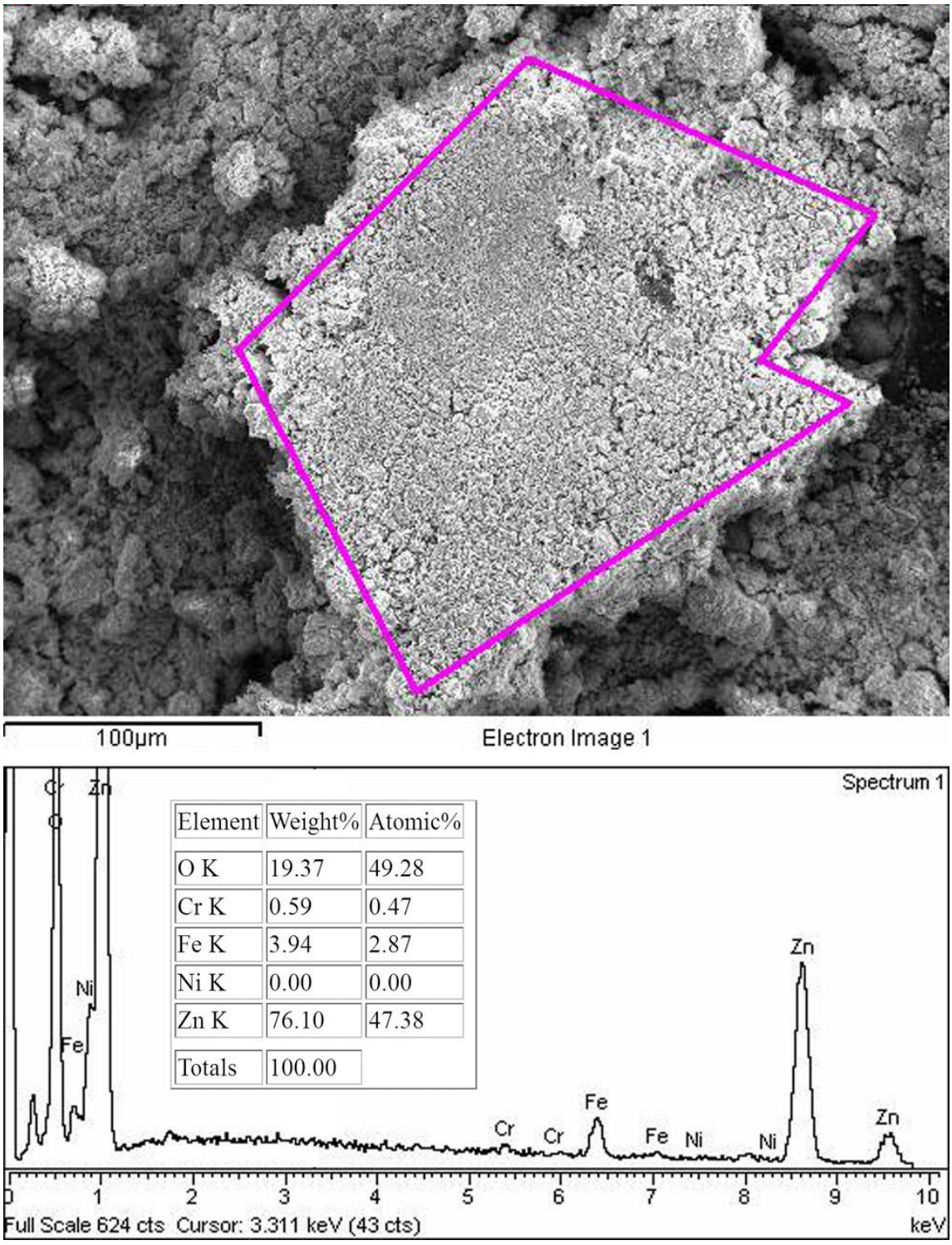

Fig. 24 FE-SEM micrograph of sample S1-5 obtained at 270 × magnification (top) and the corresponding EDS spectrum (bottom). Inset table shows the results of elemental analysis.

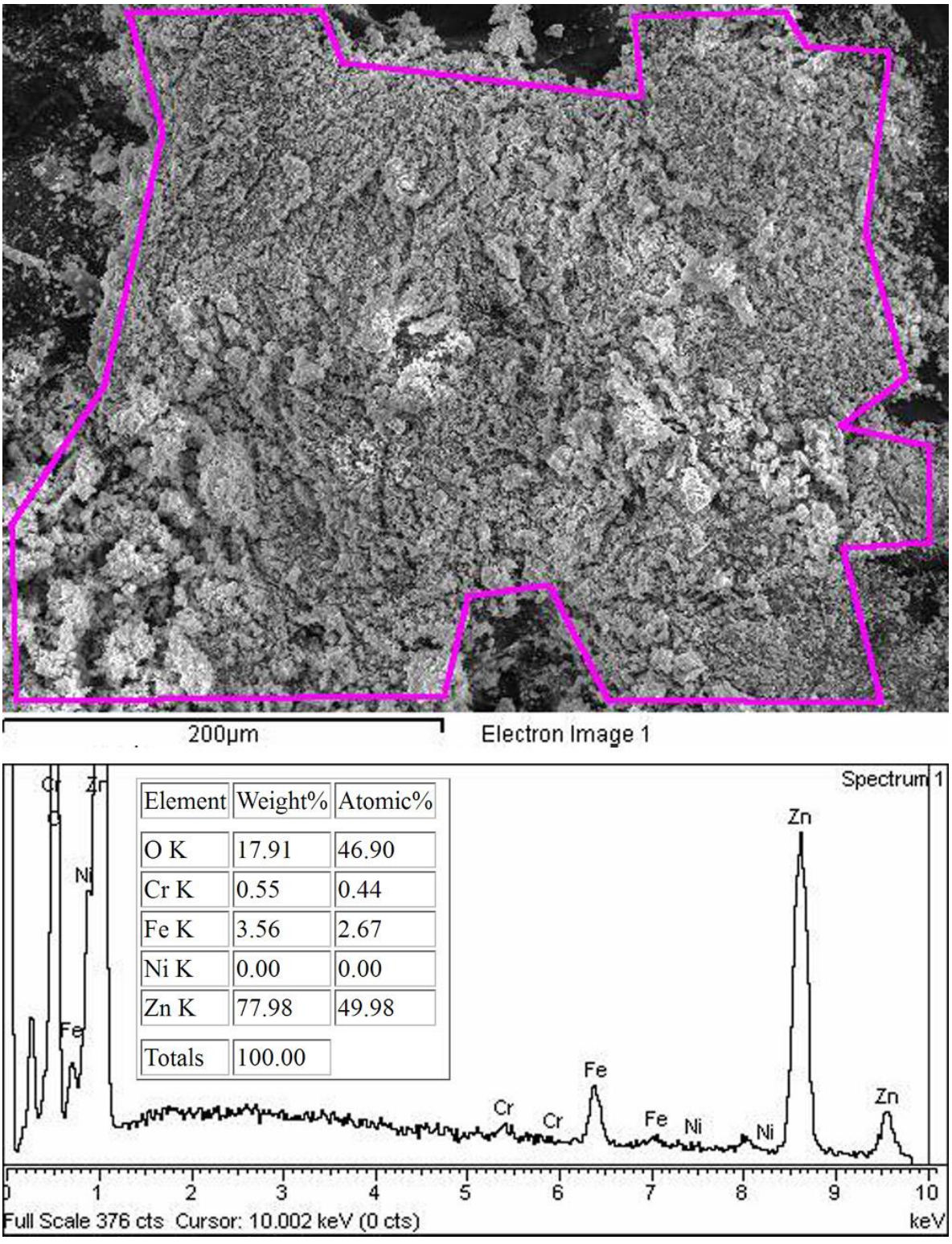

Fig. 25 FE-SEM micrograph of sample S1-9 obtained at 230 × magnification (top) and the corresponding EDS spectrum (bottom). Inset table shows the results of elemental analysis.

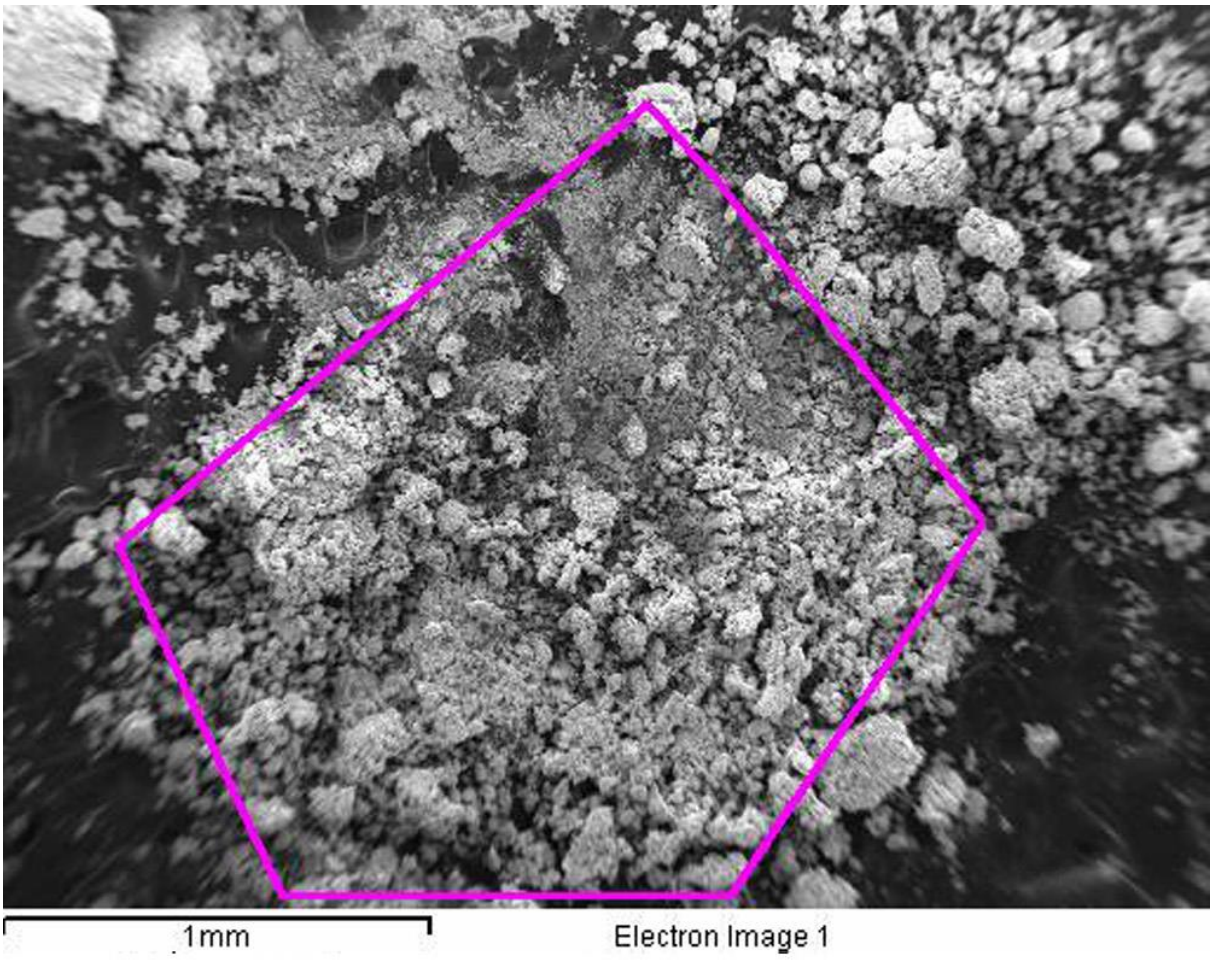

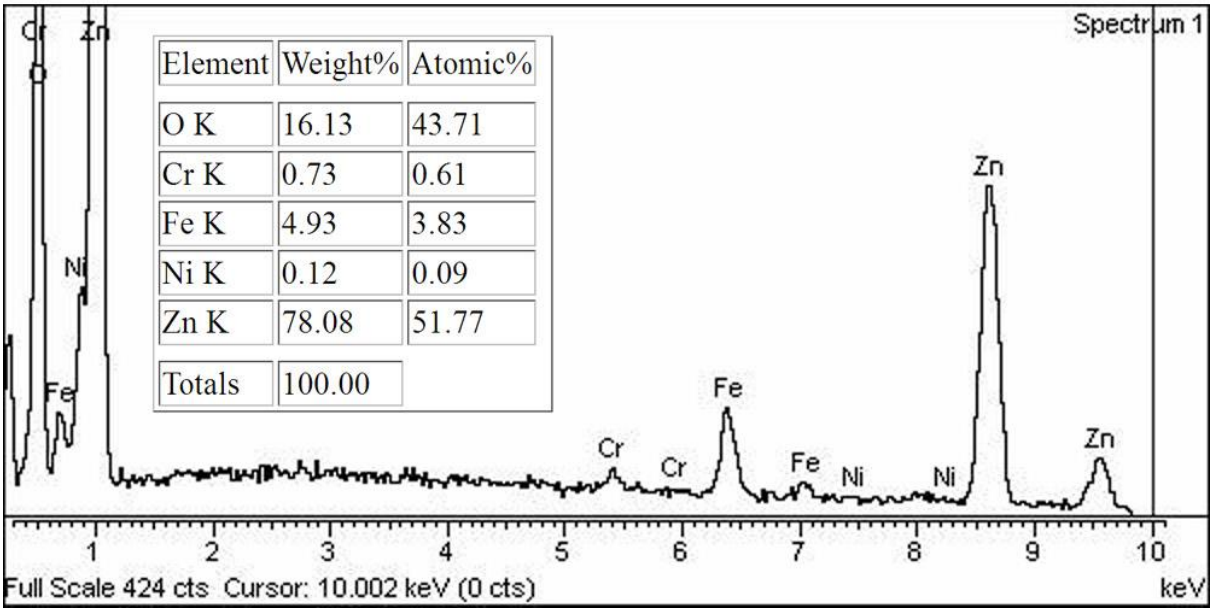

Element	Weight%	Atomic%
O K	16.13	43.71
Cr K	0.73	0.61
Fe K	4.93	3.83
Ni K	0.12	0.09
Zn K	78.08	51.77
Totals	100.00	

Fig. 26 FE-SEM micrograph of sample S1-14 obtained at 35 × magnification (top) and the corresponding EDS spectrum (bottom). Inset table shows the results of elemental analysis.

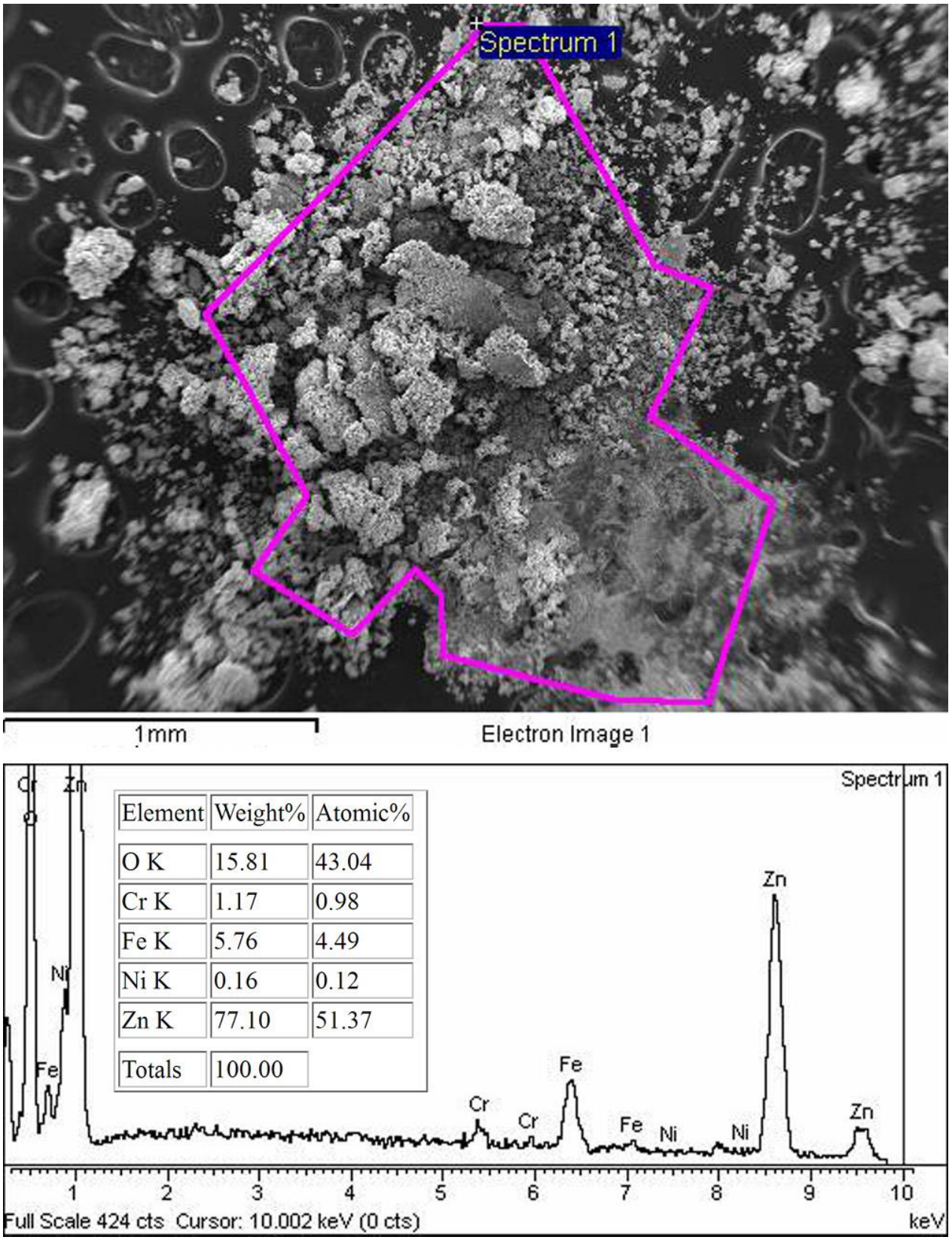

Fig. 27 FE-SEM micrograph of sample S1-20 obtained at 33 × magnification (top) and the corresponding EDS spectrum (bottom). Inset table shows the results of elemental analysis.

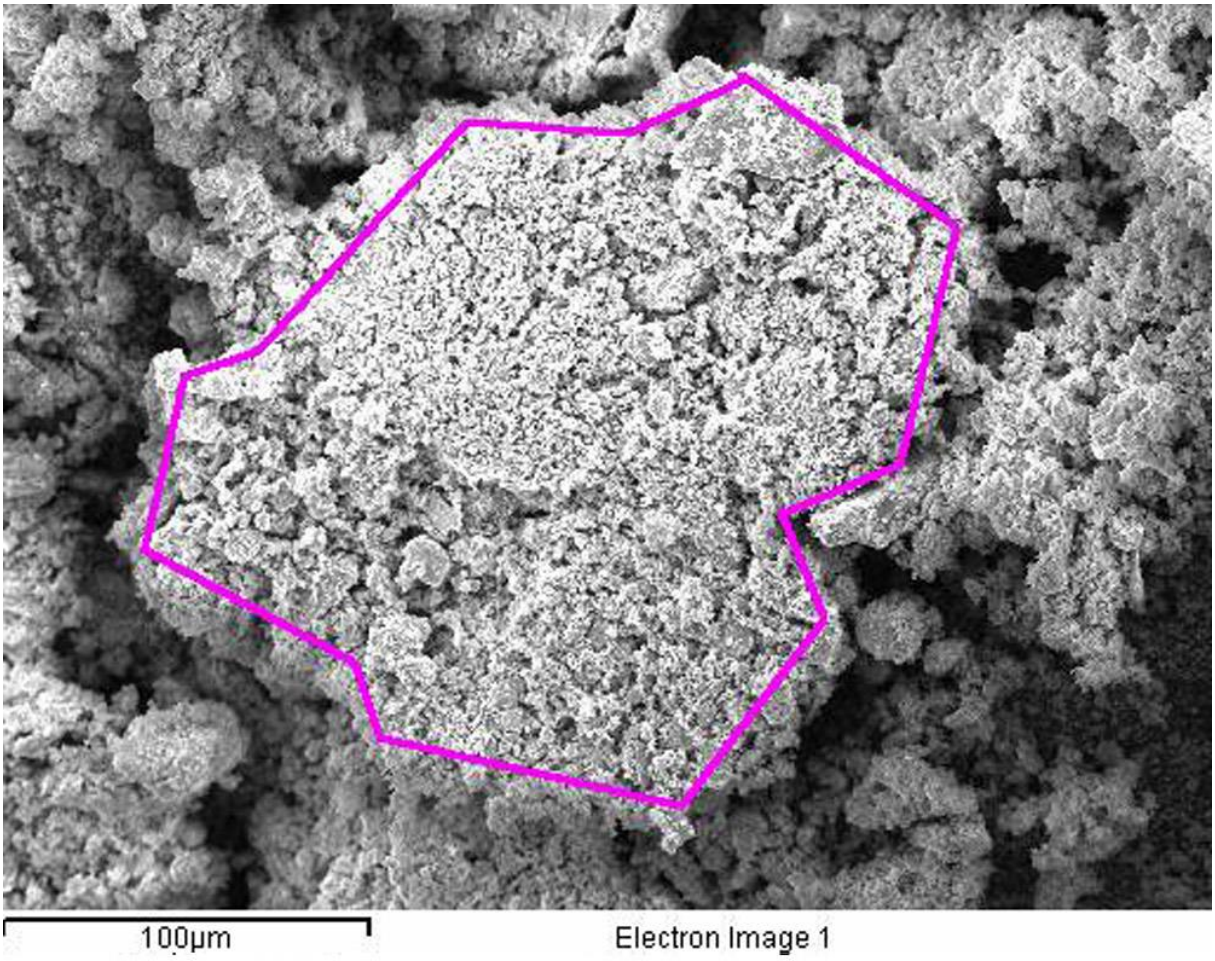

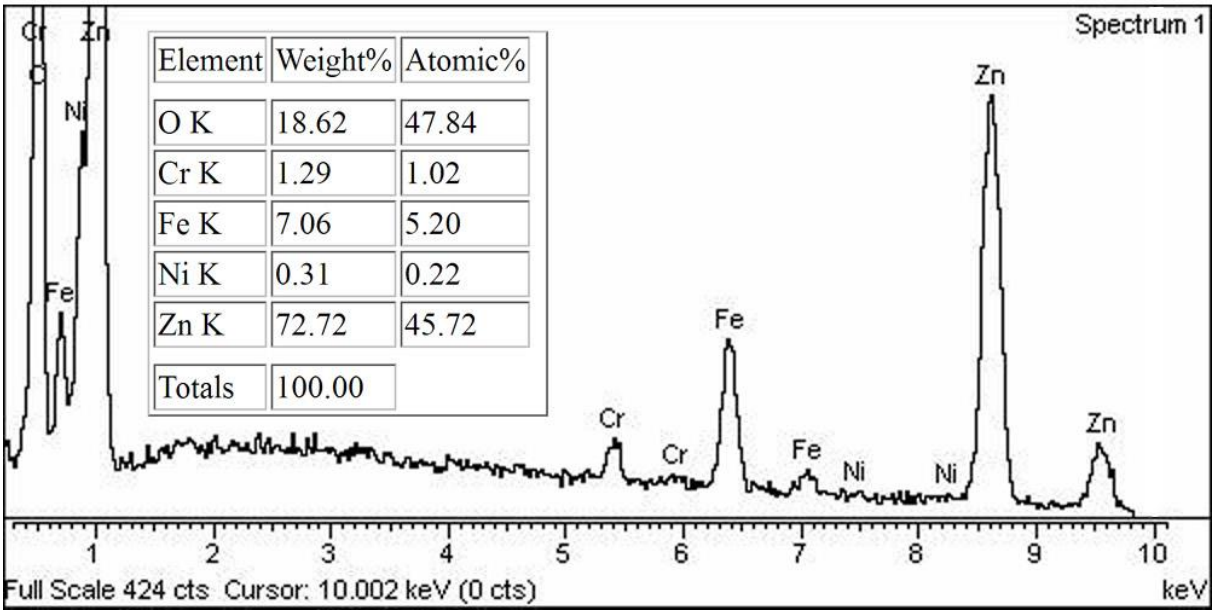

Element	Weight%	Atomic%
O K	18.62	47.84
Cr K	1.29	1.02
Fe K	7.06	5.20
Ni K	0.31	0.22
Zn K	72.72	45.72
Totals	100.00	

Fig. 28 FE-SEM micrograph of sample S1-25 obtained at 300 × magnification (top) and the corresponding EDS spectrum (bottom). Inset table shows the results of elemental analysis.

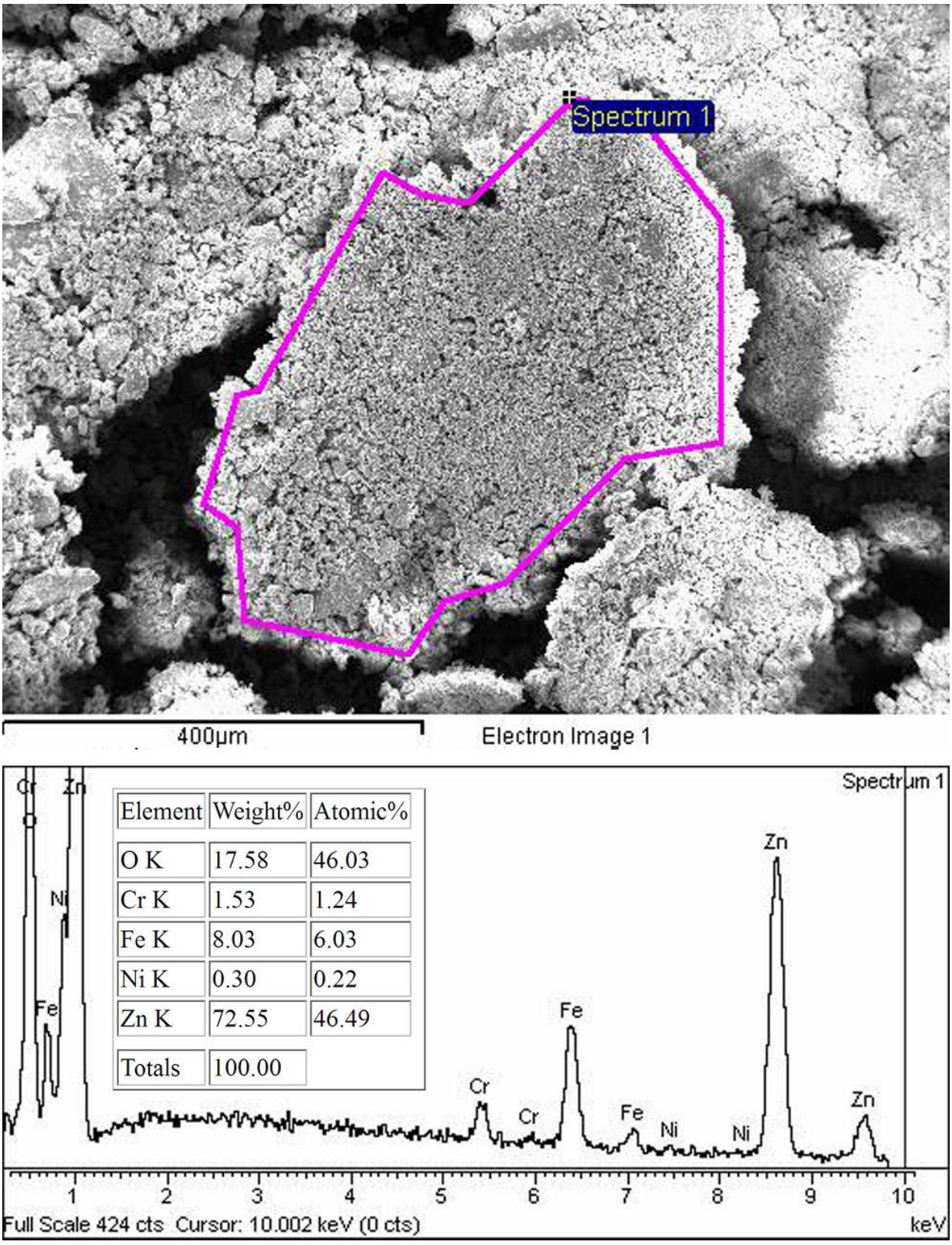

Fig. 29 FE-SEM micrograph of sample S1-30 obtained at 110 × magnification (top) and the corresponding EDS spectrum (bottom). Inset table shows the results of elemental analysis.

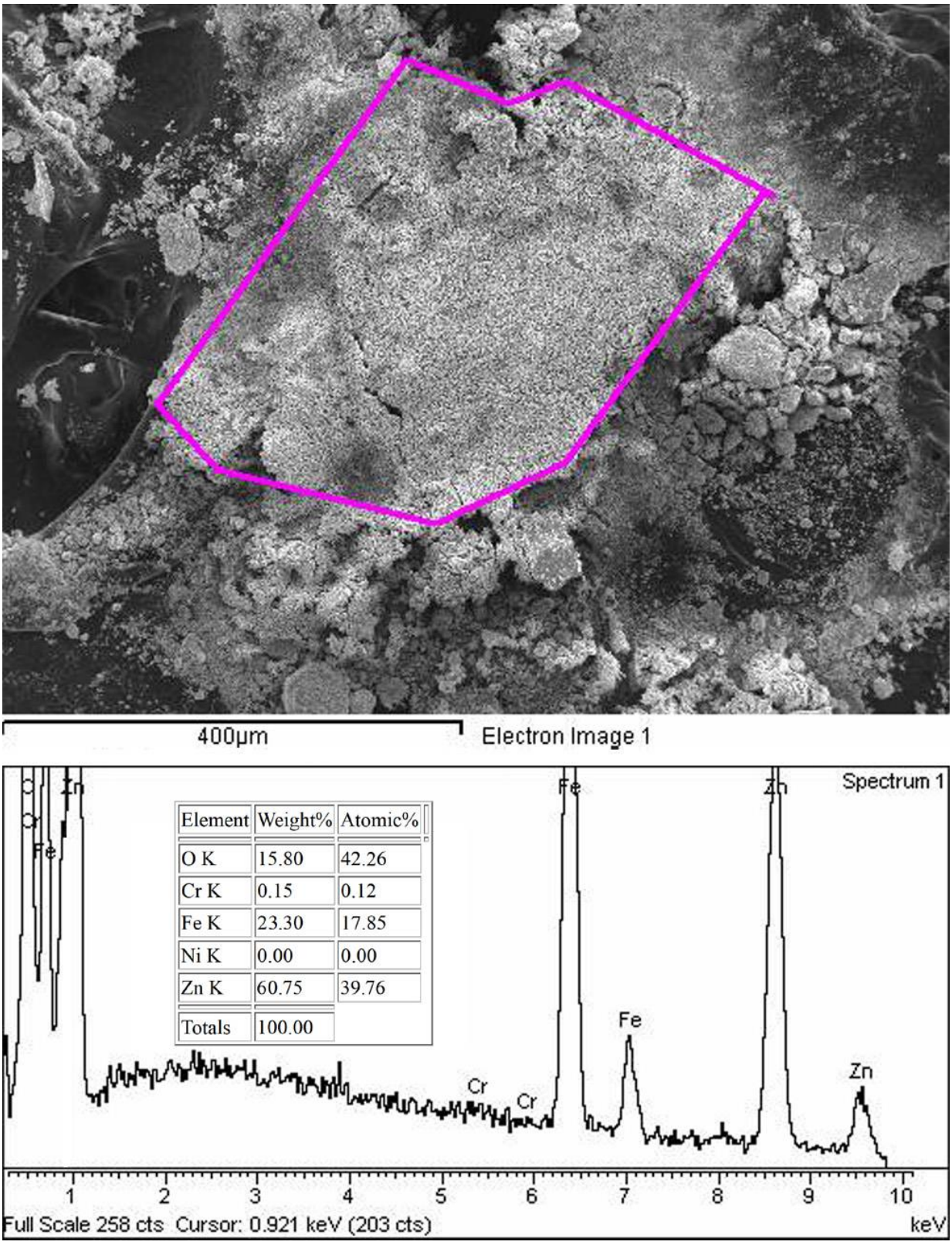

Fig. 30 FE-SEM micrograph of sample S2-1 obtained at 120 × magnification (top) and the corresponding EDS spectrum (bottom). Inset table shows the results of elemental analysis.

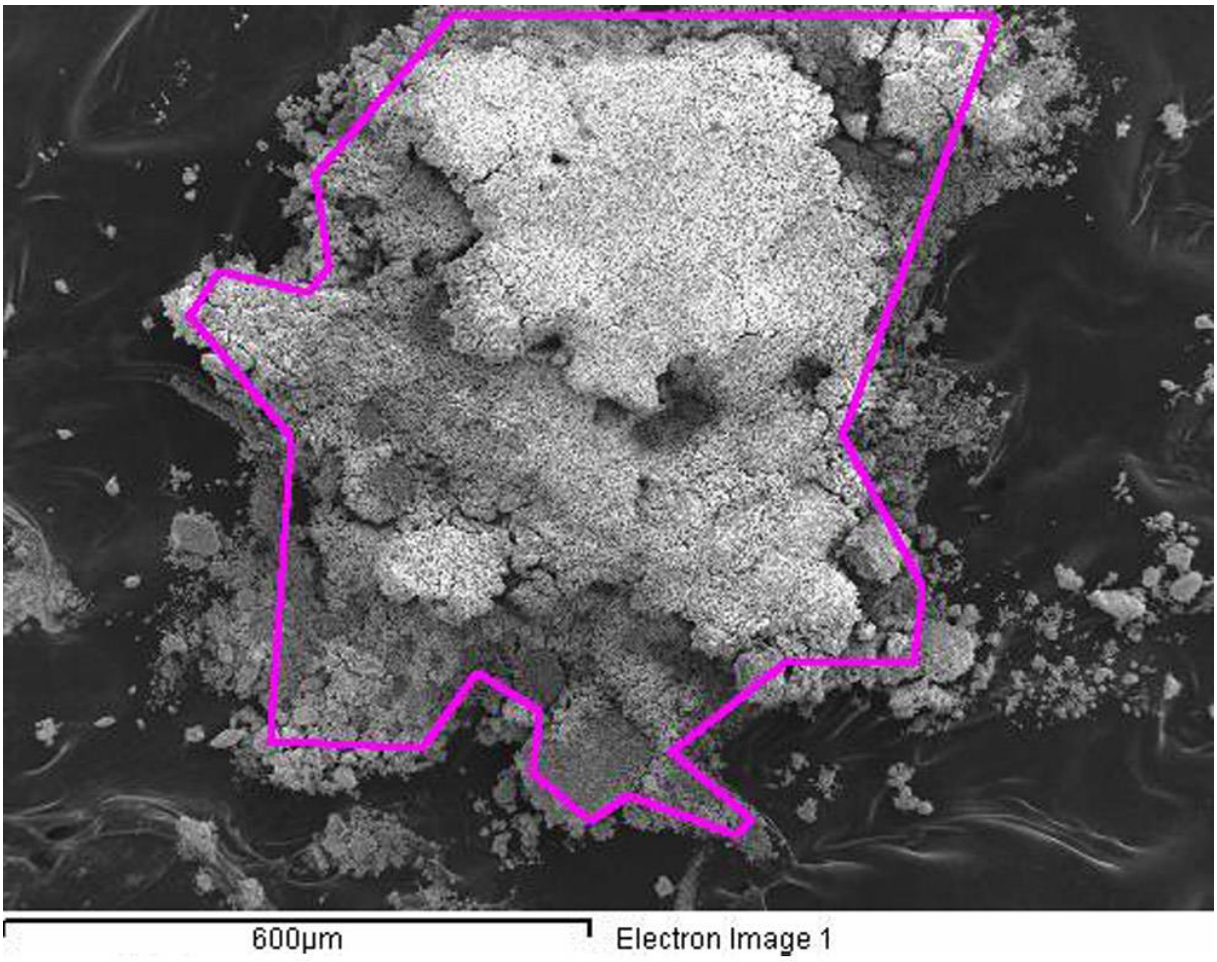

Element	Weight%	Atomic%
O K	15.15	40.91
Cr K	0.35	0.29
Fe K	26.00	20.12
Ni K	0.00	0.00
Zn K	58.50	38.68
Totals	100.00	

Fig. 31 FE-SEM micrograph of sample S2-2 obtained at 80 × magnification (top) and the corresponding EDS spectrum (bottom). Inset table shows the results of elemental analysis.

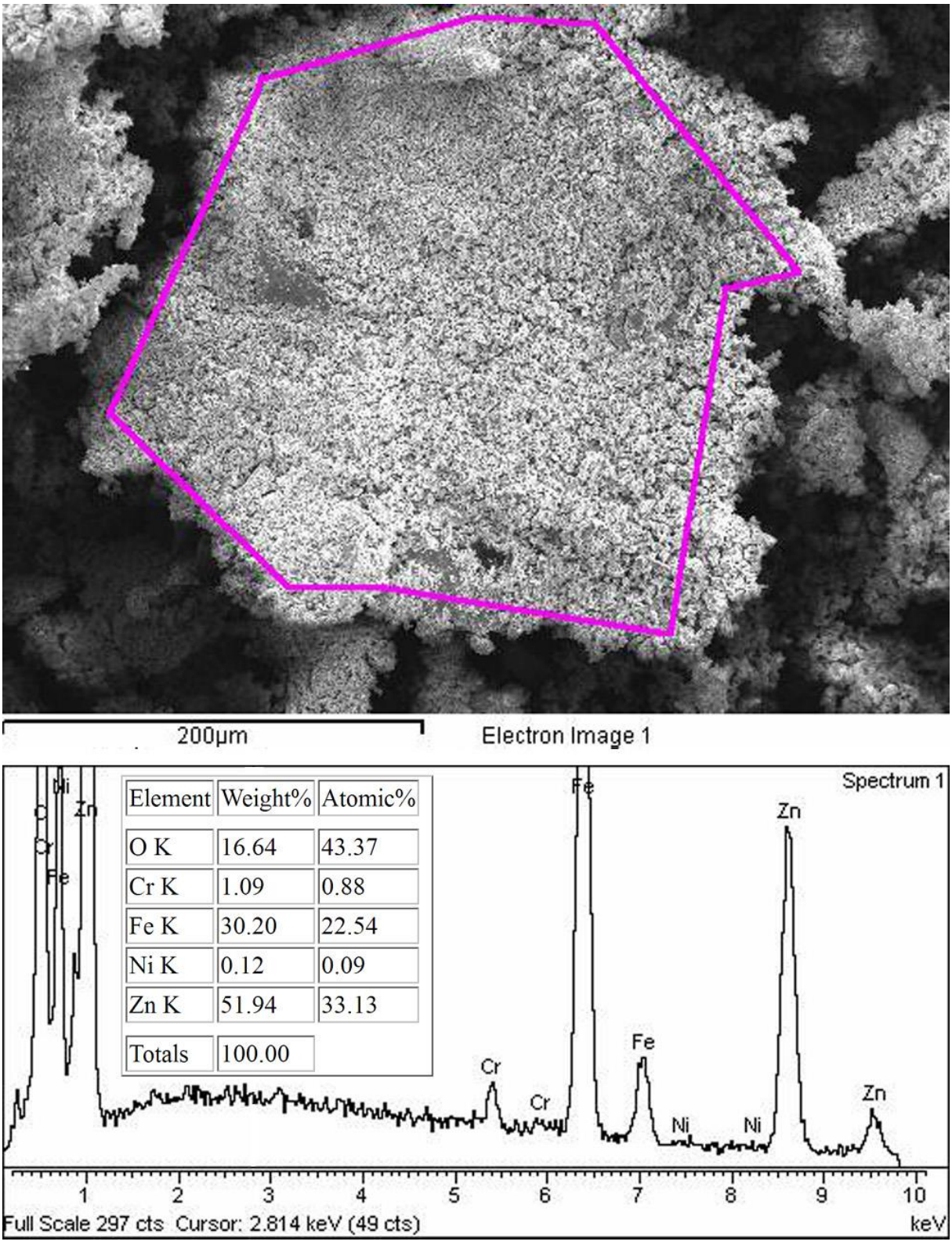

Fig. 32 FE-SEM micrograph of sample S2-5 obtained at 220 × magnification (top) and the corresponding EDS spectrum (bottom). Inset table shows the results of elemental analysis.

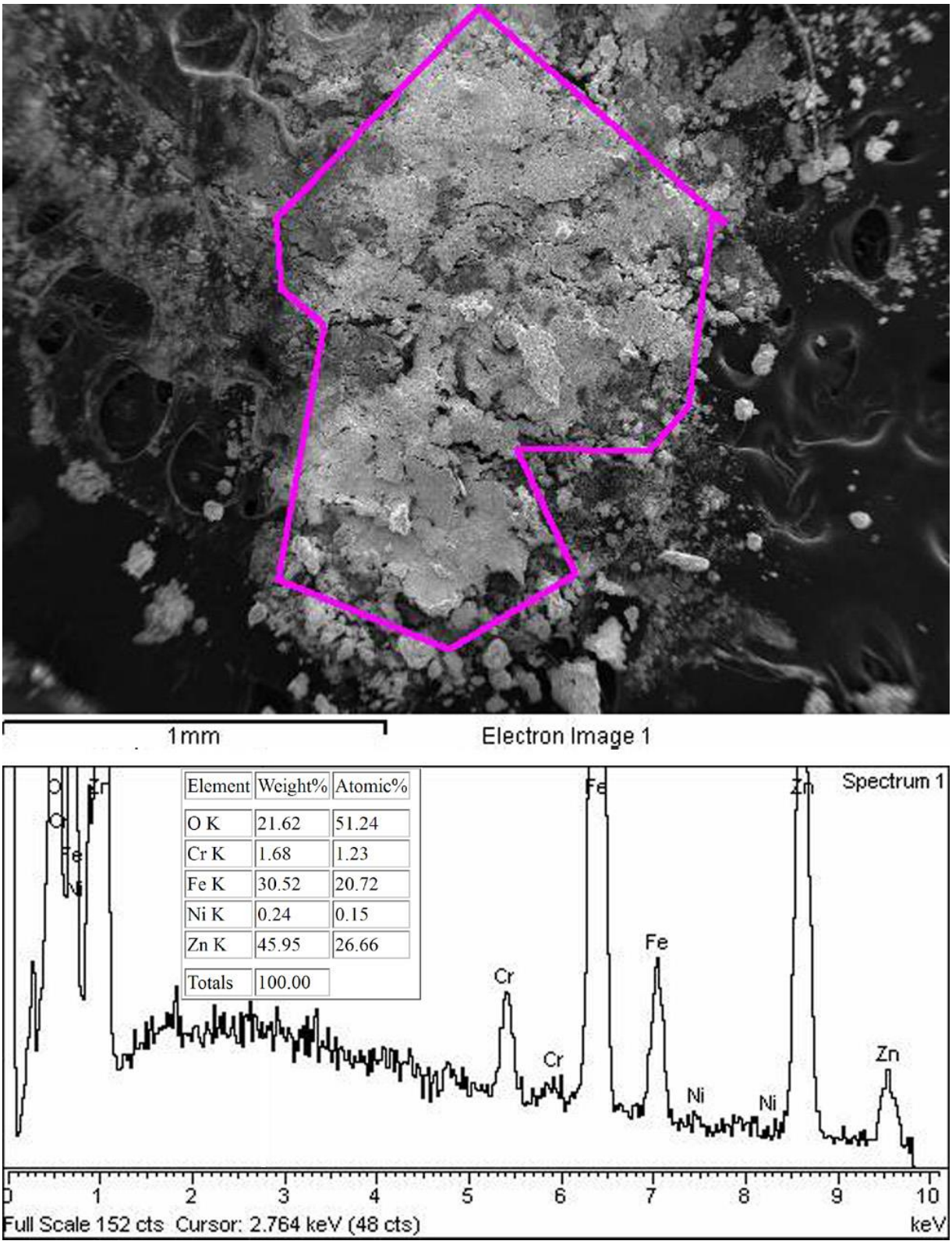

Fig. 33 FE-SEM micrograph of sample S2-9 obtained at 40 × magnification (top) and the corresponding EDS spectrum (bottom). Inset table shows the results of elemental analysis.

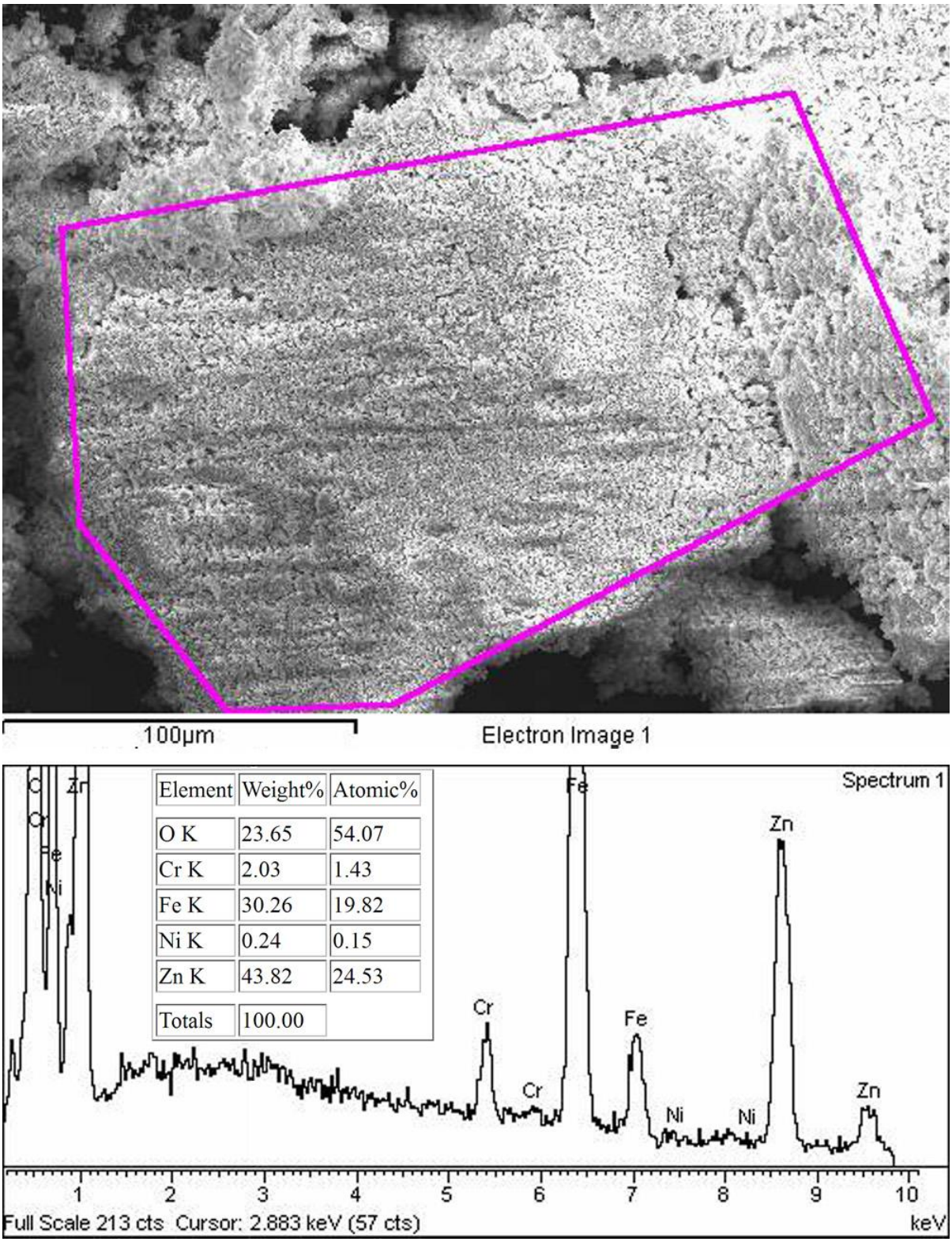

Fig. 34 FE-SEM micrograph of sample S2-14 obtained at 370 × magnification (top) and the corresponding EDS spectrum (bottom). Inset table shows the results of elemental analysis.

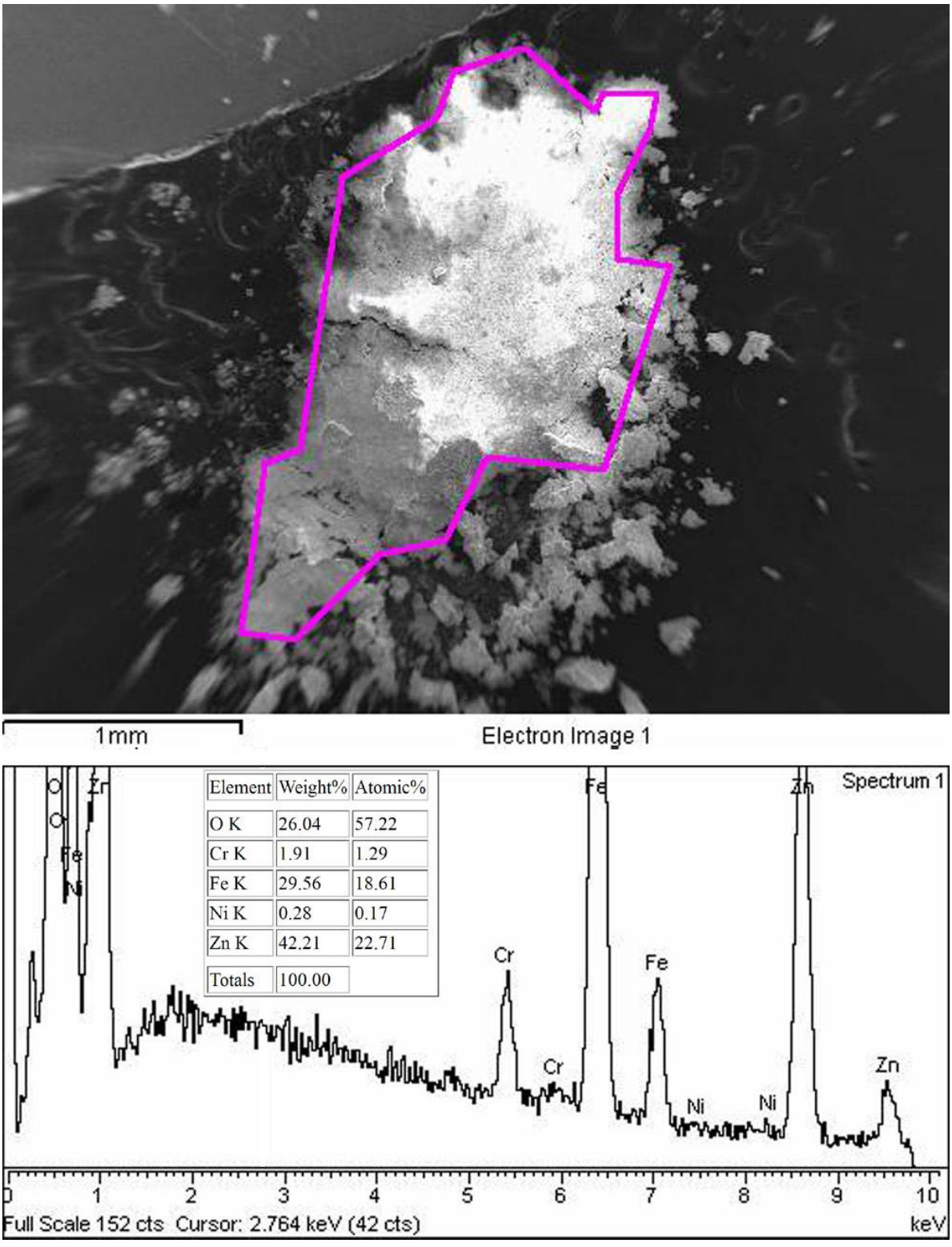

Fig. 35 FE-SEM micrograph of sample S2-20 obtained at 25 × magnification (top) and the corresponding EDS spectrum (bottom). Inset table shows the results of elemental analysis.

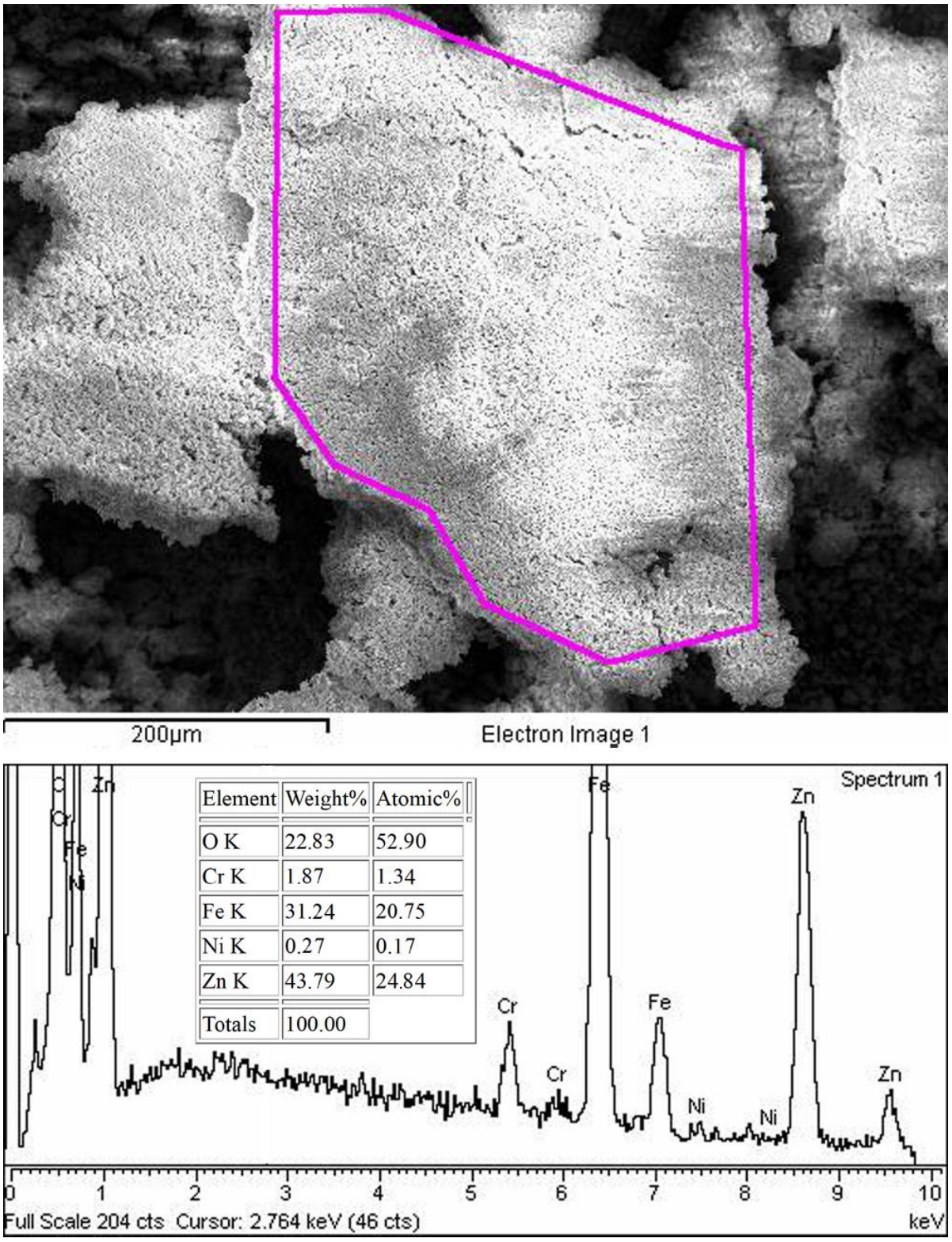

Fig. 36 FE-SEM micrograph of sample S2-25 obtained at 170 × magnification (top) and the corresponding EDS spectrum (bottom). Inset table shows the results of elemental analysis.

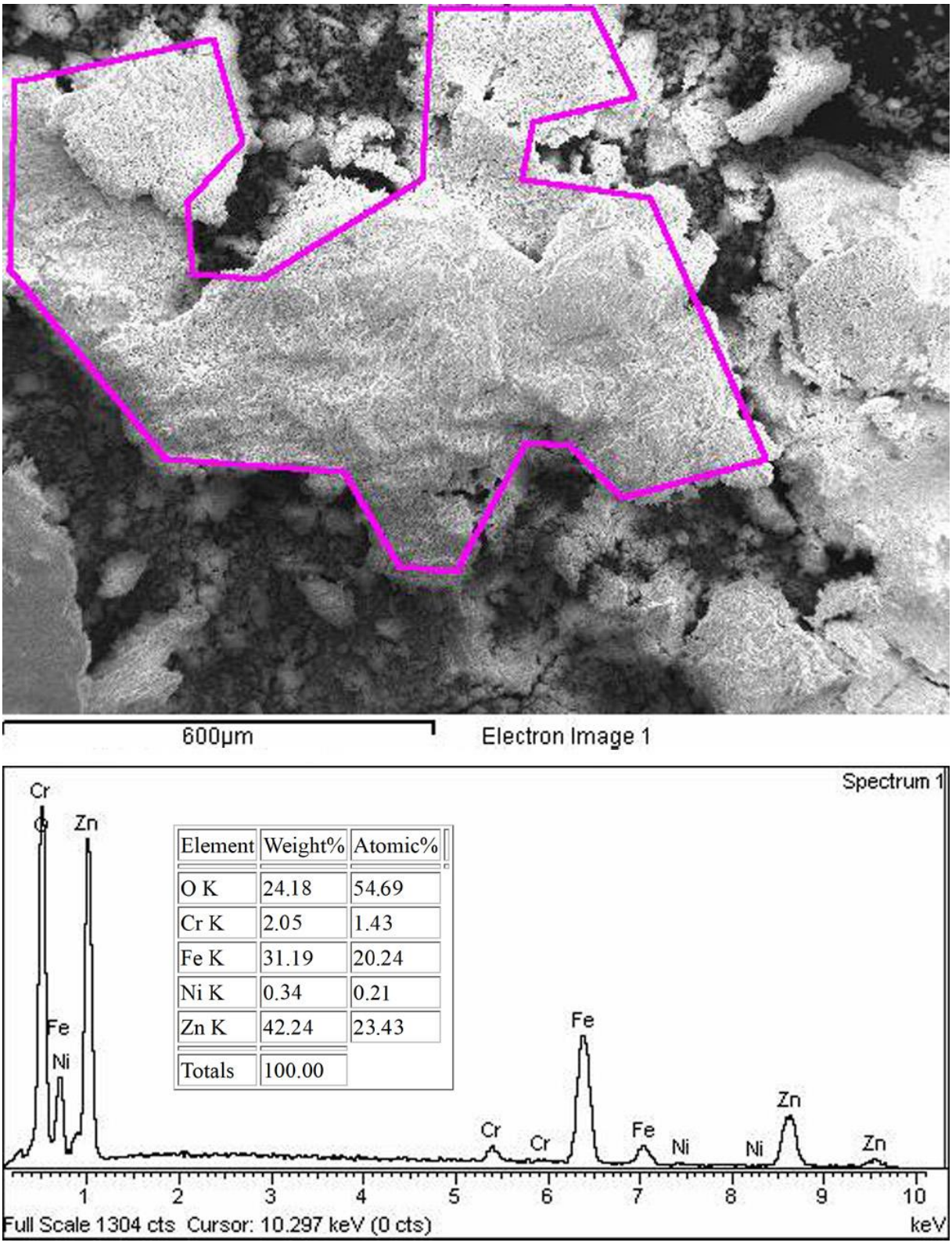

Fig. 37 FE-SEM micrograph of sample S2-30 obtained at 75 × magnification (top) and the corresponding EDS spectrum (bottom). Inset table shows the results of elemental analysis.

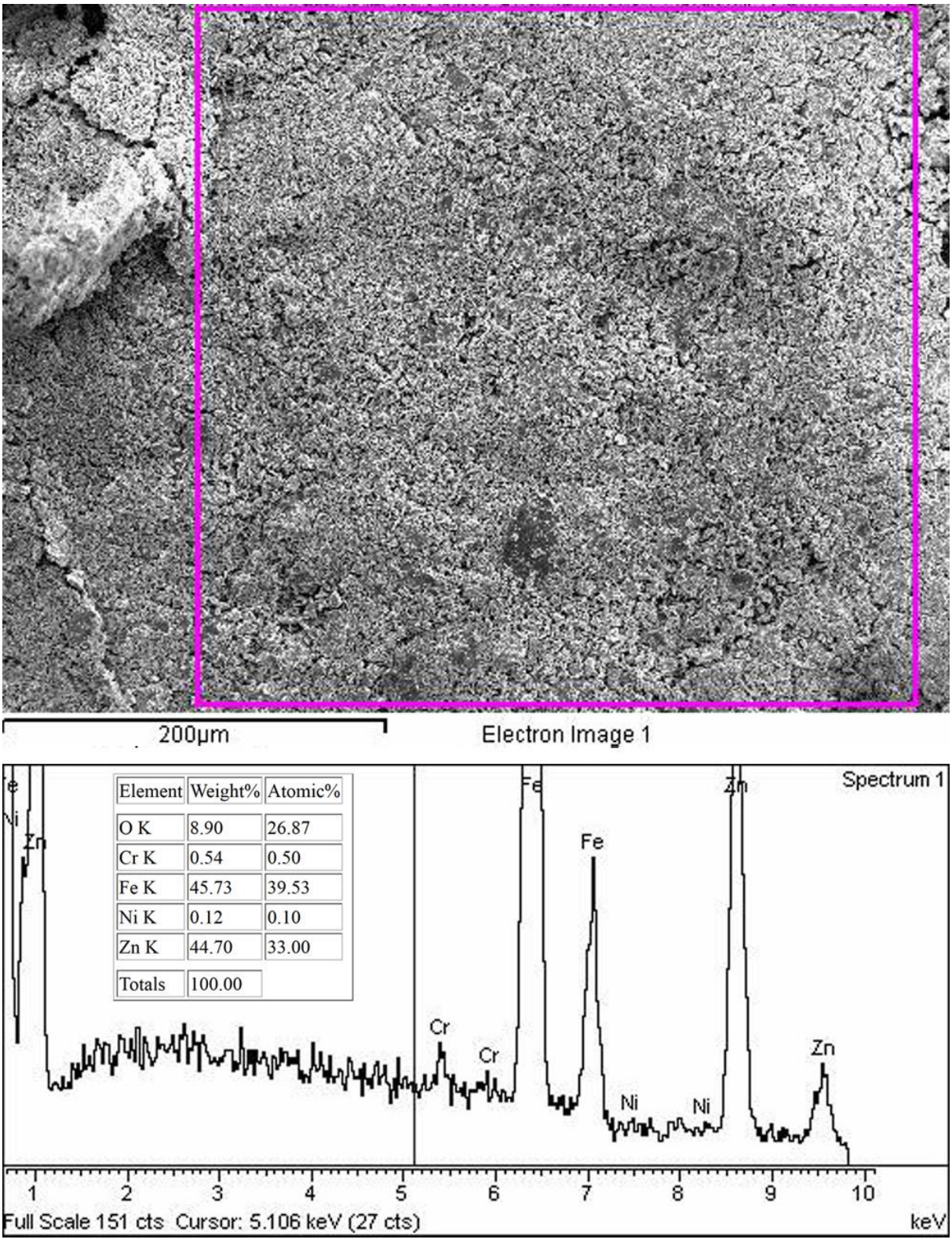

Fig. 38 FE-SEM micrograph of sample S3-1 obtained at 200 × magnification (top) and the corresponding EDS spectrum (bottom). Inset table shows the results of elemental analysis.

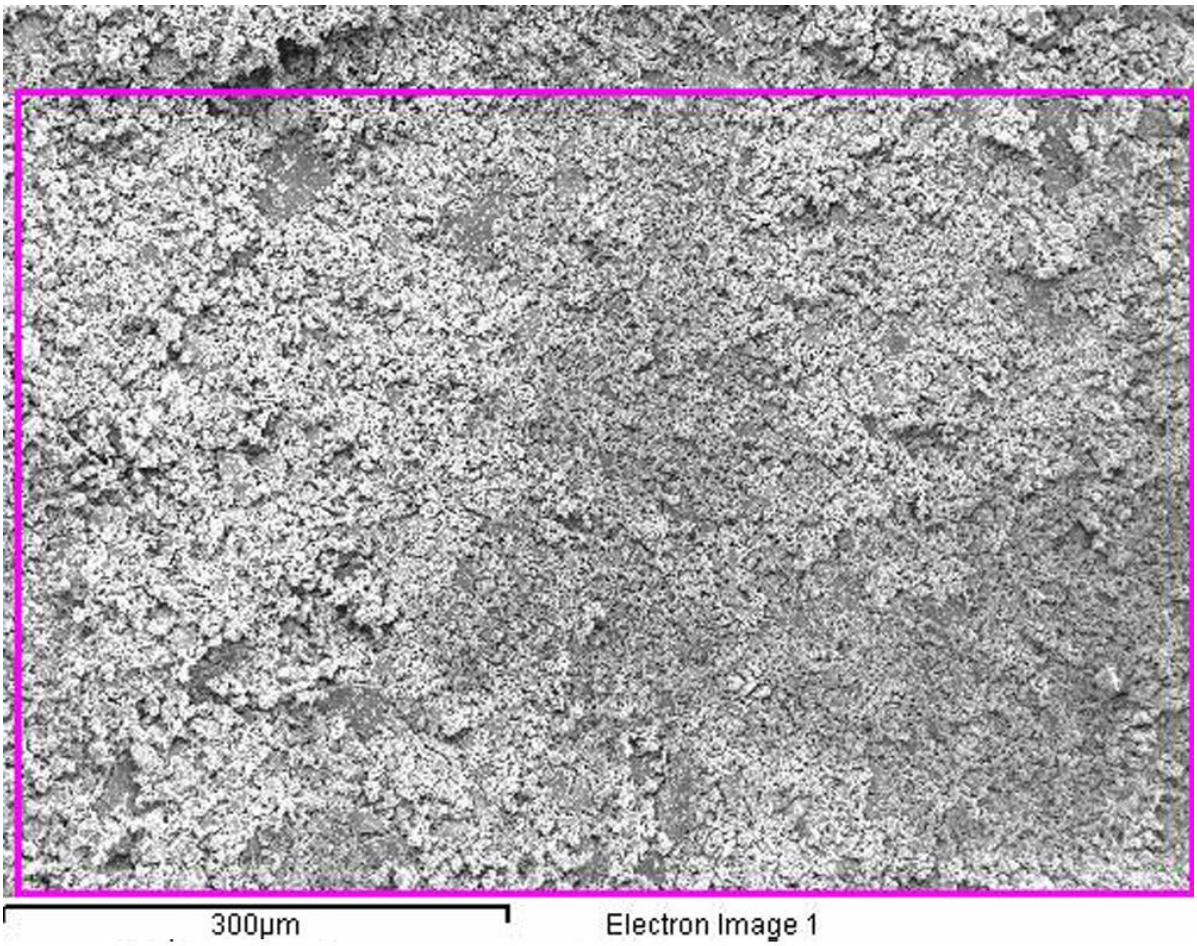

Element	Weight%	Atomic%
O K	10.17	29.57
Cr K	1.07	0.96
Fe K	51.74	43.10
Ni K	0.41	0.33
Zn K	36.62	26.06
Totals	100.00	

Fig. 39 FE-SEM micrograph of sample S3-2 obtained at 140 × magnification (top) and the corresponding EDS spectrum (bottom). Inset table shows the results of elemental analysis.

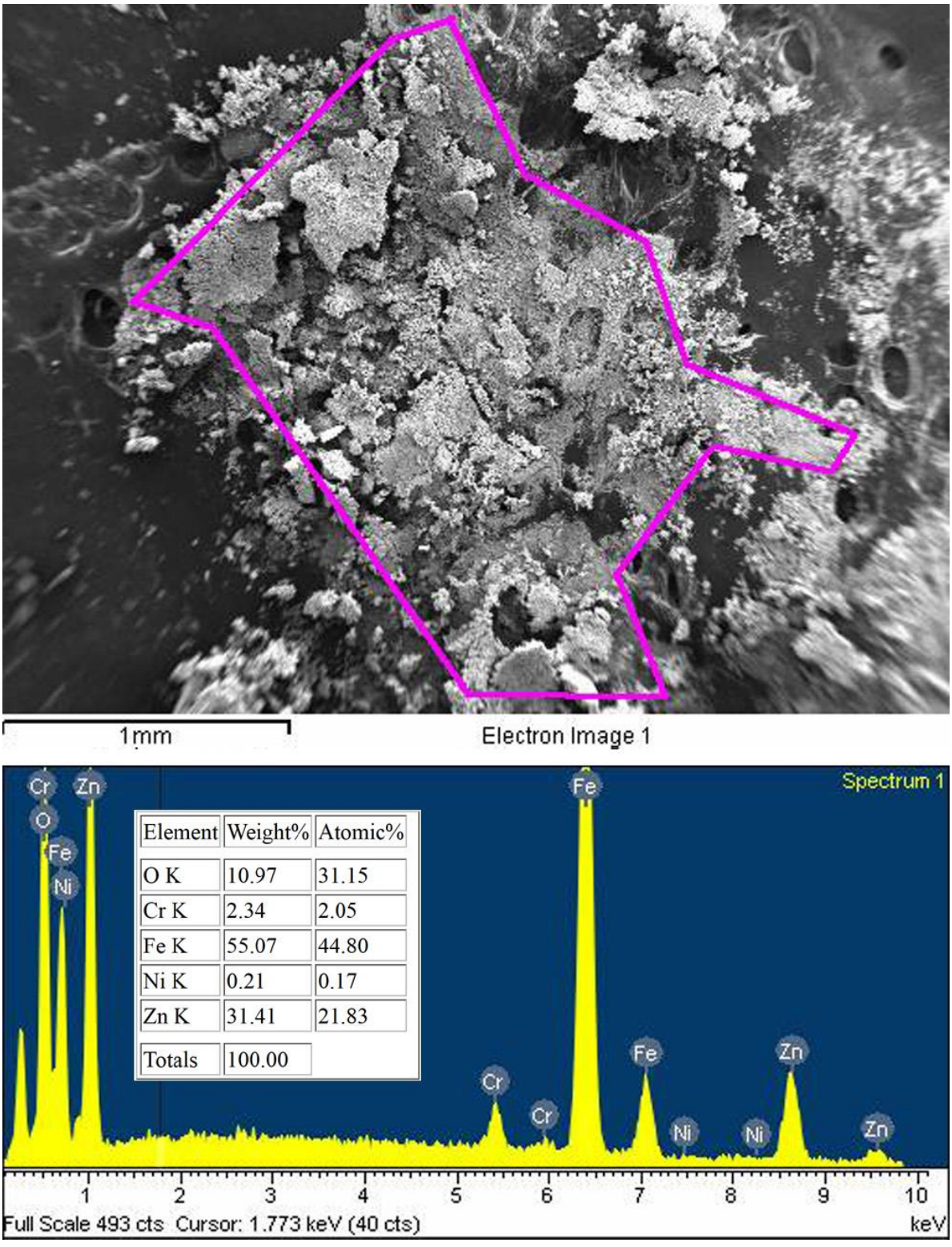

Element	Weight%	Atomic%
O K	10.97	31.15
Cr K	2.34	2.05
Fe K	55.07	44.80
Ni K	0.21	0.17
Zn K	31.41	21.83
Totals	100.00	

Fig. 40 FE-SEM micrograph of sample S3-5 obtained at 30 × magnification (top) and the corresponding EDS spectrum (bottom). Inset table shows the results of elemental analysis.

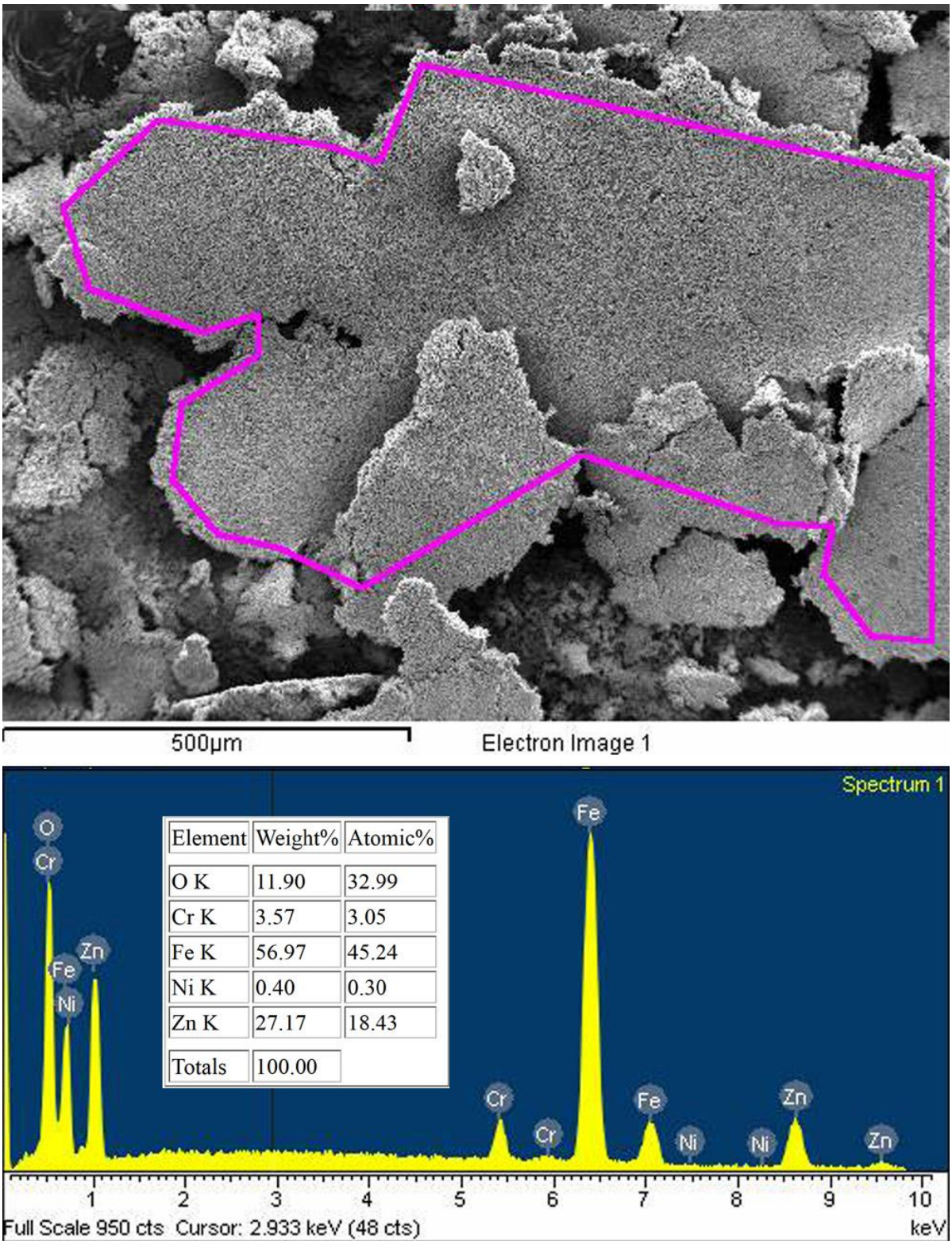

Fig. 41 FE-SEM micrograph of sample S3-9 obtained at 85 × magnification (top) and the corresponding EDS spectrum (bottom). Inset table shows the results of elemental analysis.

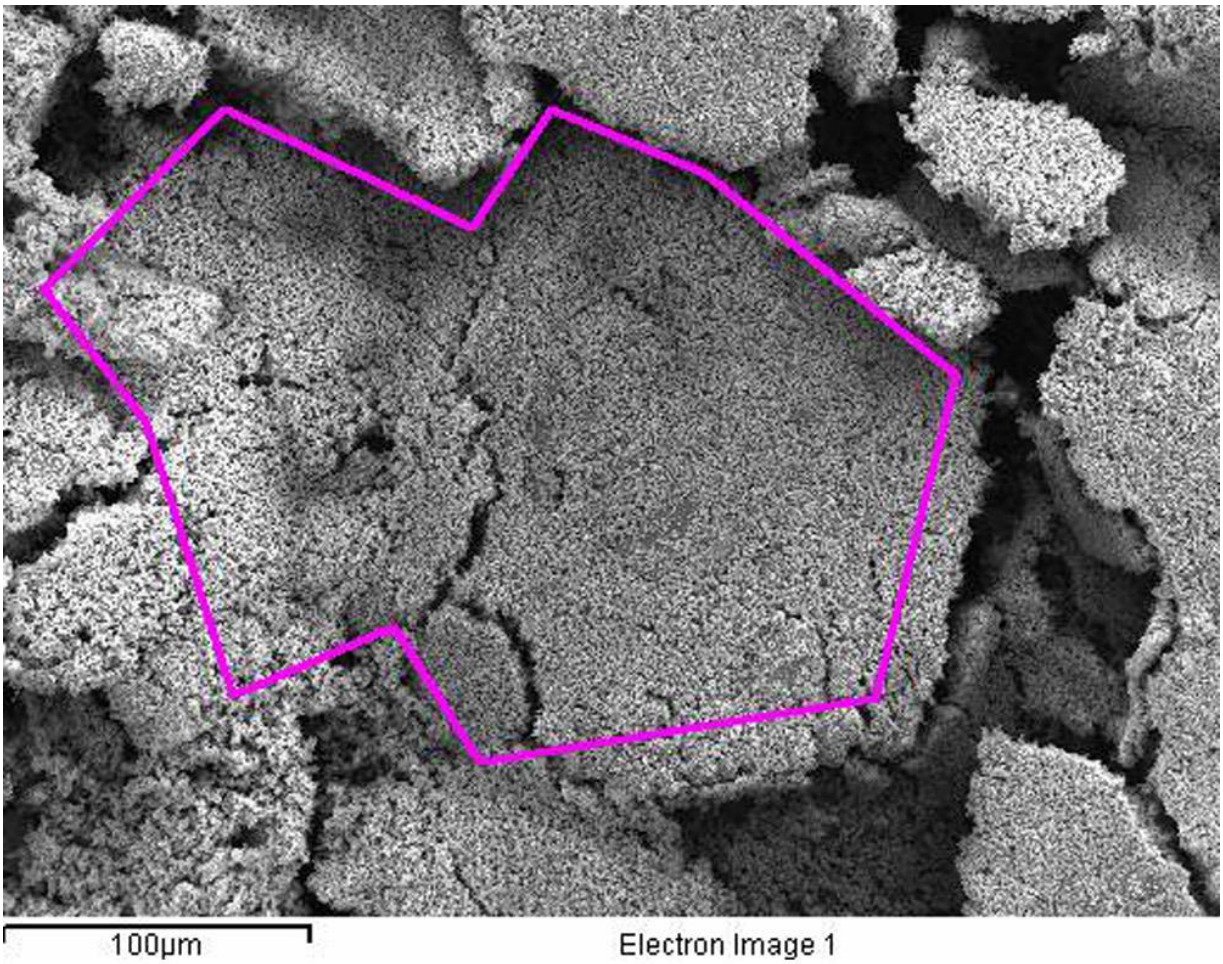

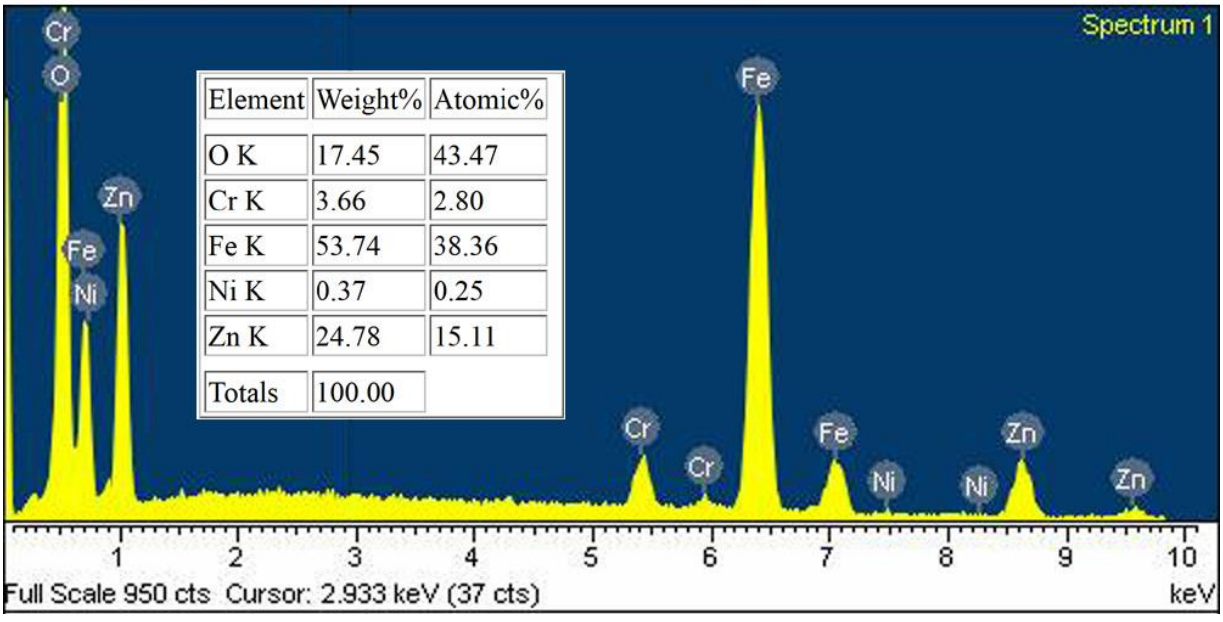

Element	Weight%	Atomic%
O K	17.45	43.47
Cr K	3.66	2.80
Fe K	53.74	38.36
Ni K	0.37	0.25
Zn K	24.78	15.11
Totals	100.00	

Fig. 42 FE-SEM micrograph of sample S3-14 obtained at 250 × magnification (top) and the corresponding EDS spectrum (bottom). Inset table shows the results of elemental analysis.

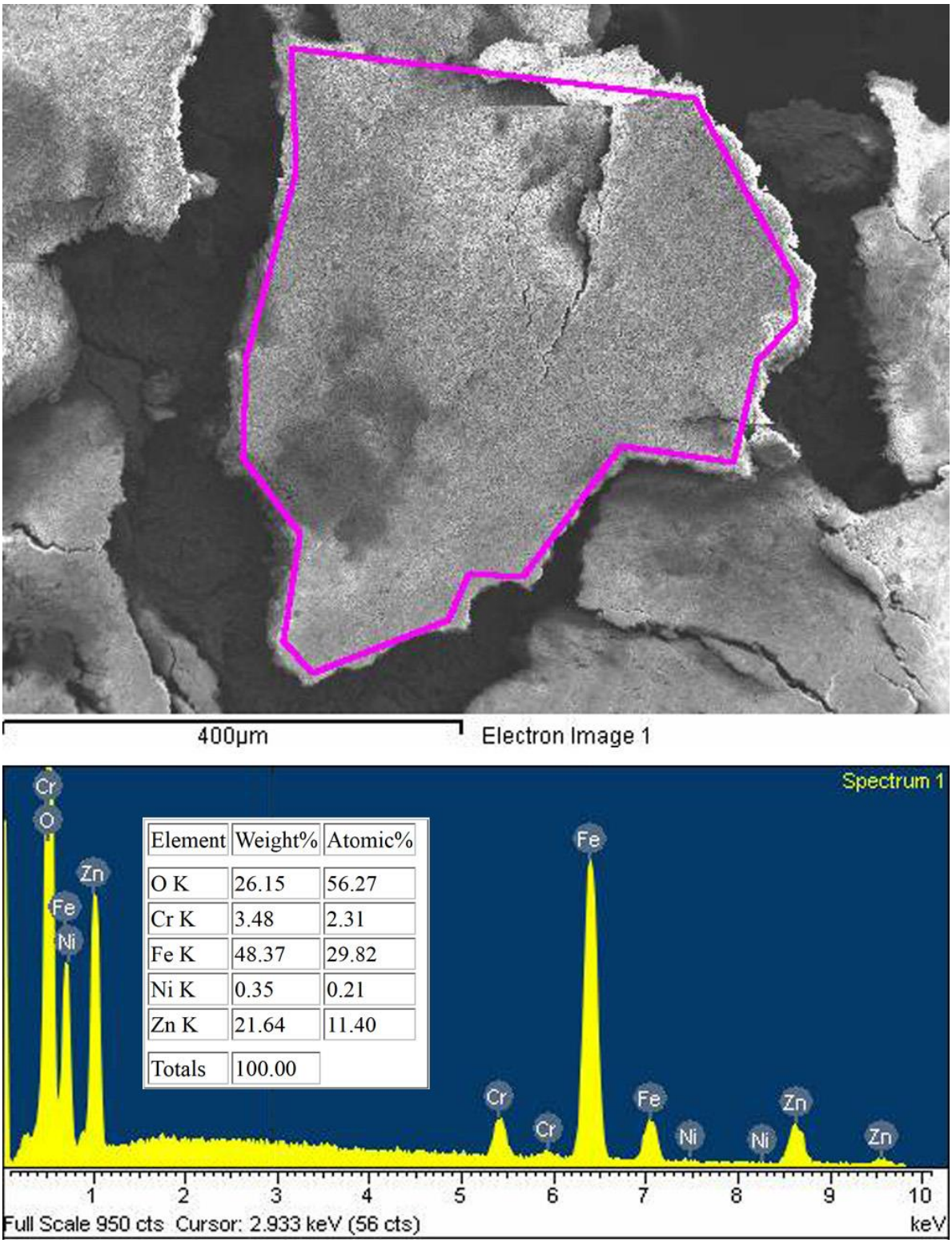

Element	Weight%	Atomic%
O K	26.15	56.27
Cr K	3.48	2.31
Fe K	48.37	29.82
Ni K	0.35	0.21
Zn K	21.64	11.40
Totals	100.00	

Fig. 43 FE-SEM micrograph of sample S3-20 obtained at 120 × magnification (top) and the corresponding EDS spectrum (bottom). Inset table shows the results of elemental analysis.

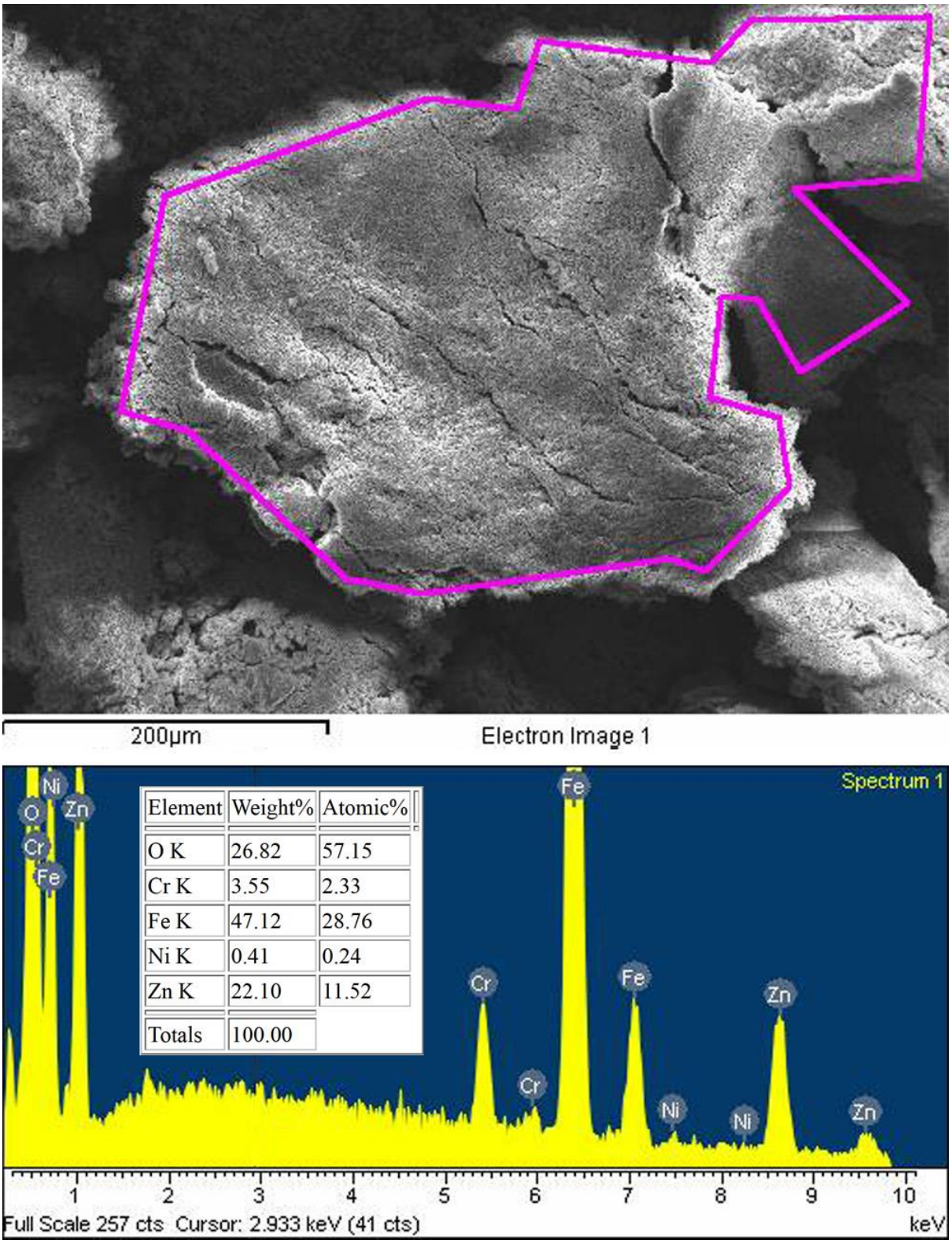

Fig. 44 FE-SEM micrograph of sample S3-25 obtained at 170 × magnification (top) and the corresponding EDS spectrum (bottom). Inset table shows the results of elemental analysis.

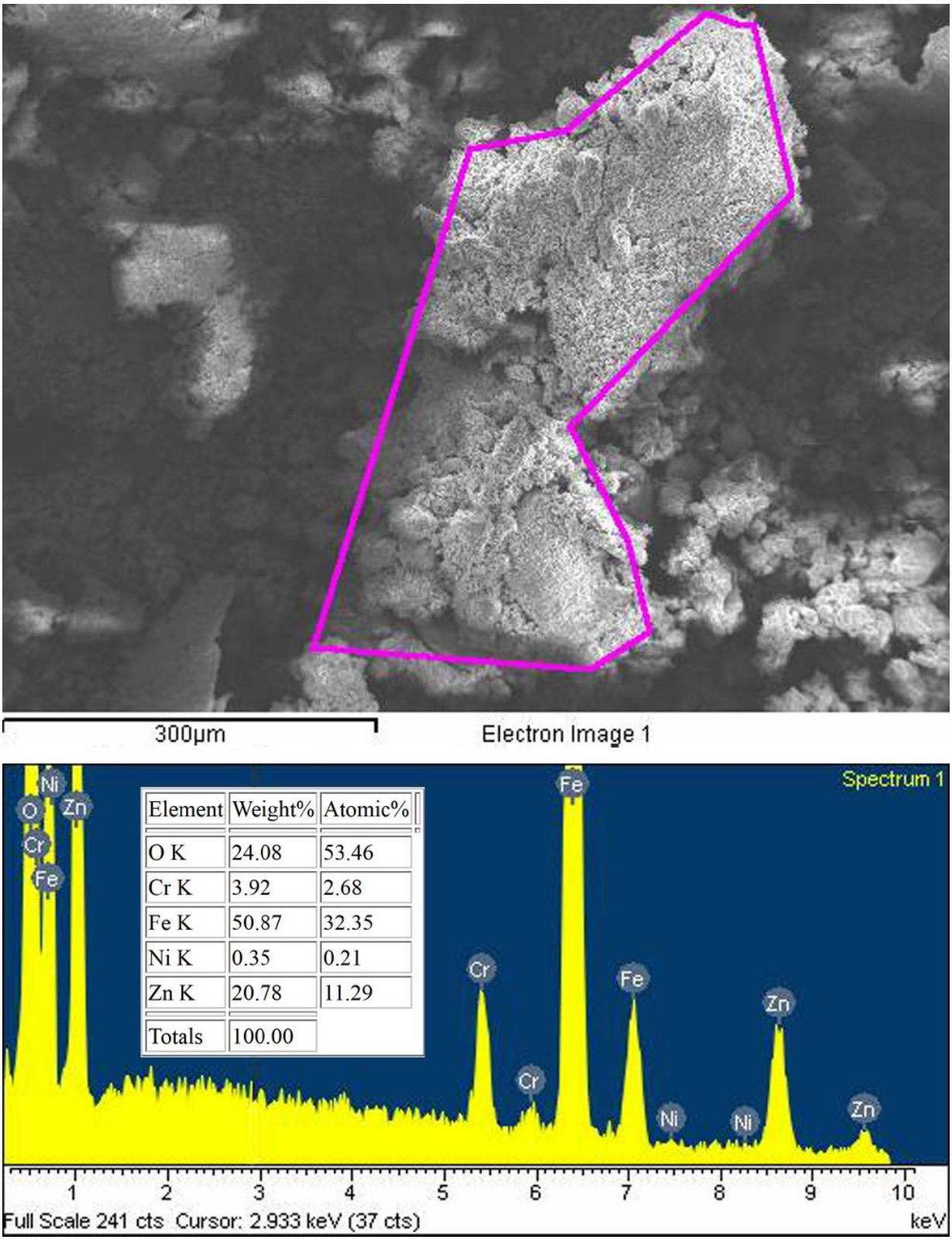

Fig. 45 FE-SEM micrograph of sample S3-30 obtained at 130 × magnification (top) and the corresponding EDS spectrum (bottom). Inset table shows the results of elemental analysis.

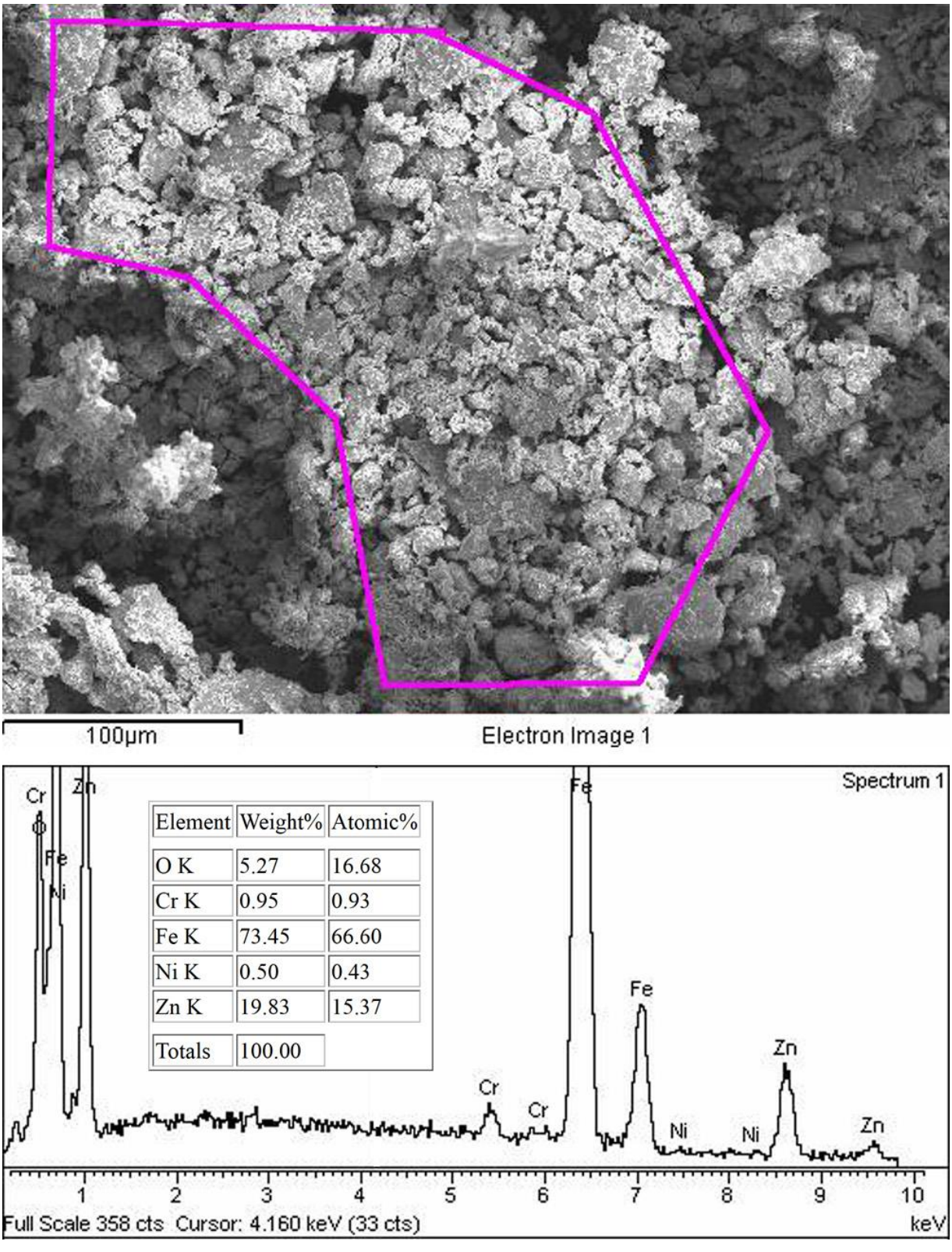

Element	Weight%	Atomic%
O K	5.27	16.68
Cr K	0.95	0.93
Fe K	73.45	66.60
Ni K	0.50	0.43
Zn K	19.83	15.37
Totals	100.00	

Fig. 46 FE-SEM micrograph of sample S4-1 obtained at 250 × magnification (top) and the corresponding EDS spectrum (bottom). Inset table shows the results of elemental analysis.

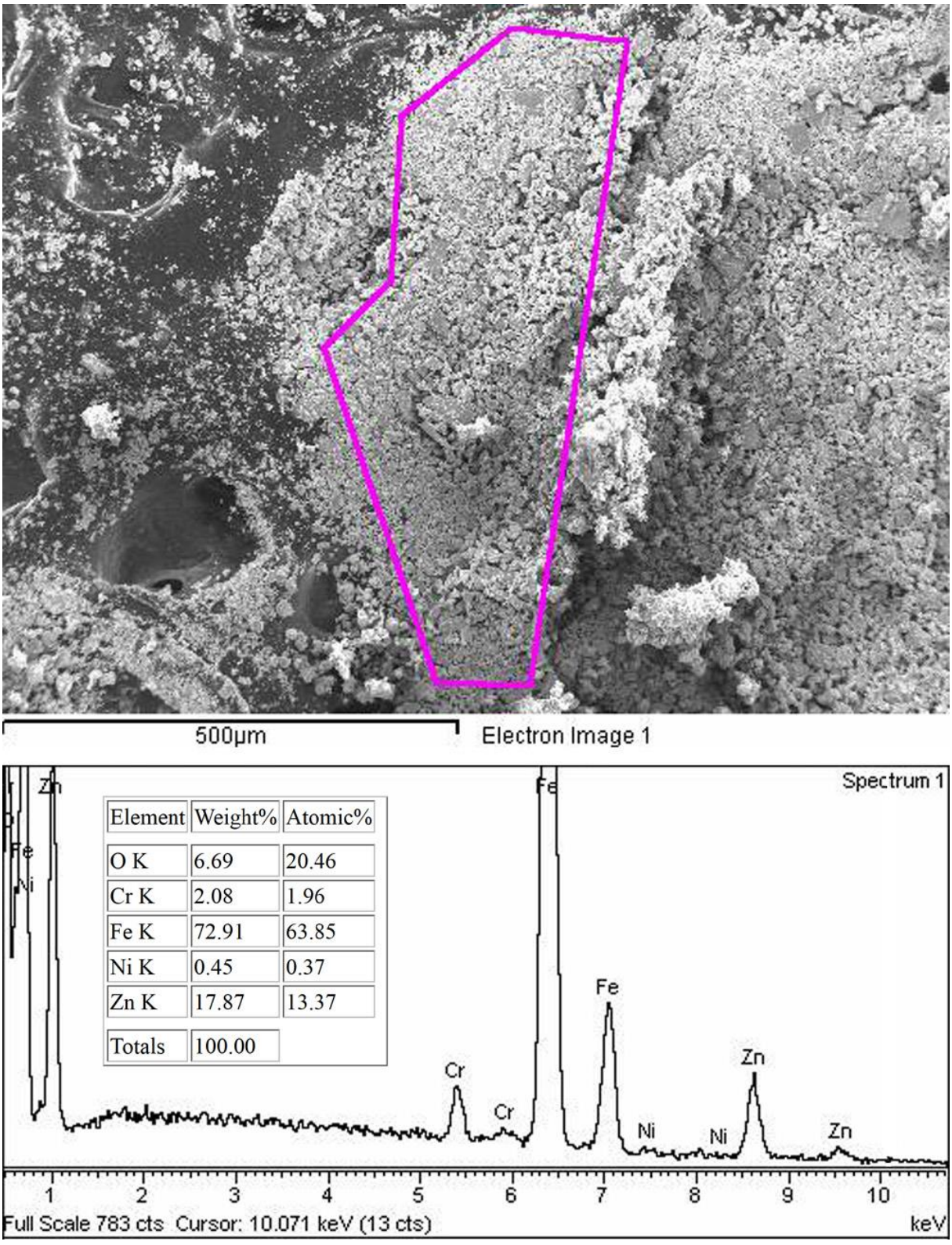

Fig. 47 FE-SEM micrograph of sample S4-2 obtained at 95 × magnification (top) and the corresponding EDS spectrum (bottom). Inset table shows the results of elemental analysis.

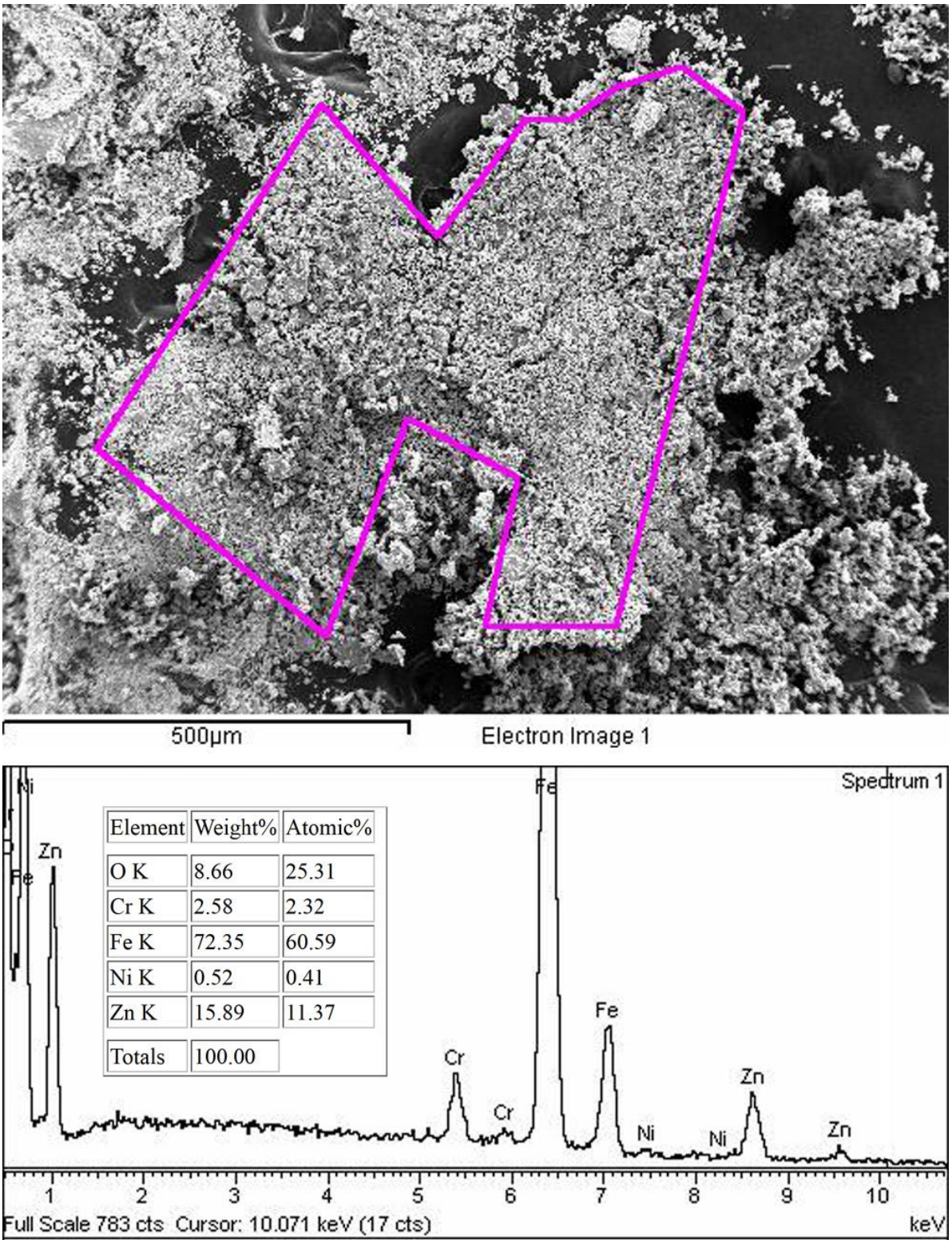

Fig. 48 FE-SEM micrograph of sample S4-5 obtained at 85 × magnification (top) and the corresponding EDS spectrum (bottom). Inset table shows the results of elemental analysis.

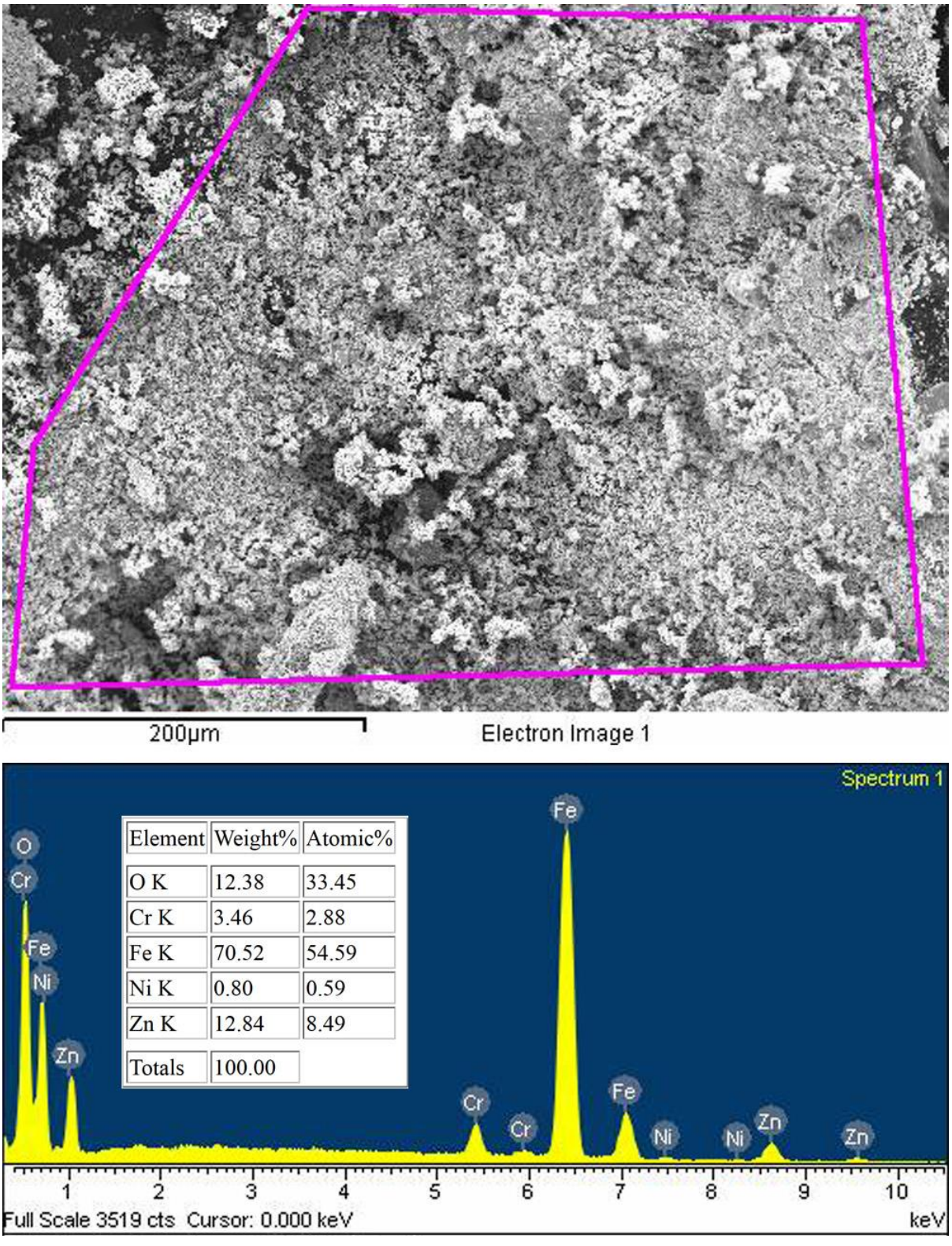

Fig. 49 FE-SEM micrograph of sample S4-9 obtained at 190 × magnification (top) and the corresponding EDS spectrum (bottom). Inset table shows the results of elemental analysis.

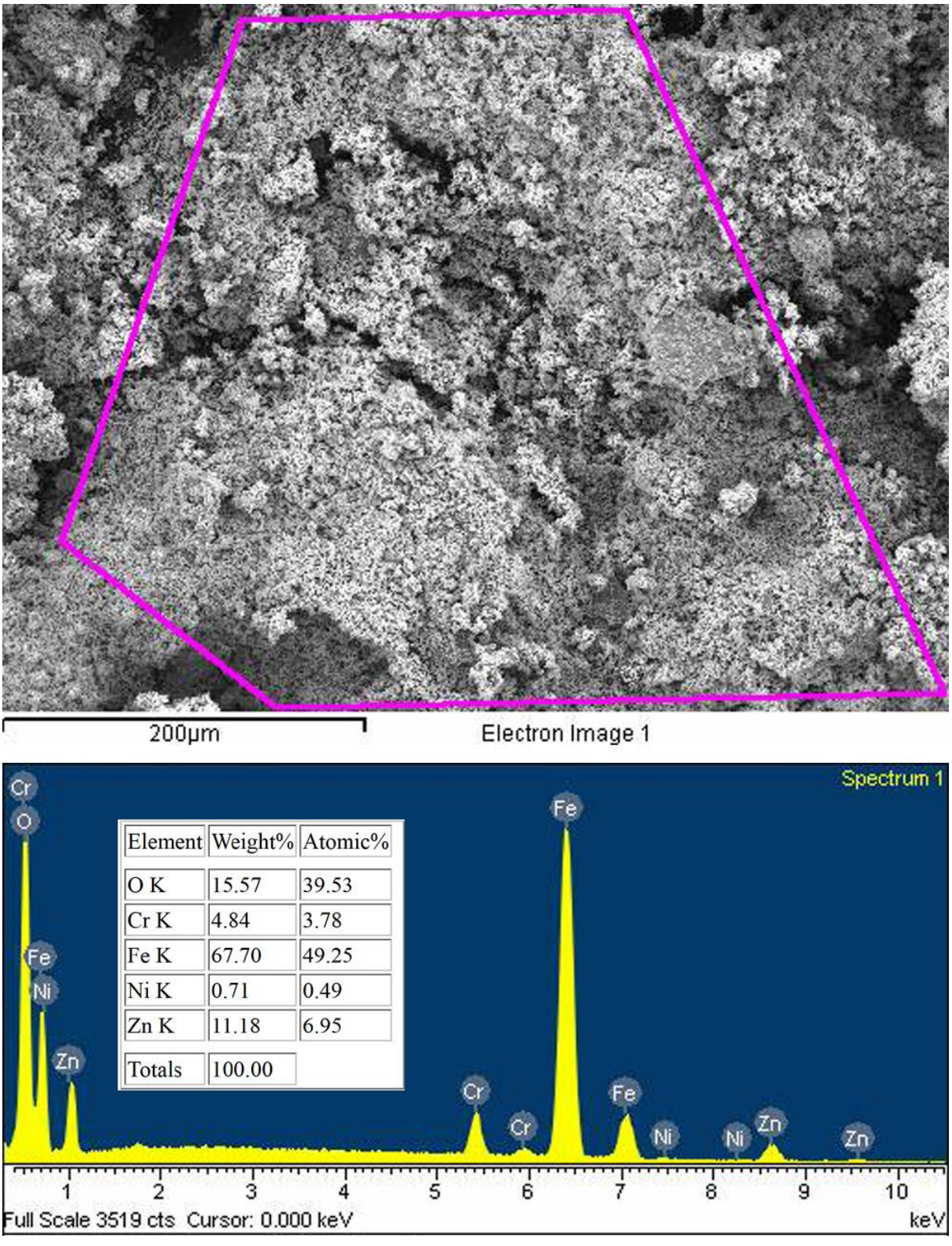

Fig. 50 FE-SEM micrograph of sample S4-14 obtained at 190 × magnification (top) and the corresponding EDS spectrum (bottom). Inset table shows the results of elemental analysis.

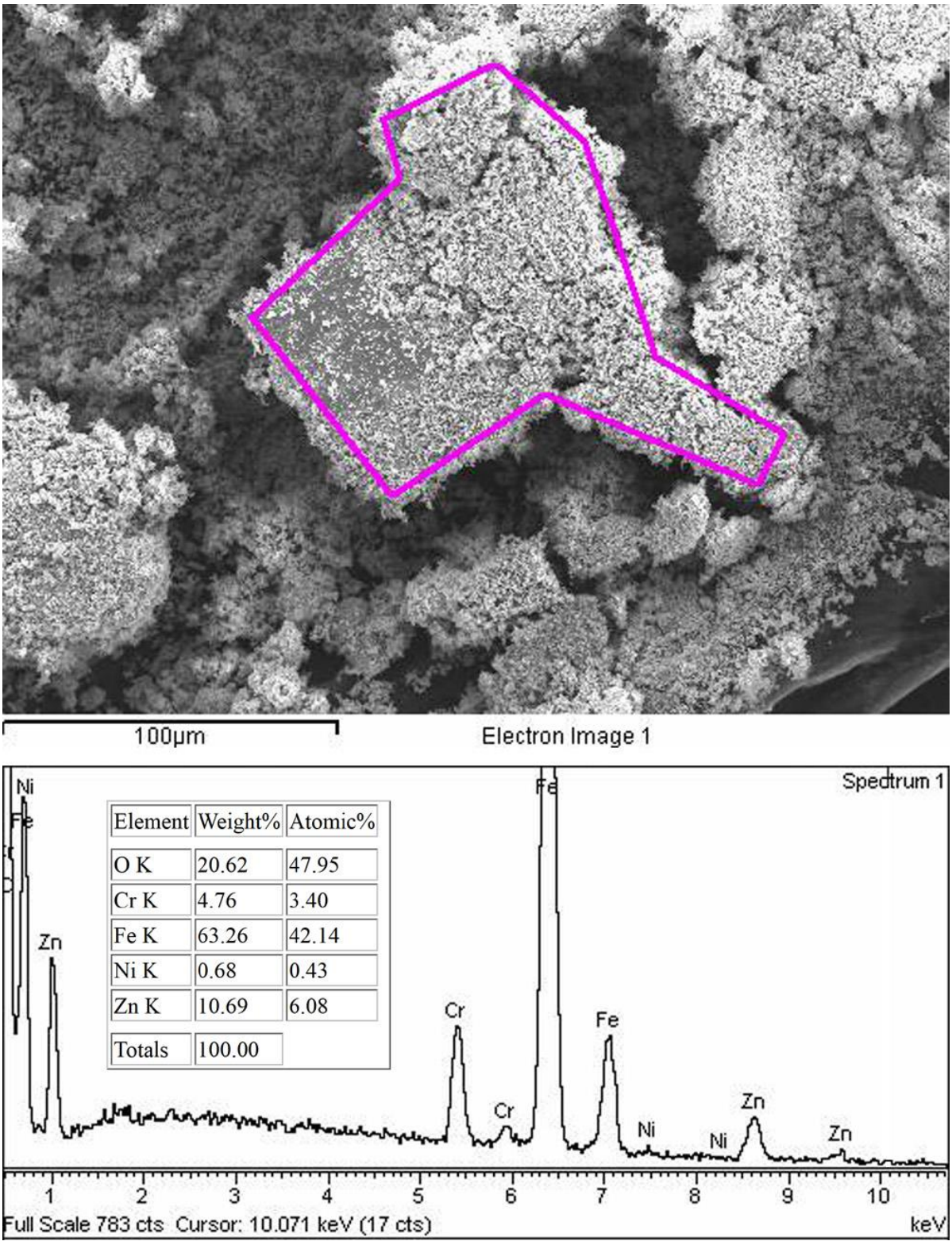

Element	Weight%	Atomic%
O K	20.62	47.95
Cr K	4.76	3.40
Fe K	63.26	42.14
Ni K	0.68	0.43
Zn K	10.69	6.08
Totals	100.00	

Fig. 51 FE-SEM micrograph of sample S4-20 obtained at 350 × magnification (top) and the corresponding EDS spectrum (bottom). Inset table shows the results of elemental analysis.

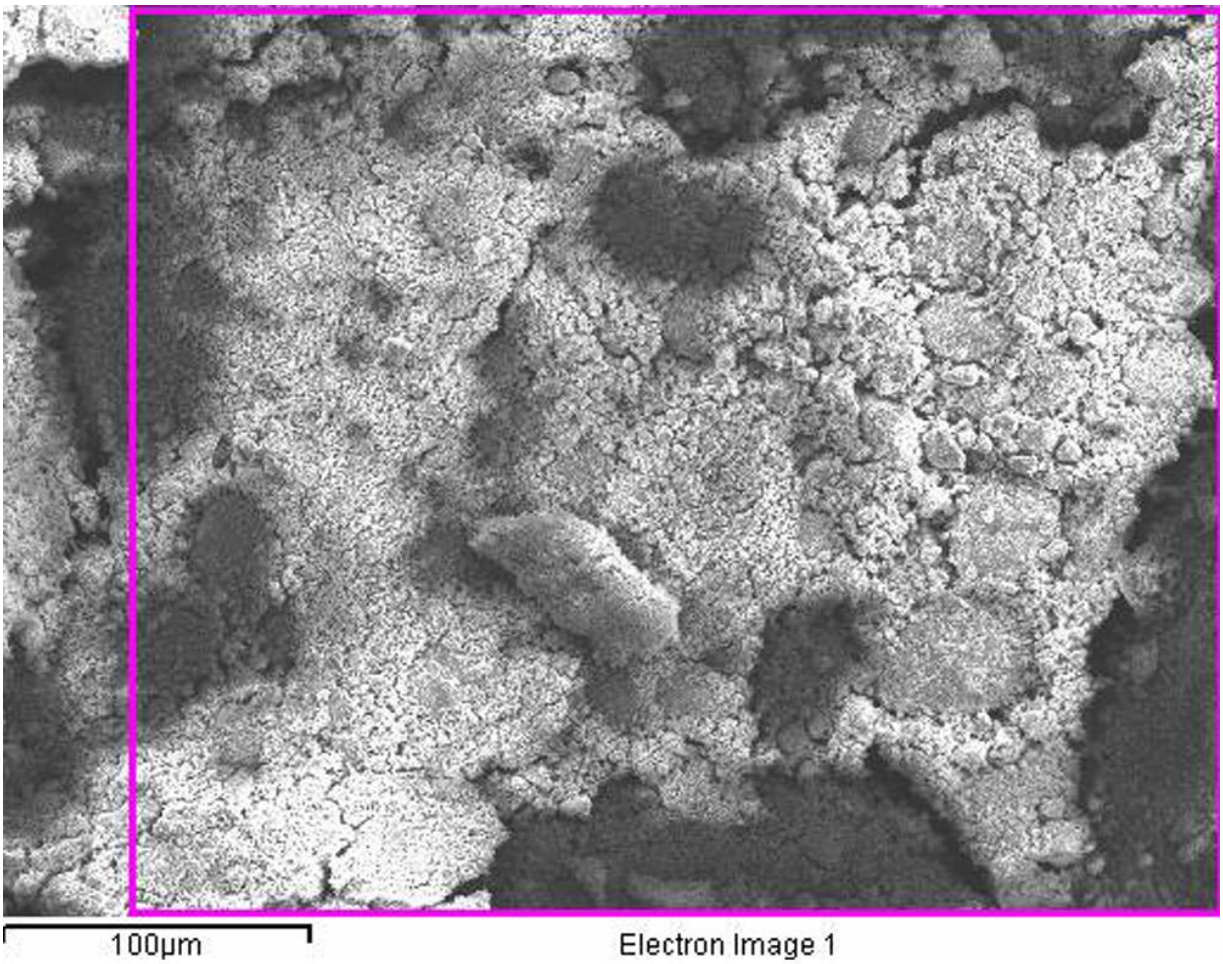

Fig. 52 FE-SEM micrograph of sample S4-25 obtained at 250 × magnification (top) and the corresponding EDS spectrum (bottom). Inset table shows the results of elemental analysis.

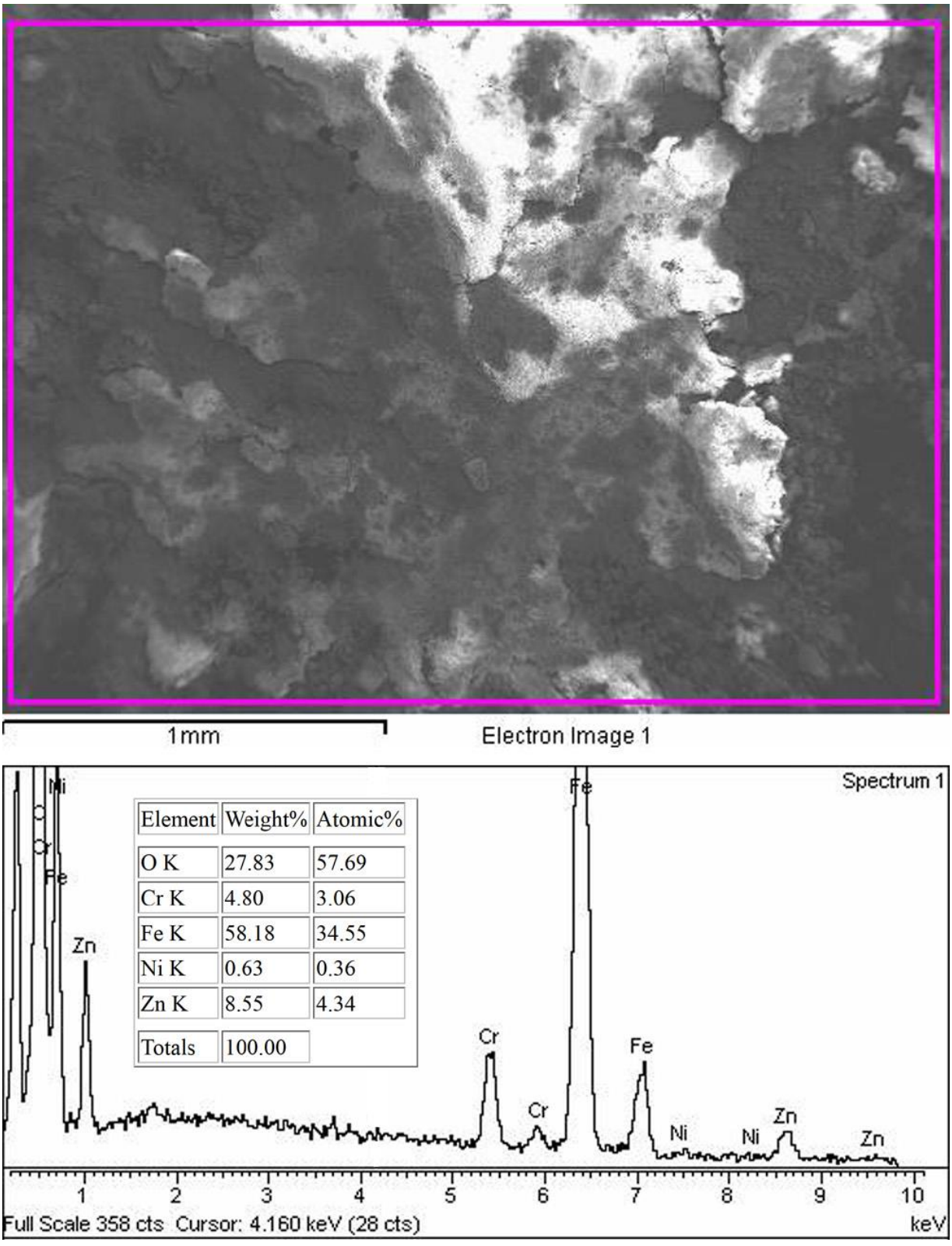

Fig. 53 FE-SEM micrograph of sample S4-30 obtained at 40 × magnification (top) and the corresponding EDS spectrum (bottom). Inset table shows the results of elemental analysis.

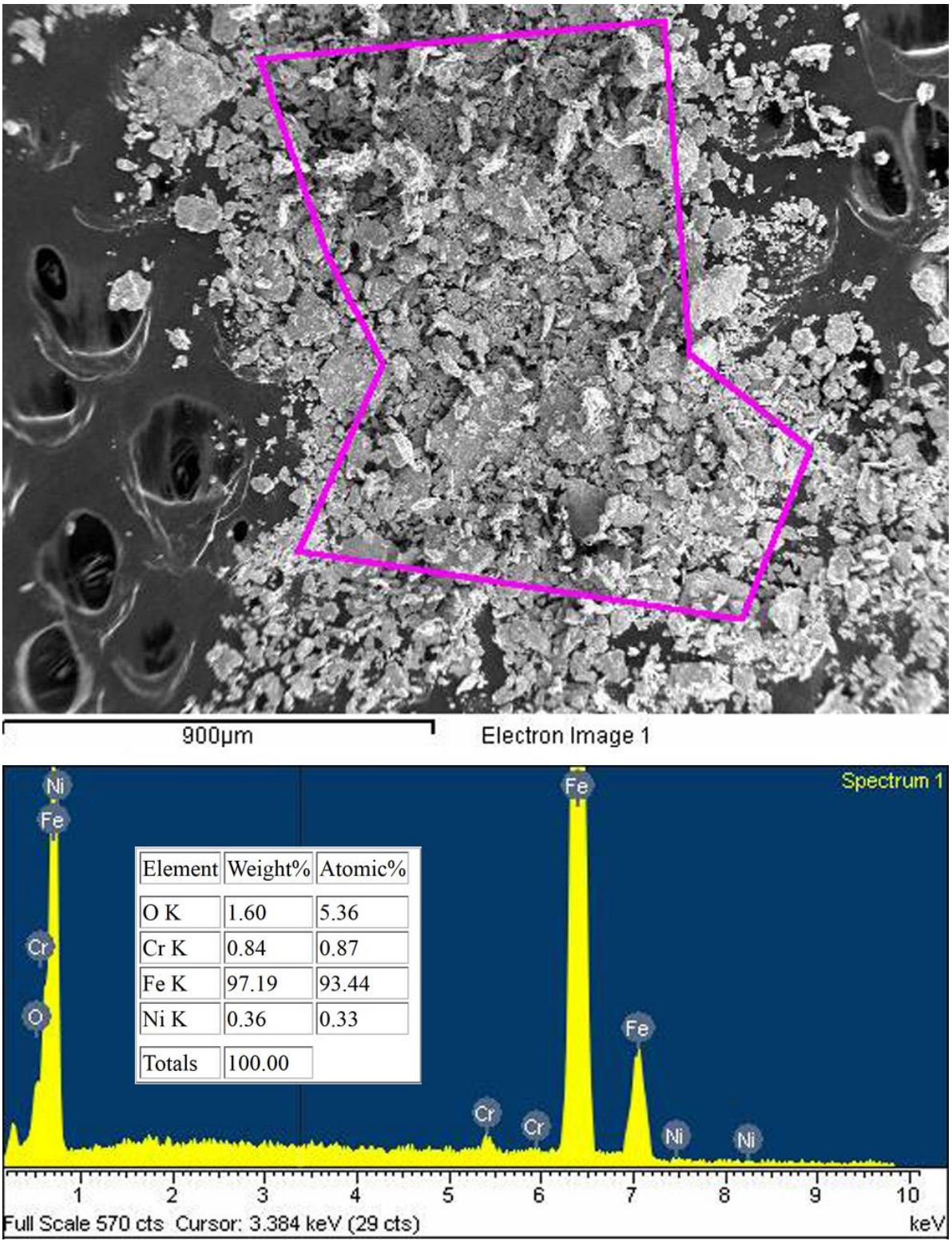

Fig. 54 FE-SEM micrograph of sample S5-1 obtained at 50 × magnification (top) and the corresponding EDS spectrum (bottom). Inset table shows the results of elemental analysis.

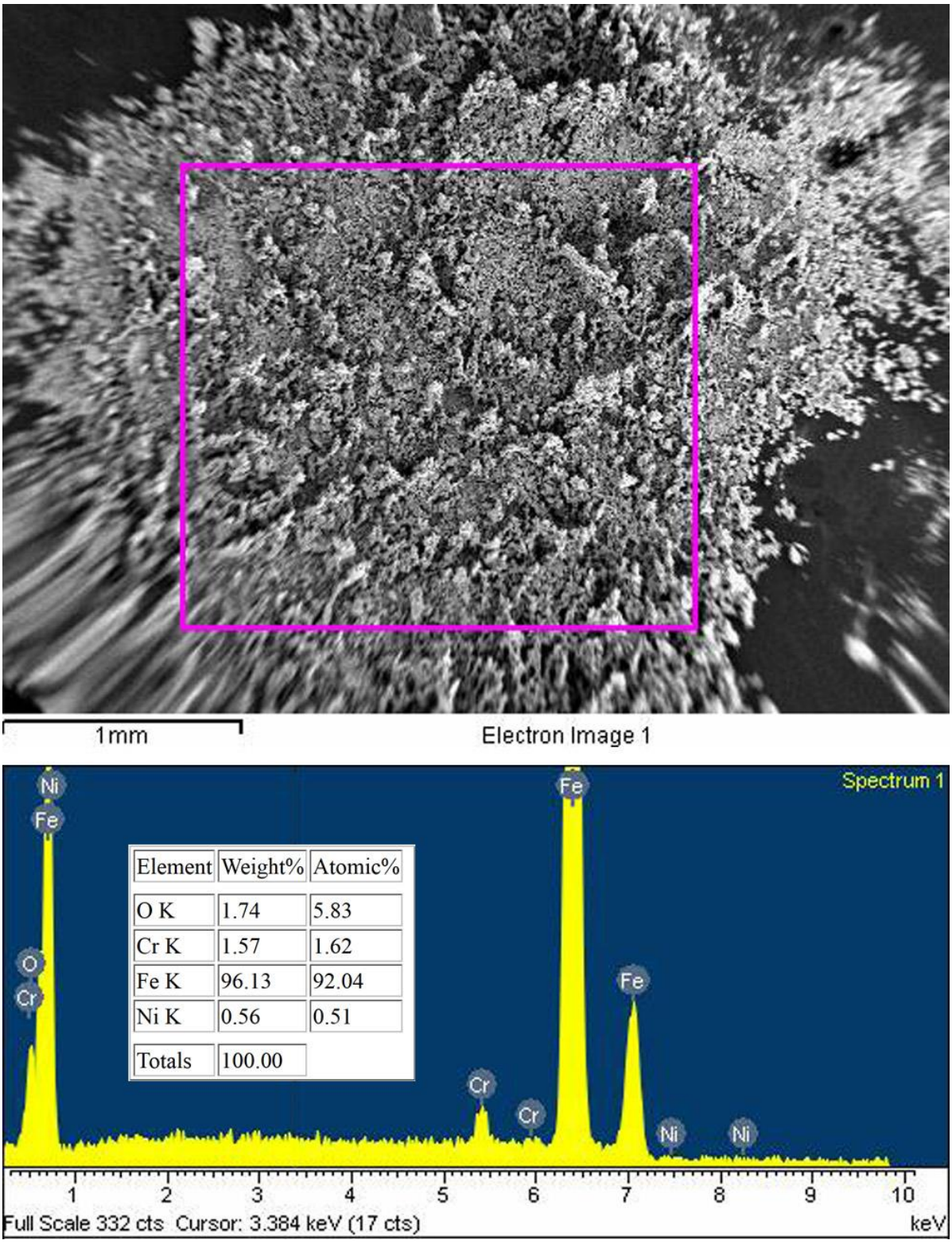

Fig. 55 FE-SEM micrograph of sample S5-2 obtained at 25 × magnification (top) and the corresponding EDS spectrum (bottom). Inset table shows the results of elemental analysis.

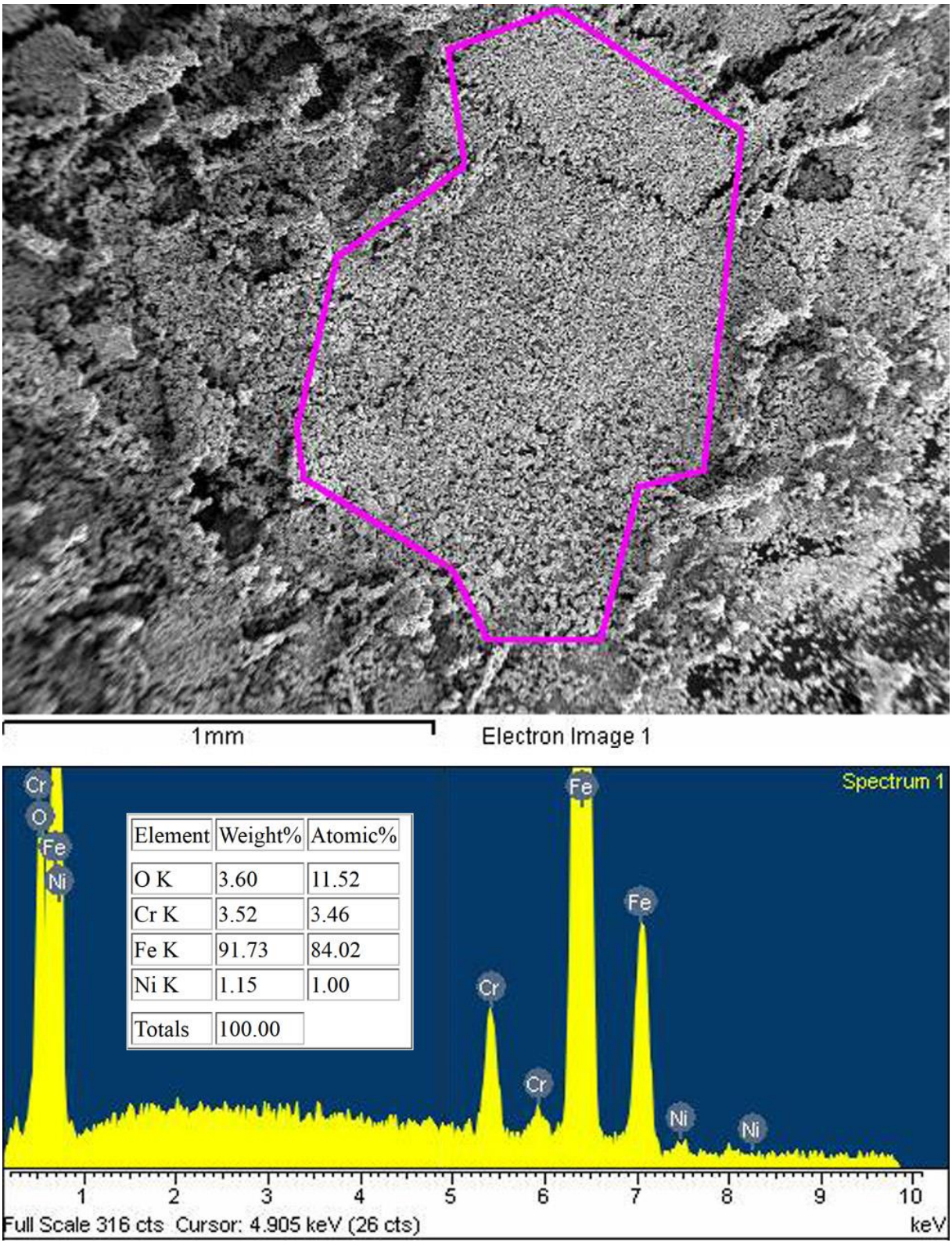

Fig. 56 FE-SEM micrograph of sample S5-5 obtained at 45 × magnification (top) and the corresponding EDS spectrum (bottom). Inset table shows the results of elemental analysis.

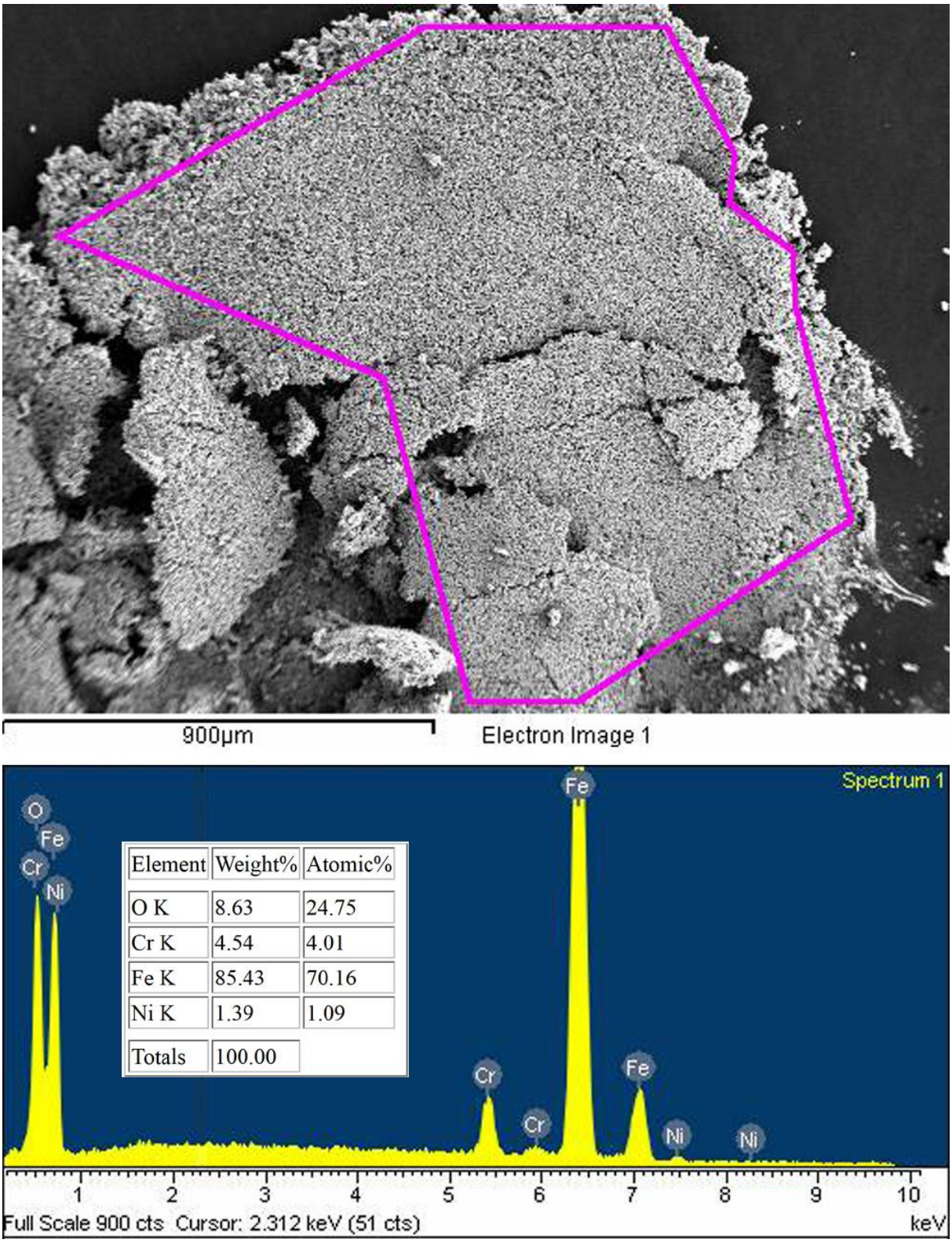

Fig. 57 FE-SEM micrograph of sample S5-9 obtained at 50 × magnification (top) and the corresponding EDS spectrum (bottom). Inset table shows the results of elemental analysis.

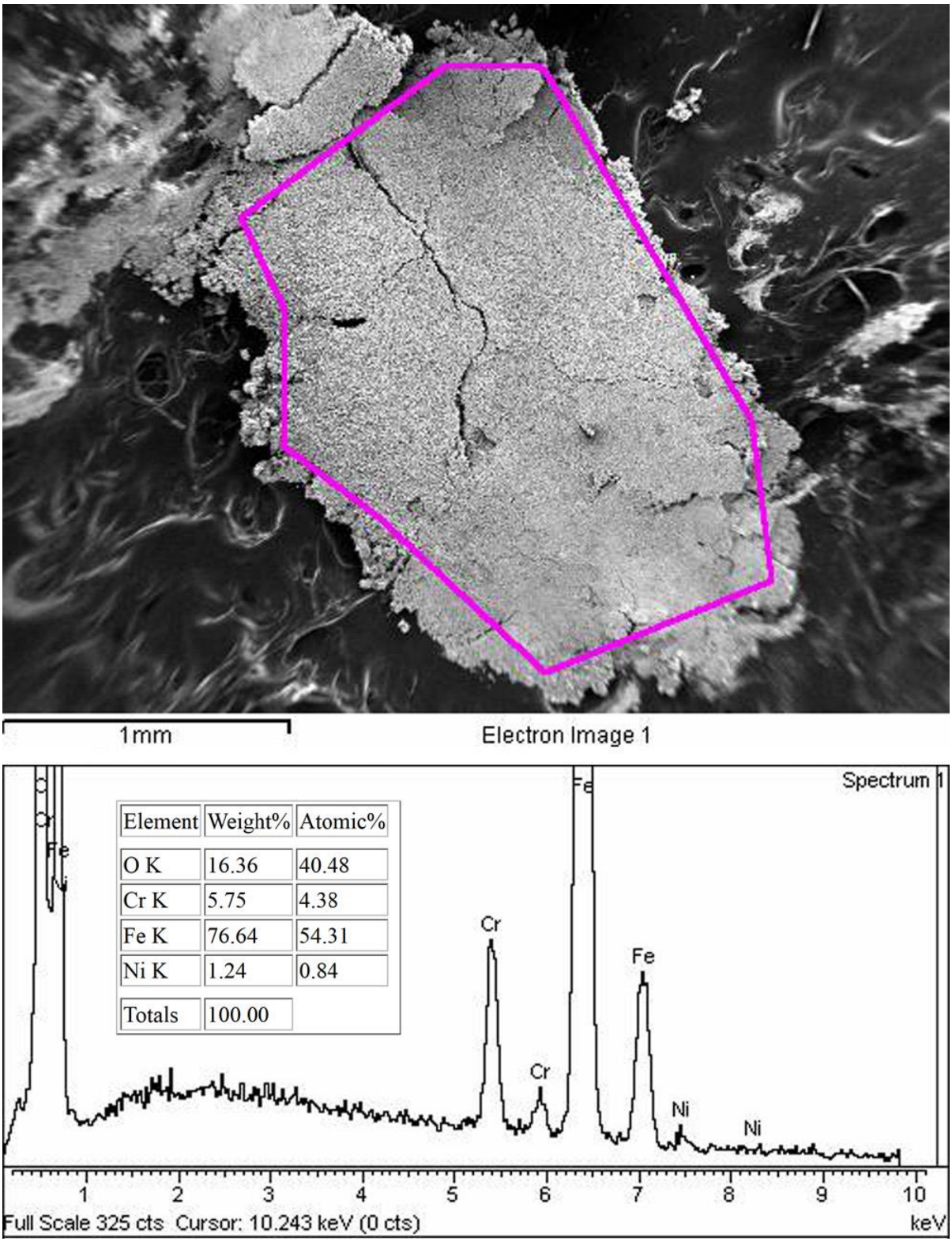

Fig. 58 FE-SEM micrograph of sample S5-14 obtained at 300 × magnification (top) and the corresponding EDS spectrum (bottom). Inset table shows the results of elemental analysis.

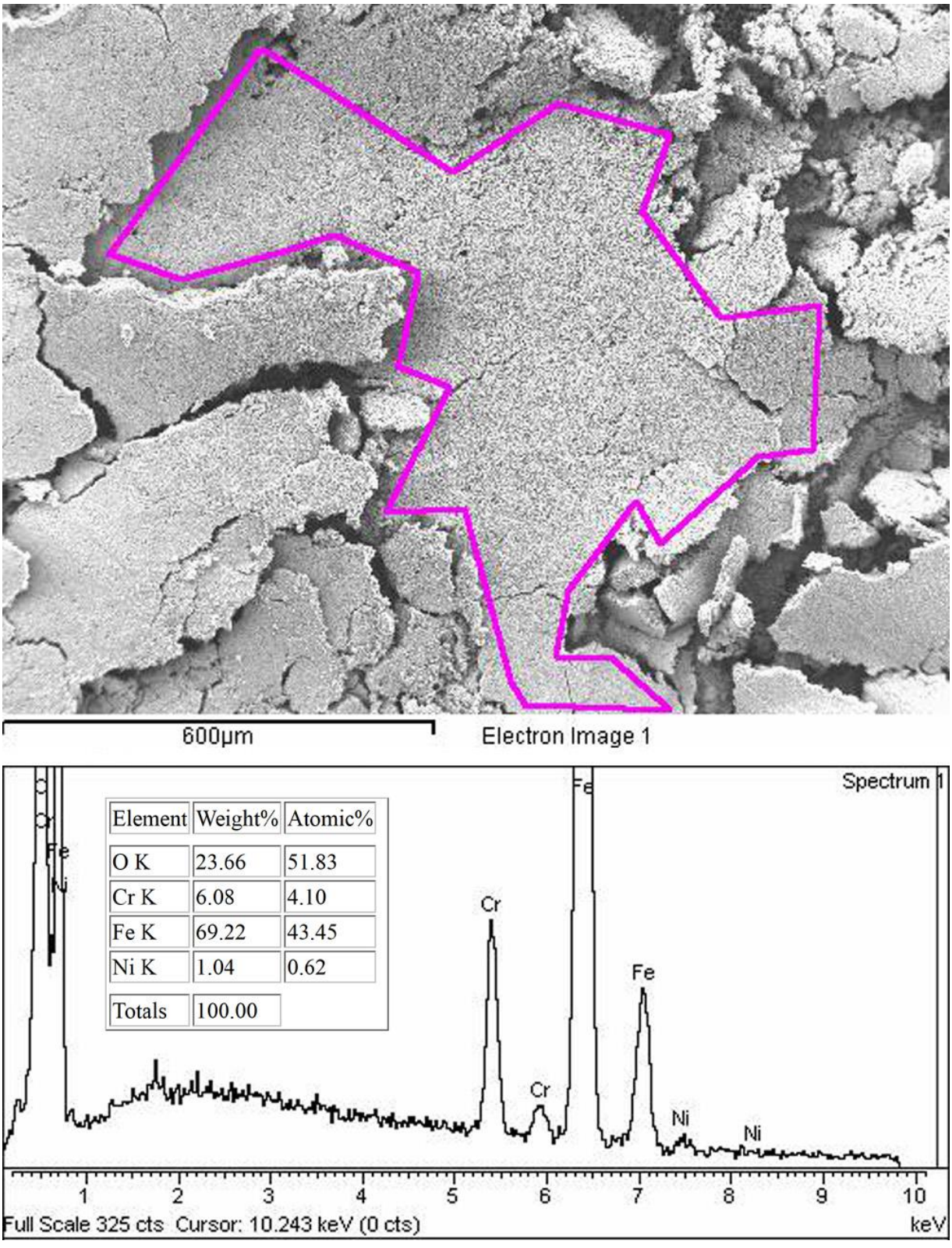

Fig. 59 FE-SEM micrograph of sample S5-20 obtained at 75 × magnification (top) and the corresponding EDS spectrum (bottom). Inset table shows the results of elemental analysis.

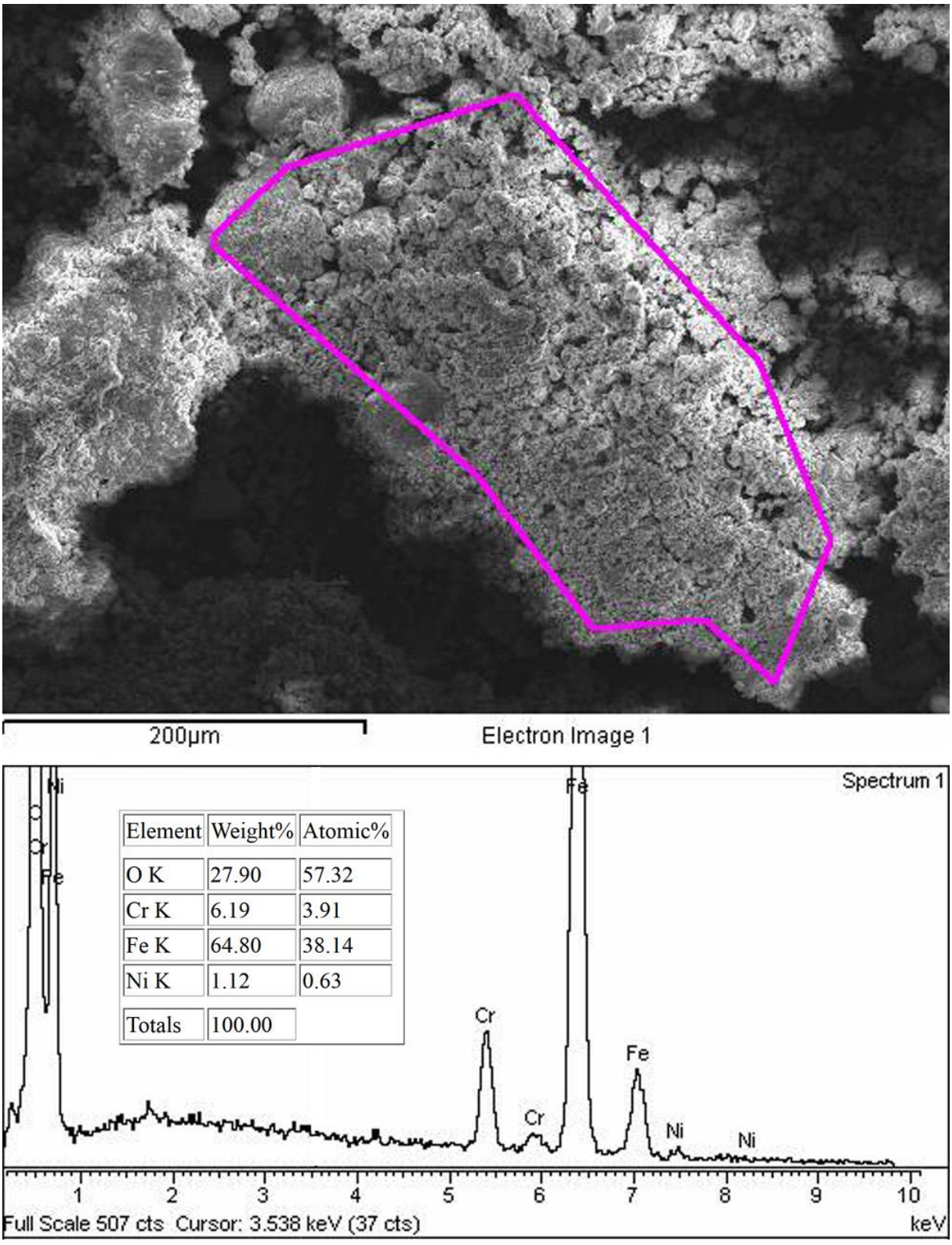

Fig. 60 FE-SEM micrograph of sample S5-25 obtained at 190 × magnification (top) and the corresponding EDS spectrum (bottom). Inset table shows the results of elemental analysis.

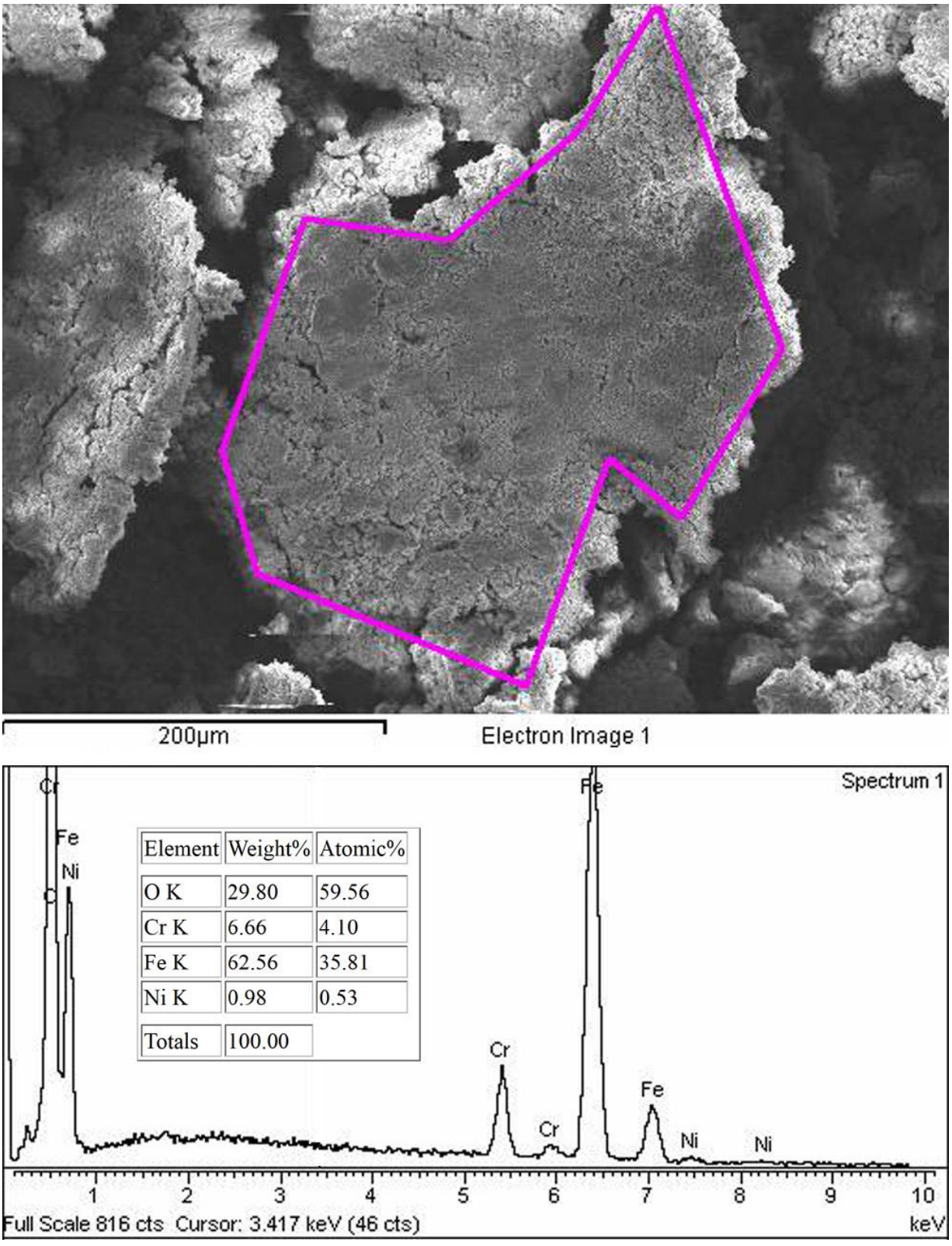

Fig. 61 FE-SEM micrograph of sample S5-30 obtained at 200 × magnification (top) and the corresponding EDS spectrum (bottom). Inset table shows the results of elemental analysis.